American Society of Hematology
2021 L Street NW, Suite 900,
Washington, DC 20036
Phone: 202-776-0544 | Fax 202-776-0545
editorial@hematology.org

# Decoding the molecular heterogeneity of pediatric monomorphic post-solid organ transplant lymphoproliferative disorders

Tracking no: BLD-2022-019543R2

Julia Salmerón-Villalobos (Centro de Investigación Biomédica en Red-Oncología (CIBERONC), Spain) Natalia Castrejon-de-Anta (Institut d'Investigacions Biomèdiques August Pi i Sunyer (IDIBAPS), Spain) Pilar Guerra-Garcia (Hospital Universitario La Paz, Spain) Joan Enric Ramis-Zaldivar (Centro de Investigación Biomédica en Red-Oncología (CIBERONC), Spain) Mònica López-Guerra (Centro de Investigación Biomédica en Red-Oncología (CIBERONC), Spain) Sara Mato (Centro de Investigación Biomédica en Red-Oncología (CIBERONC), Spain) Dolors Colomer (Hospital Clínic. IDIBAPS-CIBERONC, Spain) Francisco Diaz Crespo (Hospital General Universitario Gregorio Marañón, Spain) Javier Menarguez (Hospital General Universitario Gregorio Mara%on, Spain) Marta Garrido-Pontnou (Hospital Universitari Vall d'Hebron, Spain) Mara Andres (Hospital La Fe, Spain) Eugenia Garcia-Fernandez (Hospital Universitario La Paz, Spain) Margarita Llavador (Hospital La Fe, Spain) Gerard Frigola (Hospital Clinic of Barcelona, Spain) Noelia Garcia (Institut d'Investigacions Biomèdiques August Pi i Sunyer (IDIBAPS), Spain) Blanca Gonzalez-Farre (Centro de Investigación Biomédica en Red-Oncología (CIBERONC), Spain) Idoia martin-guerrero (UPV/EHU, Spain) Carmen Garrido-Colino (Hospital General Universitario Gregorio Marañón, Spain) Itziar Astigarraga (Hospital Universitario Cruces, University of the Basque Country, Spain) Alba Fernandez (Hospital Universitari Vall d'Hebron, Spain) Jaime Verdu-Amorós (Hospital Clínico Universitario de Valencia, Spain) Soledad Gonzalez Muñiz (Hospital Universitario Central de Asturias, Spain) Berta González-Martínez (Hospital Universitario La Paz, Spain) Verónica Celis (Hospital Sant Joan de Déu, ) Elías Campo (Centro de Investigación Biomédica en Red-Oncología (CIBERONC), Spain) Olga Balagué (Centro de Investigación Biomédica en Red-Oncología (CIBERONC), Spain) Itziar Salaverria (Centro de Investigación Biomédica en Red-Oncología (CIBERONC), Spain)

**Abstract:**
Post-transplant lymphoproliferative disorders (PTLD) represent a broad spectrum of lymphoid proliferations, frequently associated with Epstein-Barr Virus (EBV) infection. The molecular profile of pediatric monomorphic PTLDs (mPTLD) has not been elucidated and it is unknown whether they display similar genetic features as their counterpart in adult and immunocompetent (IMC) pediatric patients. In this study, we investigated 31 pediatric mPTLD after solid organ transplantation, including 24 diffuse large B-cell lymphomas (DLBCL), mostly classified as activated B-cell, and seven Burkitt lymphoma (BL), 93% of which were EBV positive. We performed an integrated molecular approach, including fluorescence *in situ* hybridization, targeted gene sequencing and copy-number (CN) arrays. Overall, PTLD-BL carried mutations in *MYC, ID3*, *DDX3X*, *ARID1A* or *CCND3* resembling IMC-BL, higher mutational burden than PTLD-DLBCL and less CN alterations than IMC-BL. PTLD-DLBCL showed a very heterogeneous genomic profile with fewer mutations and CN alterations than IMC-DLBCL. Epigenetic modifiers and genes of Notch pathway were the most recurrently mutated in PTLD-DLBCL (both 28%). Mutations in cell cycle and Notch pathways correlated with worse outcome. All seven PTLD-BL were alive after treatment with pediatric B-cell Non-Hodgkin Lymphoma protocols, whereas 54% of DLBCL patients were cured with immunosuppression reduction, rituximab and/or low-dose chemotherapy. These findings highlight the low complexity of pediatric PTLD-DLBCL, their good response to low intensity treatment and the shared pathogenesis between PTLD-BL and EBV+ IMC-BL. We also suggest new potential parameters that could help in the diagnosis and the design of better therapeutic strategies for these patients.

**Conflict of interest:** No COI declared

**COI notes:**

**Preprint server:** No;

**Author contributions and disclosures:** J.S-V performed research, analyzed data and wrote the manuscript; N.C-dA reviewed and interpreted pathological data, analyzed data and wrote the manuscript. P.G-G reviewed and interpreted clinical data, analyzed data and wrote the manuscript. J-E. R-Z, M. L-G, S.M., D.C., N.G. and I.M-G performed research and analyzed data. F. D-C, J.M., M.G., E. G-F, M. LL, G.F., B.G-F, and E.C. reviewed and interpreted pathological data. M.A., C.G-C., I.A., A.F., J.V-A., S.G-M, B.G., V.C. reviewed and interpreted clinical data. O.B. performed morphological diagnosis, analyzed data and wrote the manuscript. I.S. performed research, analyzed data, designed research and wrote the manuscript. All authors approved the final manuscript.

**Non-author contributions and disclosures:** No;

**Agreement to Share Publication-Related Data and Data Sharing Statement:** The copy-number data reported in this article have been deposited at GEO database under accession numbers GSE198253. The following secure token has been created to allow review while it remains in private status: wdidgkssvjwhzcf. Sequencing data have been deposited at the European Nucleotide Archive (ENA, accession number ERP134862).

**Clinical trial registration information (if any):**

# Decoding the molecular heterogeneity of pediatric monomorphic post-solid organ transplant lymphoproliferative disorders

**Julia Salmerón-Villalobos[1,2*], Natalia Castrejón-de-Anta[1,3*], Pilar Guerra-García[4*], Joan Enric Ramis-Zaldivar[1,2], Mónica López-Guerra[1,2,3], Sara Mato[1,2], Dolors Colomer[1,2,3], Francisco Diaz-Crespo[5], Javier Menarguez[5], Marta Garrido[6], Mara Andrés[7], Eugenia García-Fernández[8], Margarita Llavador[9], Gerard Frigola[3], Noelia García[1], Blanca González-Farré[1,2,3], Idoia Martín-Guerrero[10,12], Carmen Garrido[11], Itziar Astigarraga[12], Alba Fernández[13], Jaime Verdú-Amorós[14], Soledad González-Muñíz[15], Berta González[4], Verónica Celis[16], Elías Campo[1,2,3], Olga Balagué [1,2,3*], Itziar Salaverria[1,2*]**

*** These authors contributed equally to the study**

[1]Institut d'Investigacions Biomèdiques August Pi i Sunyer (IDIBAPS), Barcelona, Spain
[2] Centro de Investigación Biomédica en Red-Oncología (CIBERONC), Madrid, Spain
[3] Hematopathology Unit, Hospital Clínic, University of Barcelona, Barcelona Spain
[4] Pediatric Hematology and Oncology Department, Hospital Universitario La Paz. Translational Research in Pediatric Oncology, Hematopoietic Transplantation and Cell Therapy, Instituto de Investigación Hospital Universitario La Paz (IdiPaz), Madrid, Spain
[5] Pathology Department, Hospital General Universitario Gregorio Marañón, Madrid, Spain
[6] Pathology Department, Hospital Universitari Vall d'Hebron, Barcelona, Spain
[7] Pediatric Hematology and Oncology Department, Hospital Universitario y Politécnico La Fe de Valencia, Valencia, Spain
[8] Pathology Department, Hospital Universitario La Paz, Madrid, Spain
[9] Pathology Department, Hospital Universitario y Politécnico La Fe de Valencia, Valencia, Spain
[10] Genetics, Physics Anthropology and Animal Physiology, Faculty of Science and Technology, UPV/EHU, Leioa, Spain
[11] Pediatric Oncology and Hematology Department, Hospital General Universitario Gregorio Marañón, Madrid, Spain
[12] Department of Pediatrics, Osakidetza, Biocruces Bizkaia Health Research Institute, Hospital Universitario Cruces, Barakaldo, Bizkaia, Spain. Departamento de Pediatría, Universidad del Pais Vasco UPV/EHU
[13] Pediatric Oncology and Hematology Department, Hospital Universitari Vall d'Hebron, Barcelona, Spain
[14] Pediatric Oncology and Hematology Department, Hospital Clínico Universitario de Valencia, Valencia, Spain
[15] Pediatric Oncology and Hematology Department, Hospital Universitario Central de Asturias, Spain
[16] Pediatric Oncology and Hematology Department, Hospital Sant Joan de Déu, Barcelona, Spain

**Running Title:** Genetic profiling of pediatric monomorphic PTLD
**Word Count: 3959**
**Figures: 5**

**Tables: 1**
**References: 48**
**Key words:** Pediatric lymphoma, NHL, post-transplant lymphoproliferative disorders, Epstein-Barr virus, next generation sequencing

**Corresponding Authors**

Olga Balagué, MD, PhD
Pathology department, Hematopathology Unit, Hospital Clinic de Barcelona
Villarroel 170
08036 Barcelona, Spain
Email: obalague@clinic.cat

Itziar Salaverria PhD
Institut d´Investigacions Biomèdiques August Pi I Sunyer (IDIBAPS)
Rosselló 153
08036 Barcelona, Spain
Email: isalaver@recerca.clinic.cat

**Data Sharing Statement**

Copy-number and sequencing data are available at GEO and ENA under accession numbers GSE198253 and ERP134862, respectively.

**Key points**

- The mutational profile of pediatric PTLD-BL resembles immunocompetent EBV+ BL, suggesting the need of an intensive therapy.
- Pediatric PTLD-DLBCL is genetically less complex than adult PTLD-DLBCL and pediatric immunocompetent DLBCL.

**ABSTRACT**

Post-transplant lymphoproliferative disorders (PTLD) represent a broad spectrum of lymphoid proliferations, frequently associated with Epstein-Barr Virus (EBV) infection. The molecular profile of pediatric monomorphic PTLDs (mPTLD) has not been elucidated and it is unknown whether they display similar genetic features as their counterpart in adult and immunocompetent (IMC) pediatric patients. In this study, we investigated 31 pediatric mPTLD after solid organ transplantation, including 24 diffuse large B-cell lymphomas (DLBCL), mostly classified as activated B-cell, and seven Burkitt lymphoma (BL), 93% of which were EBV positive. We performed an integrated molecular approach, including fluorescence *in situ* hybridization, targeted gene sequencing and copy-number (CN) arrays. Overall, PTLD-BL carried mutations in *MYC, ID3*, *DDX3X*, *ARID1A* or *CCND3* resembling IMC-BL, higher mutational burden than PTLD-DLBCL and less CN alterations than IMC-BL. PTLD-DLBCL showed a very heterogeneous genomic profile with fewer mutations and CN alterations than IMC-DLBCL. Epigenetic modifiers and genes of Notch pathway were the most recurrently mutated in PTLD-DLBCL (both 28%). Mutations in cell cycle and Notch pathways correlated with worse outcome. All seven PTLD-BL were alive after treatment with pediatric B-cell Non-Hodgkin Lymphoma protocols, whereas 54% of DLBCL patients were cured with immunosuppression reduction, rituximab and/or low-dose chemotherapy. These findings highlight the low complexity of pediatric PTLD-DLBCL, their good response to low intensity treatment and the shared pathogenesis between PTLD-BL and EBV+ IMC-BL. We also suggest new potential parameters that

could help in the diagnosis and the design of better therapeutic strategies for these patients.

## INTRODUCTION

Post-transplant lymphoproliferative disorders (PTLD) are relatively common complications after solid organ (SOT) or hematopoietic stem cell transplantations and represent a major cause of morbidity and mortality.[1] Pediatric transplant recipients are at increased risk of developing PTLD, in part because of Epstein-Barr virus (EBV) seronegativity at the time of transplantation.[1] Three main EBV latency patterns are described in B cells, through which the virus is able to transit, distinguished by different viral gene expression profiles.[2] Characteristically, PTLDs show a latency III pattern.[3]

Diffuse large B-cell lymphoma (DLBCL) is the most common subtype of monomorphic PTLD (mPTLD) in both, adult and pediatric patients, while Burkitt lymphoma (BL) is a less frequent form, with aggressive clinical presentation and different pathological and prognostic characteristics.[4,5] These two entities are also the most frequent mature B-cell Non-Hodgkin Lymphoma (B-NHL) in immunocompetent (IMC) children and adolescents, and their genetic landscapes have been extensively studied.[6–10] In detail, sporadic BL (sBL) is characterized by t(8;14)(q24;q32)/IGH::*MYC* translocation and recurrent mutations in *ID3*, *CCND3, MYC, TP53* and *TCF3*.[6–8] Additionally, EBV-associated BL, including the endemic variant (eBL), displays less frequent mutations in those genes and higher incidence of *ARID1A* and *RHOA* mutations.[11–15] On the other hand, pediatric and young adult DLBCL lacks *BCL2* and *BCL6* primary aberrations, but similarly to adults, has recurrent 2p16/*REL* gains, 19p13/*CD70* homozygous deletions, and mutations in *SOCS1* and *KMT2D*.[9,10]

Despite the clear morphological similarities of mPTLD with lymphomas in IMC patients, few studies have systematically analyzed their biology and genetics beyond their relationship to EBV infection. The genetic profile of PTLD-BL has not been unraveled yet, whereas the few studies that describe the molecular profile of PTLD-DLBCL have been performed in adult patients.[16–18] In this sense, adult PTLD-DLBCL carries recurrent alterations in the JAK-STAT pathway,[18] lower genetic complexity of germinal center B-cell like (GCB) PTLD-DLBCL than IMC-DLBCL, and absence of mutations in key genes characteristic of IMC-DLBCL lymphomagenesis such as *SOCS1*, and genes involved in the NFKB signaling pathway as *CARD11*.[16,17] Moreover, EBV-positive (EBV+) PTLD-DLBCL patients carry a lower mutational burden than the EBV-negative (EBV-).[16] Additionally, gains of 3q, 5p, 8q and 11p, and 1p36, 12p and 17p13 losses have been described in adult PTLD-DLBCL.[19–21]

The lack of information in pediatric mPTLD also raises the question whether large B-cell lymphoma/high grade with 11q aberration (LBCL/HG-11q) and large B-cell lymphoma with *IRF4* translocation (LBCL-*IRF4*), two recently described entities predominantly occurring in children, are represented in this setting.[22,23] Of note, the mutational profile of these diseases has been well characterized in IMC population. LBCL/HG-11q lacks BL related mutations, but displays recurrent mutations in *BTG2*, *DDX3X*, *ETS1*, *EP300, GNA13* and *NFRKB,*[24,25] whereas LBCL-*IRF4* carries frequent alterations in *IRF4* and *CARD11* genes.[9]

In terms of clinical management, there is no standard of care (SOC) for mPTLD in children, a significant gap sharpened by the fact that these patients are particularly vulnerable due to risk of toxicity and rejection, and susceptibility to

infections. Reduction of immunosuppression (RIS) is generally the first treatment step, followed by rituximab, combined or not, with chemotherapy.[26,27]

The aim of this study was to delineate for the first time, the specific genetic, clinical and pathological features of pediatric mPTLD after SOT and to clarify whether the pathogenesis of these lymphomas is the same as in IMC patients. A thorough morphological review and molecular characterization of these cases, together with correlation between these aspects and clinical parameters, might help select better treatment strategies for this challenging population.

## METHODS

### Patients and samples

Thirty-one SOT-related pediatric mPTLD (≤18 years old) patients at diagnosis were recruited from pediatric transplantation Spanish national reference centers in the context of a centralized review supported by the *Sociedad Española de Hematología y Oncología Pediátricas* (SEHOP). All cases were centrally reviewed by four hematopathologists (N-CdA, B.G-F, O.B and E.C) and classified according to the revised 4th World Health Organization (WHO) classification 2017 criteria.[28] Available clinical data, details on transplant and mPTLD management were retrospectively collected (**Supplemental Table 1**).

All formalin-fixed and paraffin-embedded (FFPE) samples investigated contained more than 60% of neoplastic cells. DNA and RNA from FFPE materials were extracted using Qiagen AllPrep DNA/RNA FFPE kit (Qiagen, Hilden, Germany). Polymerase chain reaction (PCR) amplifications for clonal IGH chain gene rearrangements detection were performed according to

BIOMED-2 protocols.[29] This study was approved by the Hospital Clinic of Barcelona's Review Board (HCB/2018/0365) and was performed in accordance with the Declaration of Helsinki.

**Immunohistochemical studies, EBV infection and cell of origin (COO) determination**

Phenotypical profile was studied using standard immunohistochemistry (IHC) protocols on an automated platform (Ventana BenchmarkUltra, Roche, Switzerland). EBV infection, latency pattern and replicative phase were determined by *in situ* hybridization (EBER) and IHC (LMP-1, EBNA-2, ZEBRA) (**Supplemental Methods**; **Supplemental Table 2**). Cases were classified as GC and non-GC subtypes according to Hans algorithm.[30] Additionally, COO classification was performed using Lymph2Cx assay (NanoString Technologies, Seattle, WA).[31]

**Fluorescence *in situ* hybridization (FISH)**

FISH analyses were performed using standard protocols. Breaks at *BCL2*, *PAX5*, *BCL6*, *MYC*, IGK, *IRF4* loci, t(8;14) and t(2;8) fusions, and 11q alterations were analyzed by commercial (Metasystems, Altlußheim, Germany; Empire Genomics, Williamsville, NY; Agilent Technologies, Santa Clara, CA; Abbot, Chicago, IL; ZytoVision, Bremerhaven, Germany) or home-made FISH probes.[32]

**DNA CN alterations (CNAs) analysis**

CNAs were examined in 16 PTLD-DLBCL cases and 7 PTLD-BL, using OncoScan array (Thermo Fisher Scientific, Waltham, MA) following standard

protocols (**Supplemental Methods**). Gains, losses and CN neutral-loss of heterozygosity (CNN-LOH) regions were evaluated using Nexus Biodiscovery v9.0 software (Biodiscovery, Hawthorne, CA). Previously published CN data of pediatric IMC-BL,[33] IMC-DLBCL,[9] and adult PTLD-DLBCL[21,34] were used for comparison.

**Targeted NGS and mutational analysis**

Samples from 25 mPTLD patients, with material available, were included in the mutational analysis. The custom NGS panel interrogated 167 B-cell lymphoma related genes (**Supplemental Table 3**), including those needed to perform *LymphGen* prediction algorithm.[35] SureSelectXT Target Enrichment System Capture NGS strategy library (Agilent Technologies, Santa Clara, CA) was used before sequencing in a MiSeq equipment (Illumina, San Diego, CA) (**Supplemental Methods**). Pathway enrichment analysis was performed defining the contribution of each gene based on previous literature (**Supplemental Methods**).[36] Previously published mutational profiles of adult PTLD-DLBCL,[17,18] pediatric and young adult IMC-DLBCL,[9] pediatric sporadic and endemic BL,[6,11–13] were used for comparisons.

**Statistical methods**

Disease-free survival (DFS) was defined as time from diagnosis until lymphoma disease related death and event-free survival (EFS) was established as time to progression, death of any cause, organ loss or secondary malignancy. The Kaplan–Meier method was used to estimate the DFS and EFS distributions, whereas differences were assessed by the log-rank test.[37] Differences in the distribution of individual parameters among patient subsets were analyzed by

Fisher's exact test for categorized variables, and the Student's t-test for continuous variables. Non-parametric tests were applied when necessary. The *P*-values for multiple comparisons were adjusted using the Benjamini–Hochberg correction (false discovery rate, FDR). A *P*=0.05 cut-off was considered significant unless otherwise indicated. Statistical analyses were carried out using R software v4.1.2.

## RESULTS

### Clinical features

From the 31 recruited patients, eighteen were male and 13, female. The mean age at the time of lymphoma diagnosis was 8.7 years (range 2-17). Kidney and liver were the most frequently transplanted organs (11 and 10 patients, respectively), followed by heart (8 patients), intestine (2 cases) and lung (1 case). Twenty-four cases presented with extranodal disease, and the most frequently affected site was the gastrointestinal tract (21/29)(**Supplemental Figure 3**). Five patients had Stage IV disease (4 had bone marrow involvement, and one case had both central nervous system and bone marrow infiltration). The mean time from transplant to PTLD diagnosis was 35 months (range 2-170). Fifteen out of 31 patients (48%) had early-onset PTLD diagnosed in the first-year post-transplant, while only 6% (2/31) had very late-onset PTLD (≥10 years). Clinicopathological features are detailed in **Table 1** and **Supplemental Table 1**.

At PTLD diagnosis, EBV was detectable in blood in 23 out of 27 patients with available information, and PTLD was secondary to EBV primary infection in 47% (7/15) of the patients with known seronegativity before transplant.

**Pathological characteristics**

Individual description of clinicopathological features, COO and EBV latency pattern of mPTLD patients is detailed in **Supplemental Table 4.**

Twenty-four cases were classified as DLBCL, and seven as BL. Of note, two BL had less monotonous cytology (p28 and p29) (**Supplemental Figure 1**) and one BL (p38) (**Supplemental Figure 2**) showed DLBCL morphology. However, all 3 cases harbored typical phenotypic and molecular features and were, therefore, classified as BL. IGH gene rearrangements analysis identified a clonal peak in 23 out of 24 mPTLD. In case p27 IGH-FR3 was polyclonal, but no further analyses of IGH-FR1 and IGH-FR2 could be performed due to DNA quality.

Most DLBCL cases showed a non-GC phenotype (18/19, 95%), including four DLBCL with plasmacytic differentiation, in line with Lymph2Cx results, that showed an ABC signature in 71% (15/21), followed by 19% unclassified and 10% GCB. The seven BL were classified as GCB by either one of both methods.

EBER was positive in 28 out of 30 cases. A complete EBV latency pattern was determined in 26 cases. All seven BL were EBV+, and all 6 studied cases had a latency pattern I, whereas 21/23 DLBCL were EBV+, 60% of which had latency III. Viral replication was identified in six out of 16 analyzed cases, 5 of them among the latency pattern III group (**Table 1**).

**FISH results**

*MYC* rearrangements were detected in all seven BL. Six cases carried t(8;14)(q24;q32) translocation confirmed by IGH*::MYC* dual fusion FISH probe whereas t(2;8)(p11.2;q24) rearrangement was identified in case p28 using IGK*::MYC* dual fusion probe. Furthermore, no 11q alterations or chromosomal rearrangements involving *IRF4*, *PAX5*, *BCL2 or BCL6* were observed in the 29, 29, 29, 13 and 11 analyzed cases, respectively (**Supplemental Figure 3**).

**Copy number alteration profile**

Eleven out of the 23 pediatric mPTLD studied displayed CNAs (mean 1.5 alt/case; range 0-7) (**Figure 2A**; **Supplemental Table 5**). Seven out of the 16 (44%) PTLD-DLBCL showed CNAs (mean 1.8 alt/case), with gains of 3p and 9q21.11-q34.3 (3 cases each; 19%) being the most frequent. Four out of seven (57%) PTLD-BL displayed CNAs (mean 0.9 alt/case) with no common CNA among those cases. None of the 25 investigated cases showed the characteristic 11q alteration found in LBCL/HG-11q.

Additionally, we compared those CN profiles to the ones observed in IMC patients. Of note, pediatric PTLD-BL had lower genetic complexity than IMC-sBL[33] (0.9 alt/case vs 6.3 alt/case; $P<0.005$) and lacked the 1q23.2-q25.3 gains characteristic of BL (**Figure 2B**). Similarly, PTLD-DLBCL had less CNA than IMC-DLBCL[9] (1.8 alt/case vs 4.4 alt/case; $P<0.05$) (**Figure 2C** and **Figure 3A**) and adult PTLD-DLBCL[21,34] (**Figure 3B**), with absence of CNAs frequently observed in IMC-DLBCL[9] such as telomeric 1q31.3-q42.13 gains and losses of 6q21 and 19p13.3 (**Figure 2C**).

**Identification of mutational profiles by targeted NGS**

Eighteen DLBCL and 7 BL samples were analyzed by NGS (mean coverage 2586x, range 402-7256x). After filtering, a total of 187 somatic variants were detected in 23 out of 25 (range 0-28) mPTLD cases, 127 of them predicted as drivers (mean 5.5 driver mutation/case)(**Supplemental Methods; Supplemental Table 6**).

The mutational burden of PTLD-BL was higher than PTLD-DLBCL (7.8 vs 4.4 mutations, *P*=0.03). All 7 PTLD-BL cases carried *MYC* mutations. *ID3* and *DDX3X* variants were seen in four, *FOXO1* in three, *ARID1A* in two, and *CCND3* in one case (**Figure 4**). Four cases harbored exonic *MYC* driver mutations, three of which carried further multiple intronic mutations. Three cases had only multiple intronic mutations.

Comparison with previously published series of EBV+ and EBV- BL, both sporadic and endemic subtypes,[11–13] revealed that PTLD-BL display a mutational frequency closer to EBV+ BL, with lower incidence of *TCF3*, *CCND3*, *TP53* and *SMARCA4* mutations and higher of *ARID1A* and *FOXO1* (**Supplemental Figure 4A**). Furthermore, the recently defined IC-BL (*ID3*/*CCND3*) and DGG-BL (*DDX3X*/*GNA13*/*GNAI2*) molecular genetic subgroups seem to be represented in our PTLD-BL cohort (4 and 3 cases, respectively) (**Supplemental Figure 4B**).[15]

Differently, the mutational profile of the 18 PTLD-DLBCL was very heterogeneous with lower complexity than their counterparts in IMC patients,[9] when 94 commonly investigated genes were considered (2.4 vs 4.6 mutation/case, *P*=0.2) (**Figure 3C**; **Supplemental Table 7**). The most recurrently mutated gene was *KMT2C* in 3 cases (17%), followed by mutations

in *SPTNB5*, *TP53, NOTCH1*, *BCOR, CARD11, CD70, FAS, IL16* and *TP73* (2 cases each; 11%). The three *KMT2C* mutations were spread throughout the coding region of the gene (exons 36 and 43), while three *NOTCH1* mutations were detected in two cases, both carrying a mutation predicted to truncate the protein in its PEST domain. Of note, PTLD-DLBCL lacked the characteristic mutations of *SOCS1*, *MYD88*, *PIM1*, *BTG1*, *EZH2* and *PRDM1* genes observed in pediatric and young adult IMC-DLBCL (**Supplemental Table 7**).[9]

Pathway enrichment analysis showed that, in line with IMC-DLBCL, genes involved in epigenetic modifications were one of the most recurrently affected (5 cases). On the other hand, and differently to IMC-DLBCL, PTLD-DLBCL carried frequent mutations in Notch and MAPK pathways (5 and 2 cases, respectively), whereas lacked alterations affecting JAK-STAT pathway (**Supplemental Figure 5**). In order to discern whether these PTLD-DLBCL could belong to previously defined genetic subtypes of DLBCL,[35] *LymphGen* algorithm was applied to 19 PTLD-DLBCL. Only two cases (11%) were classified as N1, while the rest remained undetermined. These data suggest that this group of pediatric PTLD-DLBCL, mainly EBV+ (91%), do not fit in any of the established genetic DLBCL subtypes.

Moreover, comparison with adult PTLD-DLBCL[17,18] showed that pediatric PTLD-DLBCL lack mutations in *KMT2D* (30% vs 0%, *P*=0.01)*, PIK3CD, MYD88, PIM1, BTG1* and *EZH2* genes, and have lower incidence of *TP53* mutations (11% vs 32%, *P*=0.11)(**Figure 3D; Supplemental Table 7**).

**Clinical outcome and prognostic value of clinical and molecular features**

Four out of the 7 PTLD-BL (57%) presented with Stage IV. All of them underwent RIS and received chemotherapy according to the SOC for B-NHL. All seven patients were alive and in complete remission at last follow up (mean follow up 8.7 years; range 2-22 years) (**Table 1; Supplemental Table 1**).

Different to PTLD-BL, treatment strategy in PTLD-DLBCL was more heterogeneous. In detail, 7 out of 24 cases were initially treated following first-line B-NHL protocols. The remaining cases received a less aggressive regimen, mainly consisting of RIS (12 cases) and/or rituximab (12 cases). In five patients, LDCT was added (**Supplemental Table 1**).

The 5-year EFS (5y-EFS) rate was 73% in the whole cohort. Seven patients died, five of them related to lymphoma (5y-DFS 84%; **Figure 5A**). Of note, all deceased patients were PTLD-DLBCL and three of them with clinical information available, were at advanced stage (III-IV) at diagnosis. Only one out of 14 PTLD-DLBCL patients treated with less aggressive therapy (RIS, rituximab and/or LDCT) deceased because of lymphoma (5y-DFS 93%). This survival rate is in line with the one observed in patients who received intense chemotherapy (6/7 patients, 86%)(**Figure 5B**). Two of the patients died of F-PTLD before any therapy could be initiated, and there was no information available on the treatment received by the remaining case.

Of note, among PTLD-DLBCL patients, both, presence of mutations affecting cell cycle signaling (*CCND3* and *TP53*)(5y-DFS 33% vs 93%; *P*=0.008) (**Figure 5C**) and alterations of Notch pathway (*NOTCH1*, *FBXW7* and *SGK1*) (5y-DFS 50% vs 93%; *P*=0.043) (**Figure 5D**), were associated with a worse outcome.

## DISCUSSION

PTLD is a major complication in recipients of both SOT and hematopoietic stem cell transplantations and occurs in up to 20% of patients depending on the series.[5,38] In this study, we report for the first time an integrative genetic and molecular characterization of a large series of mPTLD in children and adolescents who received a SOT. Our results show relevant differences in the molecular landscape of these tumors with both PTLD in adults and DLBCL in IMC pediatric patients. Moreover, we show different molecular and clinical features between the 24 PTLD-DLBCL and 7 PTLD-BL included in the study, stressing the need for an adequate morphological and molecular diagnosis.

In detail, all seven PTLD-BL cases had a *MYC* rearrangement and, unlike PTLD-DLBCL, had a GCB phenotype and EBV latency pattern I, fully resembling IMC-BL. However, morphology ranged from typical BL cytology to less monotonous cytology or even DLBCL morphology. Nevertheless, all cases harbored typical phenotypic and molecular features of BL, highlighting the relevance of latency and COO determination in those cases. Additionally, all 7 cases depicted the mutational profile described in IMC-BL patients. Specifically, *MYC* mutations, either exonic or multiple intronic, were detected in all BL samples, followed by frequent mutations in *ID3* and *DDX3X* (4/7 cases each; 57%) and *ARID1A* (2/7 cases; 29%), with all 7 BL patients harboring, at least, one of these mutations. Our PTLD-BL also displayed lower genetic complexity than IMC-BL,[33] with absence of the characteristic 1q gains, which could be related to the EBV infection, as previously reported.[15]

Prior studies have observed differences in the mutational profile between EBV- and EBV+ BL, the latter being associated with recurrent mutations in *ARID1A* and *RHOA* and lower incidence of mutations in *ID3*, *CCND3* or *SMARCA4*.[11–

[13,15] Our 7 PTLD-BL were EBV positive, an expected higher frequency than that reported in sporadic and HIV related BL,[39] and similar to eBL.[40] All six investigated PTLD-BL had an EBV latency pattern I, typically seen in BL,[12,41] unlike other types of PTLD, where latency type III is the most prevalent.[3,42] We have also compared the mutational profile of previously published EBV+ and EBV- BL cohorts[11–13] with our cases having a mutational distribution closer to EBV+ BL.[4,5] Similarly, our cases seem to belong to the recently defined molecular subgroups highly represented in a large series of EBV+ BL tumors (DGG-BL and IC-BL) by whole-exome sequencing.[15] Despite the limited number of our PTLD-BL series, our data also confirm the lower mutational burden in IC-BL-like cases than those with DGG-BL characteristics (6 vs 13 mutations/case) and the overrepresentation of male patients within DDG-BL.

Clinically, PTLD-BL showed a longer interval between transplant and lymphoma onset compared to PTLD-DLBCL (**Table 1**) and had a more aggressive presentation (4/7 were at Stage IV) than PTLD-DLBCL (1/24). All PTLD-BL were alive and in complete remission at last follow-up after treatment with RIS and chemotherapy following SOC for mature B-cell NHL (rituximab included in 4/7).

In this line, previous studies have highlighted that PTLD-BL required chemotherapy in most cases.[26,27,43] In detail, a phase II trial proved the use of LDCT combined with rituximab to be effective in pediatric mPTLD after SOT, with a 2y-OS and EFS of 90% and 76%, respectively.[26] In this study from Gross *et al,* 4 out of 5 PTLD-BL were long-term survivors. However, *MYC* status was not known in all cases. Another non-randomized prospective multicentre trial studied a response-adapted sequential immuno-chemotherapy in PTLD after

SOT observing a 2y-OS and EFS of 86% and 67%, respectively. In half of the patients, chemotherapy could be avoided after responding to rituximab induction. Of note, in this study, 86% of PTLD-BL cases required chemotherapy.[27] All these observations claimed that PTLD-BL should be considered as an independent entity and would benefit from intensive therapeutic regimes, therefore, its distinction from other mPTLD is relevant.

On the other hand, our data show that the genetic features of pediatric PTLD-DLBCL are very heterogeneous. Latency pattern III was the most common among PTLD-DLBCL, though patterns II and I were also observed in 30% and 10% of the cases respectively, in line with previous literature on mPTLD.[3] Seven out of the 16 samples evaluated showed CNAs, with the most common alterations being gains of 3p and 9q21.11-q34.3. This CN landscape lacks characteristic alterations specific of pediatric and young adult DLBCL in IMC cases such as 1q31.3-q42.13 gains and losses of 6q21 and 19p13.3;[9] and it is also different from the one observed in adult PTLD-DLBCL, with absence of most CNAs reported in those cases.[21,34] The mutational profile was very diverse as well, with *KMT2C* being the most recurrently mutated gene (3 cases; 17%), followed by mutations in *NOTCH1* or *TP53* genes (2 cases each; 11%), among others. In terms of global mutational burden, PTLD-DLBCL showed a lower mutational load than IMC counterparts, lacking typically found *SOCS1* mutations, and the profile of affected pathways was enriched with alterations in epigenetic modifiers and Notch signaling. EBNA-2 has been described to use Notch pathway to immortalize B cells.[44] In our series, none of the ten EBNA-2 positive cases with mutational information harbored mutations in Notch pathway, while 40% (2/5) of the EBV+ PTLD-DLBCL, EBNA-2 negative had

mutations in Notch pathway, supporting an alternative role for EBNA-2 and Notch in the oncogenesis of PTLD-DLBCL.[45]

The mutational landscape of pediatric PTLD-DLBCL was different to the one reported in adult PTLD-DLBCL, either EBV+ or EBV- cases, with lack of mutations in *KMT2D* and *PIK3CD* and lower frequency of *TP53* mutations. This lack of recurrent genomic alterations in pediatric PTLD-DLBCL sheds light into the biology of these tumors, although, in order to confirm these observations, analyses in independent series by, e.g., whole-exome or whole-genome approaches need to be performed.

Regarding clinical aspects, in our series, the PTLD-DLBCL patients that were treated with less intensive schemes (14/24; 58%) had a 5y-DFS of 93%, and there was only one lymphoma related death. Furthermore, among the seven patients treated with B-NHL specific strategies (5y-DFS 86%), there was one toxic death, stressing the vulnerability of this fragile population and the need of adapting treatments to reduce toxicities.

In summary, the different genetic background of pediatric PTLD-DLBCL in comparison with adult PTLD-DLBCL and IMC children and young adults, and the response to different treatment strategies, suggest that perhaps less intensive schemes with only RIS and rituximab or LDCT, could be a therapeutic option in selected patients. Additionally, correlation analyses between molecular features and clinical outcome revealed that alterations in the cell cycle signaling and Notch pathway were associated with a worse outcome. The real impact of these alterations as potential biomarkers needs to be further investigated.

Moreover, previous studies in adult PTLD have reported association of EBV latency pattern III and replication with a significantly shorter survival and early PTLD onset.[3] In pediatric mPTLD, patients with EBV latency III and viral replication presented a shorter time from transplant to PTLD diagnosis (8.2 vs 47.6 months; *P*=0.004) and a tendency towards a worse prognosis (2y-DFS 60 vs 82%; *P*=0.33) (**Supplemental Figure 6B**). Although EBV latency pattern is currently not available for clinicians, its inclusion in the design of future therapeutic strategies should be considered.

The incidence of LBCL/HG-11q and LBCL-*IRF4* in pediatric mPTLD had not been previously investigated. Remarkably, Ferreiro *et al*[46] described an overrepresentation of LBCL/HG-11q in a subset of molecularly defined adult BL in the post-transplant setting. Interestingly, in our pediatric mPTLD, no 11q aberrations were identified by FISH and/or CN arrays. Similarly, although 20 mPTLD with DLBCL diagnosis expressed IRF4/MUM1, none of the 23 investigated cases displayed *IRF4* rearrangements. These results suggest the rarity of LBCL/HG-11q and LBCL-*IRF4* in pediatric mPTLD, although larger series of cases should validate these observations. Also, *PAX5* alterations, previously reported to occur in B-NHL in the post-transplant setting and associated with unfavorable outcome,[3,47,48] were absent in pediatric mPTLD, suggesting that *PAX5* is not a key gene related to lymphomagenesis in these patients.

Altogether, we performed a multidisciplinary genome-wide analysis of a large series of pediatric SOT-associated mPTLD for the first time, observing distinct molecular profiles among PTLD-BL and PTLD-DLBCL. Additionally, PTLD-BL

showed similarities with EBV+ IMC-BL whereas PTLD-DLBCL was genetically different than adult PTLD and IMC-DLBCL counterpart.

Moreover, although the low number of patients included and the diverse therapeutic approaches in our series is a limitation, our analyses support previous evidence stating that PTLD-DLBCL in SOT recipients can respond to less intensive treatment.[26,27] Further prospective studies should be undertaken to corroborate our findings and help in defining more personalized therapeutic strategies for these patients.

## ACKNOWLEDGMENTS

We thank the centers of the Sociedad Española de Hematología y Oncología Pediátricas (SEHOP) that submitted cases for centralized review and to Silvia Martín, Helena Suarez, Nuria Orellana and Silvia Ruiz for their excellent technical and administrative assistance. We thank Adela Rodriguez from Hospital Clínic for helping to confirm the non-deleterious effect of *BRCA2* mutations. We are indebted to the IDIBAPS Genomics Core Facility and to HCB-IDIBAPS Biobank-Tumor Bank and Biobanc de l'Hospital Infantil Sant Joan de Déu, Hospital Universitario Virgen del Rocío-Instituto de Biomedicina de Sevilla Biobank (ISCIII-Red de Biobancos PT13/0010/0056) all three integrated in the National Network Biobanks of ISCIII for the sample and data procurement. This work was funded by Fondo de Investigaciones Sanitarias Instituto de Salud Carlos III (ISCIII) through the projects "Miguel Servet Program MSII18/0015" and "PI18/00471" (I.S.) and European Regional Development Fund "Una manera de hacer Europa", Asociación Española Contra el Cáncer (AECC CICPFI6025SALA), Generalitat de Catalunya Suport Grups de Recerca (2017-SGR-1107 I.S.). J.E.R-Z was supported by a fellowship from Generalitat de Catalunya AGAUR FI-DGR 2017 (2017 FI_B01004). N.G has been continuously supported by Acció instrumental d'incorporació de científics i tecnòlegs PERIS (SLT002/16/00336 and SL017/20/000204) from Generalitat de Catalunya. E.C. is an Academia Researcher of the "Institució Catalana de Recerca i Estudis Avançats" (ICREA) of the Generalitat de Catalunya. This work was developed at the Centro Esther Koplowitz, Barcelona, Spain.

## AUTHOR CONTRIBUTION

J.S-V performed research, analyzed data and wrote the manuscript; N. C-dA reviewed and interpreted pathological data, analyzed data and wrote the manuscript. P.G-G reviewed and interpreted clinical data, analyzed data and wrote the manuscript. J-E. R-Z, M. L-G, S.M., D.C., N.G., and I.M-G performed research and analyzed data. F. D-C, J.M., M.G., E. G-F, M. LL, G.F., B.G-F, and E.C. reviewed and interpreted pathological data. M.A., C.G-C, I.A., A.F., J.V-A., S.G-M, B.G., V.C. reviewed and interpreted clinical data. O.B. performed morphological diagnosis, analyzed data and wrote the manuscript. I.S. performed research, analyzed data, designed research and wrote the manuscript. All authors approved the final manuscript.

## CONFLICT OF INTEREST DISCLOSURES

The authors declare no conflict of interest.

## REFERENCES


1. Dharnidharka VR, Tejani AH, Ho P-L, Harmon WE. Post-Transplant Lymphoproliferative Disorder in the United States: Young Caucasian Males are at Highest Risk. *Am. J. Transplant.* 2002;2:993–998.

2. Chabay PA, Preciado M V. EBV primary infection in childhood and its relation to B-cell lymphoma development: a mini-review from a developing region. *Int. J. cancer*. 2013;133(6):1286–1292.

3. Gonzalez-Farre B, Rovira J, Martinez D, et al. In vivo intratumoral Epstein-Barr virus replication is associated with XBP1 activation and early-onset post-transplant lymphoproliferative disorders with prognostic implications. *Mod. Pathol.* 2014;27(12):1599–1611.

4. Picarsic J, Jaffe R, Mazariegos G, et al. Post-transplant Burkitt lymphoma is a more aggressive and distinct form of post-transplant lymphoproliferative disorder. *Cancer*. 2011;117(19):4540–4550.

5. Mynarek M, Schober T, Behrends U, Maecker-Kolhoff B. Posttransplant lymphoproliferative disease after pediatric solid organ transplantation. *Clin. Dev. Immunol.* 2013;2013:814973.

6. Schmitz R, Young RM, Ceribelli M, et al. Burkitt lymphoma pathogenesis and therapeutic targets from structural and functional genomics. *Nature*. 2012;490(7418):116–120.

7. Love C, Sun Z, Jima D, et al. The genetic landscape of mutations in Burkitt lymphoma. *Nat. Genet.* 2012;44(12):1321–1325.

8. Richter J, Schlesner M, Hoffmann S, et al. Recurrent mutation of the ID3 gene in Burkitt lymphoma identified by integrated genome, exome and transcriptome sequencing. *Nat. Genet.* 2012;44(12):1316–1320.

9. Ramis-Zaldivar JE, Gonzalez-Farré B, Balagué O, et al. Distinct molecular profile of IRF4-rearranged large B-cell lymphoma. *Blood*. 2020;135(4):274–286.

10. Newman AM, Zaka M, Zhou P, et al. Genomic abnormalities of TP53 define distinct risk groups of paediatric B-cell non-Hodgkin lymphoma. *Leukemia*. 2022;36(3):781–789.

11. Abate F, Raffaella Ambrosio M, Mundo L, et al. Distinct Viral and Mutational Spectrum of Endemic Burkitt Lymphoma. *PLOS Pathog.* 2015;11(10):e1005158.

12. Kaymaz Y, Oduor CI, Yu H, et al. Comprehensive Transcriptome and Mutational Profiling of Endemic Burkitt Lymphoma Reveals EBV Type-Specific Differences. *Mol. cancer Res.* 2017;15(5):563–576.

13. Grande BM, Gerhard DS, Jiang A, et al. Genome-wide discovery of somatic coding and noncoding mutations in pediatric endemic and sporadic Burkitt lymphoma. *Blood*. 2019;133(12):1313–1324.

14. Richter J, John K, Staiger AM, et al. Epstein–Barr virus status of sporadic Burkitt lymphoma is associated with patient age and mutational features. *Br. J. Haematol.* 2022;196(3):681–689.

15. Thomas N, Dreval K, Gerhard DS, et al. Genetic Subgroups Inform on Pathobiology in Adult and Pediatric Burkitt Lymphoma. *Blood*.

2023;141(8):904–916.

16. Gebauer N, Gebauer J, Tristan Hardel T, et al. Prevalence of targetable oncogenic mutations and genomic alterations in Epstein-Barr virus-associated diffuse large B-cell lymphoma of the elderly. *Leuk. Lymphoma*. 2015;56(4):1100–1106.

17. Menter T, Juskevicius D, Alikian M, et al. Mutational landscape of B-cell post-transplant lymphoproliferative disorders. *Br. J. Haematol.* 2017;178(1):48–56.

18. Butzmann A, Sridhar K, Jangam D, et al. Mutations in JAK/STAT and NOTCH1 Genes Are Enriched in Post-Transplant Lymphoproliferative Disorders. *Front. Oncol.* 2022;11:790481.

19. Poirel HA, Bernheim A, Schneider A, et al. Characteristic pattern of chromosomal imbalances in posttransplantation lymphoproliferative disorders: Correlation with histopathological subcategories and EBV status. *Transplantation*. 2005;80(2):176–184.

20. Rinaldi A, Kwee I, Poretti G, et al. Comparative genome-wide profiling of post-transplant lymphoproliferative disorders and diffuse large B-cell lymphomas. *Br. J. Haematol.* 2006;134(1):27–36.

21. Rinaldi A, Capello D, Scandurra M, et al. Single nucleotide polymorphism-arrays provide new insights in the pathogenesis of post-transplant diffuse large B-cell lymphoma. *Br. J. Haematol.* 2010;149(4):569–577.

22. Alaggio R, Amador C, Anagnostopoulos I, et al. The 5th edition of the World Health Organization Classification of Haematolymphoid Tumours:

Lymphoid Neoplasms. *Leukemia*. 2022;36:1720–1748.

23. Campo E, Jaffe ES, Cook JR, et al. The International Consensus Classification of Mature Lymphoid Neoplasms: A Report from the Clinical Advisory Committee. *Blood*. 2022;140(11):1229–1253.

24. Gonzalez-Farre B, Ramis-Zaldivar JE, Salmeron-Villalobos J, et al. Burkitt-like lymphoma with 11q aberration: A germinal center-derived lymphoma genetically unrelated to Burkitt lymphoma. *Haematologica*. 2019;104(9):1822–1829.

25. Wagener R, Seufert J, Raimondi F, et al. The mutational landscape of Burkitt-like lymphoma with 11q aberration is distinct from that of Burkitt lymphoma. *Blood*. 2019;133(9):962–966.

26. Gross TG, Orjuela MA, Perkins SL, et al. Low-dose chemotherapy and rituximab for posttransplant lymphoproliferative disease (PTLD): a Children's Oncology Group Report. *Am. J. Transplant*. 2012;12(11):3069–3075.

27. Maecker-Kolhoff B, Beier R, Zimmermann M, et al. Response-Adapted Sequential Immuno-Chemotherapy of Post-Transplant Lymphoproliferative Disorders in Pediatric Solid Organ Transplant Recipients: Results from the Prospective Ped-PTLD 2005 Trial. *Blood*. 2014;124(21):4468–4468.

28. Swerdlow SH, Campo E, Harris NL, Jaffe ES, Pileri SA , Stein H, Thiele J (Eds): WHO Classification of Tumours of Haematopoietic and Lymphoid Tissues (Revised 4th edition). IARC: Lyon 2017

29. Van Dongen J, Langerak AW, Brü Ggemann M, et al. Design and standardization of PCR primers and protocols for detection of clonal immunoglobulin and T-cell receptor gene recombinations in suspect lymphoproliferations: Report of the BIOMED-2 Concerted Action BMH4-CT98-3936. *Leukemia*. 2003;17(12):2257–2317.

30. Hans CP, Weisenburger DD, Greiner TC, et al. Confirmation of the molecular classification of diffuse large B-cell lymphoma by immunohistochemistry using a tissue microarray. *Neoplasia*. 2004;103(2):275–282.

31. Scott DW, Wright GW, Williams PM, et al. Determining cell-of-origin subtypes of diffuse large B-cell lymphoma using gene expression in formalin-fixed paraffin-embedded tissue. *Blood*. 2014;123(8):1214–1217.

32. Salaverria I, Philipp C, Oschlies I, et al. Translocations activating IRF4 identify a subtype of germinal center-derived B-cell lymphoma affecting predominantly children and young adults. *Blood*. 2011;118(1):139–148.

33. Scholtysik R, Kreuz M, Klapper W, et al. Detection of genomic aberrations in molecularly defined burkitt's lymphoma by array-based, high resolution, single nucleotide polymorphism analysis. *Haematologica*. 2010;95(12):2047–2055.

34. Finalet Ferreiro J, Morscio J, Dierickx D, et al. EBV-Positive and EBV-Negative Posttransplant Diffuse Large B Cell Lymphomas Have Distinct Genomic and Transcriptomic Features. *Am. J. Transplant.* 2016;16(2):414–425.

35. Wright GW, Huang DW, Phelan JD, et al. A Probabilistic Classification Tool for Genetic Subtypes of Diffuse Large B Cell Lymphoma with Therapeutic Implications. *Cancer Cell*. 2020;37(4):551-568.e14.

36. Karube K, Enjuanes A, Dlouhy I, et al. Integrating genomic alterations in diffuse large B-cell lymphoma identifies new relevant pathways and potential therapeutic targets. *Leukemia*. 2018;32(3):675–684.

37. Cheson BD, Pfistner B, Juweid ME, et al. Revised response criteria for malignant lymphoma. *J. Clin. Oncol.* 2007;25(5):579–586.

38. Penn I. Cancers Complicating Organ Transplantation. *N. Engl. J. Med.* 1990;323(25):1767–1769.

39. Navari M, Etebari M, Falco G De, et al. The presence of Epstein-Barr virus significantly impacts the transcriptional profile in immunodeficiency-associated Burkitt lymphoma. *Front. Microbiol.* 2015;6(JUN):556.

40. Kelly GL, Stylianou J, Rasaiyaah J, et al. Different Patterns of Epstein-Barr Virus Latency in Endemic Burkitt Lymphoma (BL) Lead to Distinct Variants within the BL-Associated Gene Expression Signature. *J. Virol.* 2013;87(5):2882–2894.

41. Murata T, Sugimoto A, Inagaki T, et al. Molecular Basis of Epstein-Barr Virus Latency Establishment and Lytic Reactivation. *Viruses*. 2021;13(12):2344.

42. Tse E, Kwong Y-L. Epstein Barr virus-associated lymphoproliferative diseases: the virus as a therapeutic target. *Exp. Mol. Med.* 2015;47(1):e136.

43. Afify Z, Orjuela-Grimm M, Smith CM, et al. Burkitt lymphoma after solid-organ transplant: Treatment and outcomes in the paediatric PTLD collaborative. *Br. J. Haematol.* 2022;200(3):297–305.

44. Grossman SR, Johannsen E, Tong X, Yalamanchili R, Kieff E. The Epstein-Barr virus nuclear antigen 2 transactivator is directed to response elements by the JKc recombination signal binding protein. *Med. Sci.* 1994;91:7568–7572.

45. Höfelmayr H, Strobl LJ, Marschall G, Bornkamm GW, Zimber-Strobl U. Activated Notch1 Can Transiently Substitute for EBNA2 in the Maintenance of Proliferation of LMP1-Expressing Immortalized B Cells. *J. Virol.* 2001;75(5):2033–2040.

46. Ferreiro JF, Morscio J, Dierickx D. Post-transplant molecularly defined Burkitt lymphomas are frequently MYC-negative and characterized by the 11q-gain/ loss pattern. *Haematologica*. 2015;100(7):e275–e279.

47. Poppe B, De Paepe P, Michaux L, et al. PAX5/IGH rearrangement is a recurrent finding in a subset of aggressive B-NHL with complex chromosomal rearrangements. *Genes Chromosom. Cancer*. 2005;44(2):218–223.

48. Fasan O, Willmott C, Czepulkowski B, et al. Epstein-Barr virus-related post-transplant lymphoproliferative disorder with t(9;14)(p11∼12;q32). *Cancer Genet. Cytogenet.* 2003;142(2):134–136.

**Table 1.** Clinicopathological characteristics of 31 pediatric B-cell monomorphic PTLD patients

| | PTLD-DLBCL, n= 24 | PTLD-BL, n = 7 | Total, n = 31 |
|---|---|---|---|
| Mean age (range, years old) | 8 (2-17) | 12 (6-16) | 9 (2-17) |
| Male | 13/24 (54%) | 5/7 (71%) | 18/31 (58%) |
| Female | 11/24 (46%) | 2/7 (29%) | 13/31 (42%) |
| Localization | | | |
| Extranodal involvement | 17/23 (74%) | 6/7 (86%) | 23/30 (77%) |
| Gastrointestinal tract | 17/23 (74%) | 4/6 (67%) | 21/29 (72%) |
| Stage | | | |
| Stage I | 1/19 (5%) | 1/7 (14%) | 2/26 (8%) |
| Stage II | 3/19 (16%) | 0/7 (0%) | 3/26 (11%) |
| Stage III | 14/19 (74%) | 2/7 (29%) | 16/26 (62%) |
| Stage IV | 1/19 (5%) | 4/7 (57%) | 5/26 (19%) |
| Cell of origin (NanoString and/or Hans algorithm)[&] | | | |
| GCB | 2/22 (9%) | 7/7 (100%) | 9/29 (31%) |
| ABC/non-GCB | 20/22 (91%) | 0/7 (0%) | 20/29 (69%) |
| EBER Hybridization positive | 21/23 (91%) | 7/7 (100%) | 28/30 (93%) |
| EBV replication | 6/11 (55%) | 0/5 (0%) | 6/16 (38%) |
| Latency pattern | | | |
| Latency I | 2/20 (10%) | 6/6 (100%) | 8/26 (31%) |
| Latency II | 6/20 (30%) | 0/6 (0%) | 6/26 (23%) |
| Latency III* | 12/20 (60%) | 0/6 (0%) | 12/26 (46%) |
| Mean time from transplant to PTLD diagnosis (range, months) | 24 (2-141) | 74.4 (32-170) | 35 (2-170) |
| Early-onset PTLD | 15/24 (63%) | 0/7 (0%) | 15/31 (48%) |
| Alive with no evidence of disease | 17/24 (71%) | 7/7 (100%) | 24/31 (77%) |
| Died of disease | 5/24 (21%) | 0/7 (0%) | 5/31 (16%) |
| Fulminant-PTLD | 3/5 (60%) | 0/0 (0%) | 3/5 (60%) |
| Follow up (median) | 1.3 years | 5.2 years | 2.7 years |
| (range) | (10 days – 14.1 years) | (2.1 – 22.6 years) | (10 days – 22.6 years) |
| 5y-DFS | 78.9% | 100% | 83.7% |

ABC: activated B cell; GCB, germinal center B cell; EBER: Epstein-Barr virus-encoded small RNAs; EBV, Epstein-Barr Virus; DFS: disease-free survival.
*In the absence of LMP-1 assessability, two cases with latency pattern IIb-III are included in latency pattern III group.

[&] Unclassified cases by NanoString analysis were classified according to Hans algorithm results.

## FIGURE LEGENDS

**Figure 1. Morphological, immunohistochemical and genetic features of two prototypical post-SOT mPTLD, Burkitt lymphoma (BL) (case p11) and diffuse large B-cell lymphoma (DLBCL) (case p10), respectively. Case p11**: **(A)** H&E, original magnification at 400x. **(B)** Tumor cells are diffusely positive for CD10 (Immunostain, original magnification at 400x). **(C)** *In situ* hybridization for EBV RNA is positive in tumor cells (*In situ* hybridization, original magnification at 400x). **(D-F)** Neoplastic cells are negative for LMP1 **(D)**, EBNA2 **(E)** and Zebra **(F)** immunostains, indicating a latency pattern I (Immunostains, original magnification at 400x). **(G)** FISH using *MYC* Break-Apart Probe (BAP) shows a signal constellation of one colocalized signal (yellow arrow) and two split signals (green and red arrows) in accordance with the gene rearrangement. **Case p10**: **(H)** DLBCL with focal plasmacytic differentiation, (H&E, original magnification at 400x). **(I)** Atypical cells are diffusely positive for MUM1 (Immunostain, original magnification at 400x). **(J-L)** LMP1 **(J)**, EBNA2 **(K)** and ZEBRA **(L)** immunostains show positive tumor cells, reflecting a pattern III of latency (Immunostains, original magnification at 400x). **(M-N)** FISH using BAP for *MYC* **(M)** and *IRF4* **(N)** genes show a normal pattern with two colocalizations in each nucleus for both hybridizations (yellow arrows).

**Figure 2. (A) Global CN profile of 23 B-cell post-SOT mPTLD**. X-axis represents chromosomes from 1 to Y and p to q. The Y-axis indicates frequency of each genomic alteration among the analyzed cases; CN gains are represented in blue and CN losses are depicted in red. Chromosomal bands of regions altered in more than 10% cases are indicated in the plot. **(B)** Comparative plot of CN profile comparison with previously published data on

BL[33] and **(C)** DLBCL[9] in IMC patients. Asterisks indicate significant differences between both groups according to Fisher's exact test raw *P*<0.1, considering a minimum number of altered cases n=3.

**Figure 3. Comparison between pediatric PTLD-DLBCL, pediatric and young adult IMC-DLBCL[9] and adult PTLD-DLBCL[17,18,21,34] in terms of (A-B) copy number alterations (CNA) and (C-D) mutational frequencies**. The vertical axis of (A) and (C) represents number of alterations and the two groups are separated in the X-axis (PTLD-DLBCL represented in purple and IMC-DLBCL represented in blue). Asterisks in (A) mark significant differences between both groups according to Wilcoxon rank-sum test *P*<0.05. The vertical axis of (B) and (D) represents frequency of alteration (%), with the different CNA in (B) and genes in (D) represented in the horizontal axis. Asterisks in (B) mark significant differences between adult and pediatric PTLD-DLBCL, according to Fisher's exact test *P*-<0.1 and in (D) indicate significant differences between adult, either EBV+ or negative, and pediatric PTLD-DLBCL, according to Fisher's exact test * *P*<0.1 and ** *P*<0.05.

**Figure 4. Molecular CN and mutational information on 25 B-cell post-SOT mPTLD.** Each column corresponds to a case, the top histogram depicts number of CN alteration (CNA) and each row of the bottom plot represents a gene, where dark blue color marks driver mutation. Only genes with driver mutation in more than two cases are represented. Blue in *MYC*-R row indicates *MYC* rearrangement was detected by FISH using *MYC* BAP and, in cases p11, p15, p22, p29, p38 and p42, also using IGH::*MYC* DF probe whereas in case p28, IGK::*MYC* DF probe was used. NA: Not available; DLBCL: diffuse large B-cell lymphoma, BL: Burkitt lymphoma; COO: cell of origin; GCB: germinal center B-

cell, ABC: activated B-cell; RIS: reduction of immunosuppression; LDCT: low-dose chemotherapy: SOC-BNHL: standard-of-care for B-NHL.

**Figure 5**. **(A) Event-free survival (EFS) and disease-free survival (DFS) probabilities within the complete cohort. (B) DFS probability of PTLD-DLBCL** patients treated with reduction of immunosuppression (RIS) and/or rituximab (R) and/or low-dose chemotherapy (LDCT) compared to that of cases treated with standard-of-care for B-NHL (SOC-BNHL). **(C) DFS probability of PTLD-DLBCL patients** according to mutations affecting cell cycle signaling and **(D)** Notch pathway.

Figure 1

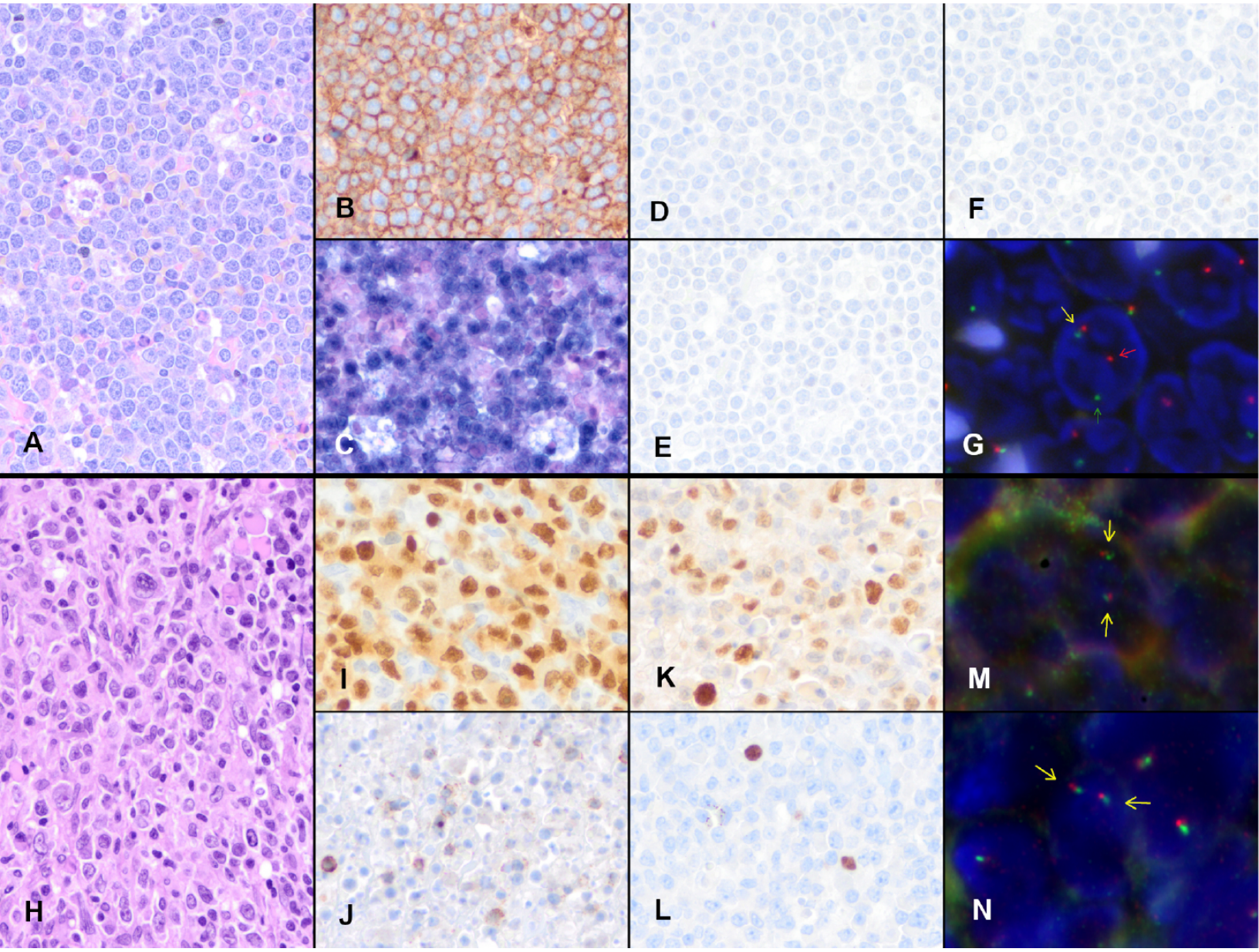

Figure 2

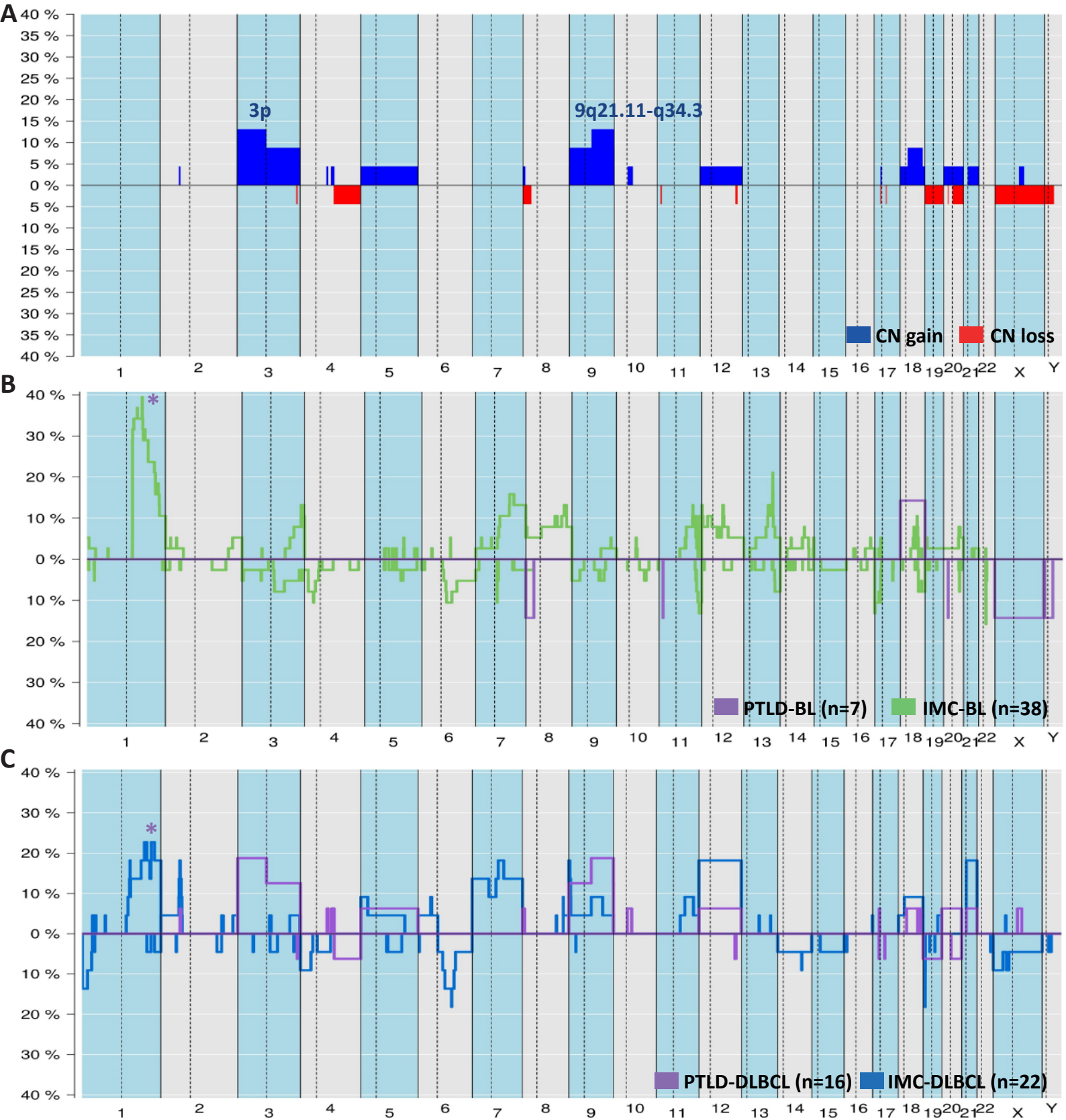
A
3p
9q21.11-q34.3
CN gain
CN loss
B
PTLD-BL (n=7)
IMC-BL (n=38)
C
PTLD-DLBCL (n=16)
IMC-DLBCL (n=22)

Figure 3

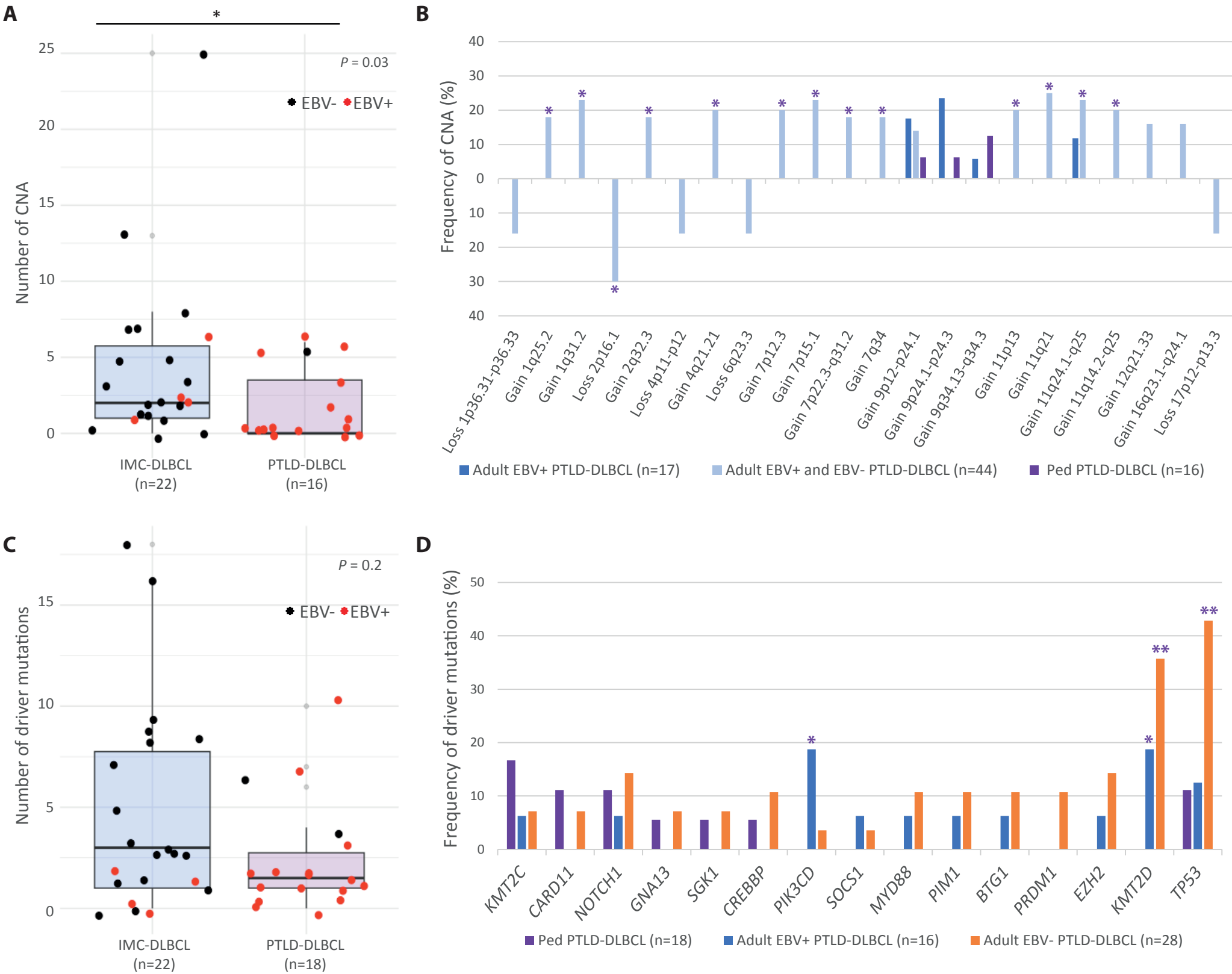
A
*
P = 0.03
EBV- EBV+
Number of CNA
25
20
15
10
5
0
IMC-DLBCL (n=22)
PTLD-DLBCL (n=16)
B
Frequency of CNA (%)
40
30
20
10
0
10
20
30
40
Loss 1p36.31-p36.33
Gain 1q25.2
Gain 1q31.2
Loss 2p16.1
Gain 2q32.3
Loss 4p11-p12
Gain 4q21.21
Loss 6q23.3
Gain 7p12.3
Gain 7p15.1
Gain 7p22.3-q31.2
Gain 7q34
Gain 9p12-p24.1
Gain 9p24.1-p24.3
Gain 9q34.13-q34.3
Gain 11p13
Gain 11q21
Gain 11q24.1-q25
Gain 11q14.2-q25
Gain 12q21.33
Gain 16q23.1-q24.1
Loss 17p12-p13.3
Adult EBV+ PTLD-DLBCL (n=17)
Adult EBV+ and EBV- PTLD-DLBCL (n=44)
Ped PTLD-DLBCL (n=16)
C
P = 0.2
EBV- EBV+
Number of driver mutations
15
10
5
0
IMC-DLBCL (n=22)
PTLD-DLBCL (n=18)
D
Frequency of driver mutations (%)
50
40
30
20
10
0
KMT2C
CARD11
NOTCH1
GNA13
SGK1
CREBBP
PIK3CD
SOCS1
MYD88
PIM1
BTG1
PRDM1
EZH2
KMT2D
TP53
Ped PTLD-DLBCL (n=18)
Adult EBV+ PTLD-DLBCL (n=16)
Adult EBV- PTLD-DLBCL (n=28)

Figure 4

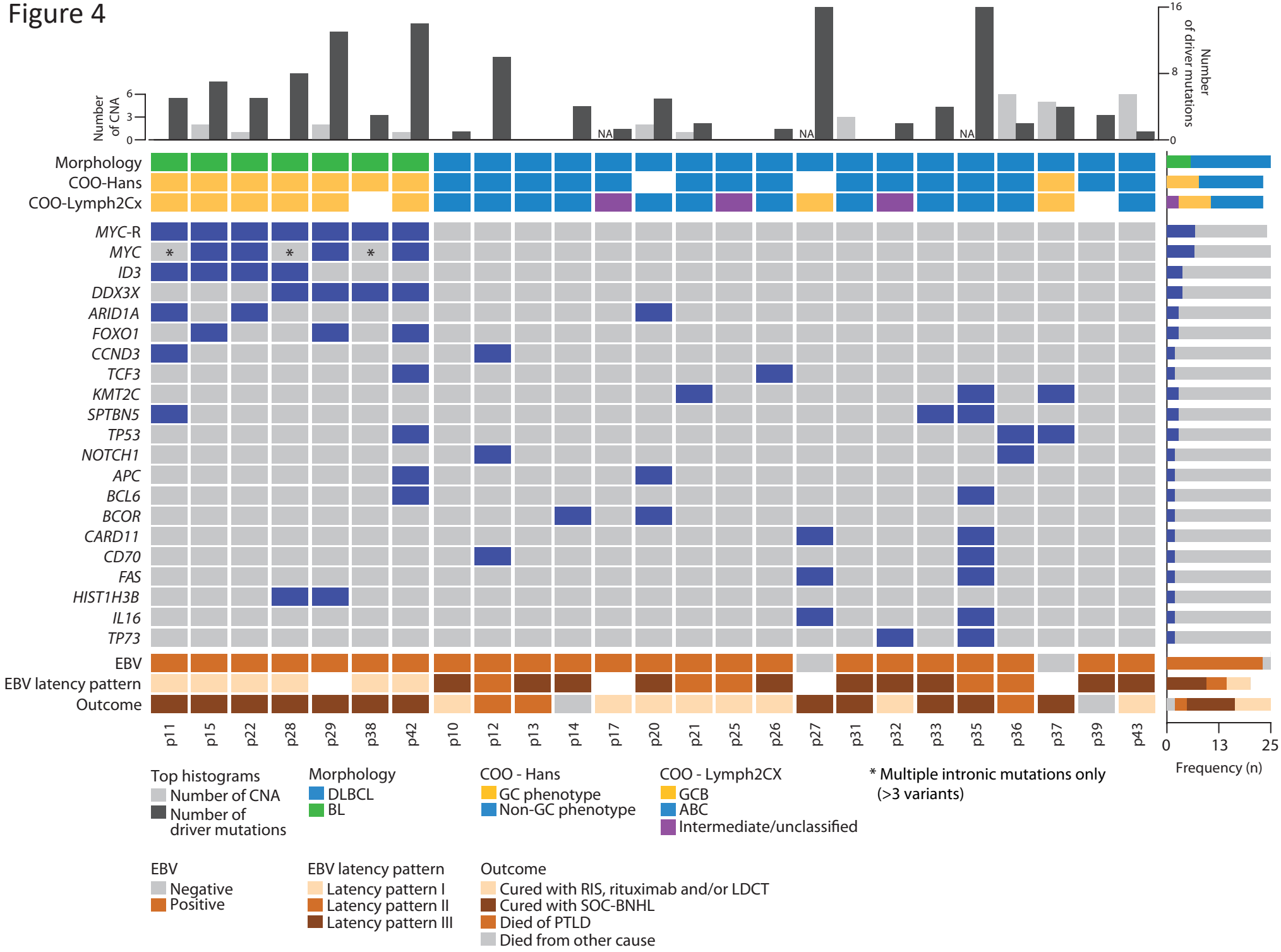
Number of CNA
0
3
6
NA
Number of driver mutations
0
8
16
Morphology
COO-Hans
COO-Lymph2Cx
MYC-R
MYC
ID3
DDX3X
ARID1A
FOXO1
CCND3
TCF3
KMT2C
SPTBN5
TP53
NOTCH1
APC
BCL6
BCOR
CARD11
CD70
FAS
HIST1H3B
IL16
TP73
EBV
EBV latency pattern
Outcome
p11
p15
p22
p28
p29
p38
p42
p10
p12
p13
p14
p17
p20
p21
p25
p26
p27
p31
p32
p33
p35
p36
p37
p39
p43
0
13
25
Frequency (n)
Top histograms
Number of CNA
Number of driver mutations
Morphology
DLBCL
BL
COO - Hans
GC phenotype
Non-GC phenotype
COO - Lymph2CX
GCB
ABC
Intermediate/unclassified
* Multiple intronic mutations only (>3 variants)
EBV
Negative
Positive
EBV latency pattern
Latency pattern I
Latency pattern II
Latency pattern III
Outcome
Cured with RIS, rituximab and/or LDCT
Cured with SOC-BNHL
Died of PTLD
Died from other cause

Figure 5

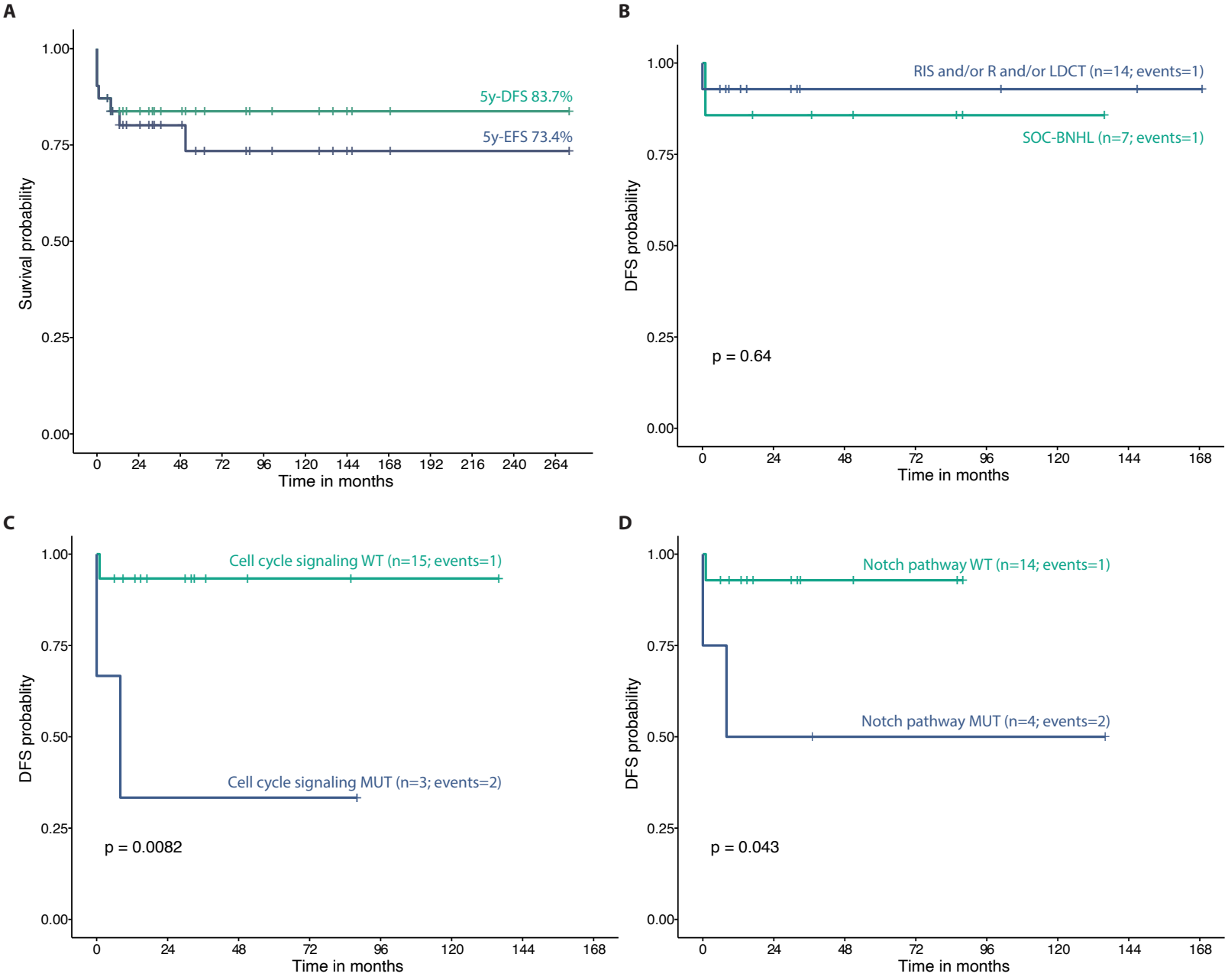
A
Survival probability
1.00
0.75
0.50
0.25
0.00
5y-DFS 83.7%
5y-EFS 73.4%
0
24
48
72
96
120
144
168
192
216
240
264
Time in months
B
DFS probability
RIS and/or R and/or LDCT (n=14; events=1)
SOC-BNHL (n=7; events=1)
p = 0.64
Time in months
C
DFS probablity
Cell cycle signaling WT (n=15; events=1)
Cell cycle signaling MUT (n=3; events=2)
p = 0.0082
Time in months
D
DFS probability
Notch pathway WT (n=14; events=1)
Notch pathway MUT (n=4; events=2)
p = 0.043
Time in months

# Supplemental Material

# Salmeron *et al*

## Supplemental Methods

### EBV latency pattern immunohistochemical evaluation

The latency pattern was assessed using EBNA-2 and LMP-1 antibodies available in our lab (Supplemental Table 2) and established according to the study from Murata T et al, Viruses 2021.[1]

In detail, when EBER was positive, and both EBNA-2 and LMP-1 were negative, the case was considered to show a latency pattern I, whereas when both markers were positive it was regarded as a latency pattern III. A case showing EBNA-2 positivity and LMP-1 negativity was considered a latency phase IIb, conversely, EBNA-2 negativity and LMP-1 positivity phenotype was regarded as a latency pattern IIa.

### COO determination according to Lymph2Cx assay (NanoString, Seattle, WA, USA)

Four hundred nanograms of total RNA from FFPE samples were processed using Gene Expression Lymph2Cx NanoString Assay. First, Probe Mixes A and B and hybridization master mix (including the TagSet) were prepared and split into the 12 tubes containing the samples to analyze. Samples were then incubated in a PCR machine, for 16 hours at 67ºC. In the next morning, on the deck of the NanoString nCounter Prep Station, purified Target/Probe complexes are eluted off and are immobilized in the cartridge for data collection on the nCounter Digital Analyzer. This instrument collects data, yielding hundreds of thousands of target molecule counts, using a microscope objective and a CCD camera. Digital images are processed on the nCounter Digital Analyzer and the barcode counts are tabulated in a comma separated value (CSV) format, which can be downloaded via a memory stick.

### Library preparation SureSelectXT and Targeted sequencing approach

A total of 25 formalin fixed paraffin embedded (FFPE) samples were processed using SureSelectXT (Agilent Technologies, Santa Clara, CA) a custom panel interrogating 167 genes, that was designed according to previous literature in DLBCL and other B-cell

lymphomas in both adult and children population (**Supplemental Table 3**), including those needed to perform *LymphGen* prediction algorithm.[2] A total of 100ng of genomic DNA were sheared using the Covaris S220 focused-ultra sonicator (Covaris, Woburn, MA) to a target peak size of 150–200 bp. Library preparation was performed using SureSelectXT Custom Capture Library baits as described in SureSelectXT Target Enrichment System protocol (Agilent Technologies, Santa Clara, CA). For amplification of the post capture libraries, 10 to 13 cycles were performed depending on the initial sample quality. The libraries were qualified using the Bioanalyzer HS (Agilent Technologies, Santa Clara, CA), quantified with the KAPA Library Quantification Kit (Kapa Biosystems, Wilmington, Massachusetts) and sequenced in a MiSeq instrument (Illumina, San Diego, CA) in a paired-end run of 150 bp. The average sequencing coverage of the across regions was 2554x (range 255-7421x) and over 84% of the targeted regions were covered by at least 100x.

FASTQ files were generated by MiSeq control software and quality control of the raw data was performed using the FastQC tool (https://www.bioinformatics.babraham.ac.uk/projects/fastqc/). Sequencing reads were subsequently aligned to the human reference genome (GRCh37/hg19) using the Burrows-Wheeler Aligner–MEM algorithm.[3] Variant calling was performed using two different variant callers, Somatic Variant Caller (Illumina, San Diego, CA) and Mutect2 (Genome Analysis Toolkit (GATK), version 4.0.3)[4] and variants were annotated using the VariantStudio software v3.0 and ANNOVAR, respectively.[5] For Somatic Variant Caller (Illumina, San Diego, CA), default settings were used to analyze sequencing results and to call the variants. Low quality or low coverage calls (total depth <20) were excluded. For Mutect2 variants, low quality variants were also excluded using FilterMutectCalls (GATK) with default thresholds. Only variants identified by both algorithms were considered. We excluded variants affecting non-interrogated regions and known polymorphisms described in the GnomAD, 1000 Genomes and/or ExAC03 database (latest version included in ANNOVAR) with more than 0.1% frequency in normal population. In order to exclude

artifacts, each variant was also inspected with the Integrative Genomics Viewer (IGV, Broad Institute, version 2.3) software (**Supplemental Figure 2**). Variants detected in *BRCA2* were specifically consulted in ClinVar database (https://www.ncbi.nlm.nih.gov/clinvar/), which reports relationships between human variations and phenotypes, regarding their clinical significance and they were excluded after confirmation of their benign effect. Variant detected in case p27 was additionally detected in DNA extracted from blood sample (data not shown).

**Driver prediction by mutation effect**

Since no germline DNA was available and in order to select somatic variants, potential driver mutations were predicted according to previously published criteria[6] in which the 90% of the mutations classified as functional were demonstrated to be somatic. Inclusion criteria were: 1) variants described previously as somatic or functional on previous reports or COSMIC, 2) all truncating variants (nonsense, frameshift, splice donor or acceptor mutations; and 3) the remaining missense variants that were predicted to be functionally deleterious using Mutation Assessor[7] or SIFT predictor if a score was not provided by Mutation Assessor.[8] Other functional predictors as Polyphen-2 (Polymorphism Phenotyping-2)[9], CADD (Combined Annotation Dependent Depletion)[10] and CHASM-3.1[11] were also applied. In detail, there were 96 non-synonymous missense driver SNVs, 12 frameshift indels, 3 in-frame deletions, 3 splicing variants and 9 nonsense mutations.

**Copy number analysis**

DNAs from 23 samples were hybridized on an OncoScan array (ThermoFisher Scientific inc.). Gains and losses and copy number neutral-loss of heterozygosity (CNN-LOH) regions were evaluated and visually inspected using Nexus Biodiscovery version 9.0 software (Biodiscovery, Hawthorne, CA). Human reference genome was GRCh37/hg19. The copy number alterations (CNAs) with minimum size of 100 kb and CNN-LOH larger than 5 Mb

were considered informative. Published CN data from pediatric IMC-BL[12] and IMC-DLBCL,[13] adult PTLD-DLBCL[14,15] were used for comparison.

## Supplemental Figures

**Supplemental Figure 1**. **Cases p28 and p29 showing an intermediate morphology between DLBCL and a BL, with *MYC* gene rearrangement. (A)** Case p28 shows a quite monotonous proliferation of medium-sized lymphocytes, with a round-oval irregular nucleus, finely clumped chromatin in most of them, some demonstrating a small nucleoli, abundant mitosis figures and intermingled scattered body tangible macrophages (H&E, original magnification at 400x). **(B)** FISH with IGK::*MYC* dual fusion probe demonstrates the presence of fusion signals, consistent with the t(2;8) translocation. **(C)** Case p29 demonstrates a rather monotonous proliferation of medium-sized lymphocytes, with round irregular nucleus and finely clumped chromatin with conspicuous nucleoli. **(D)** FISH with *MYC* break-apart probe exhibits split signals, in accordance to the presence of the *MYC* gene rearrangement.

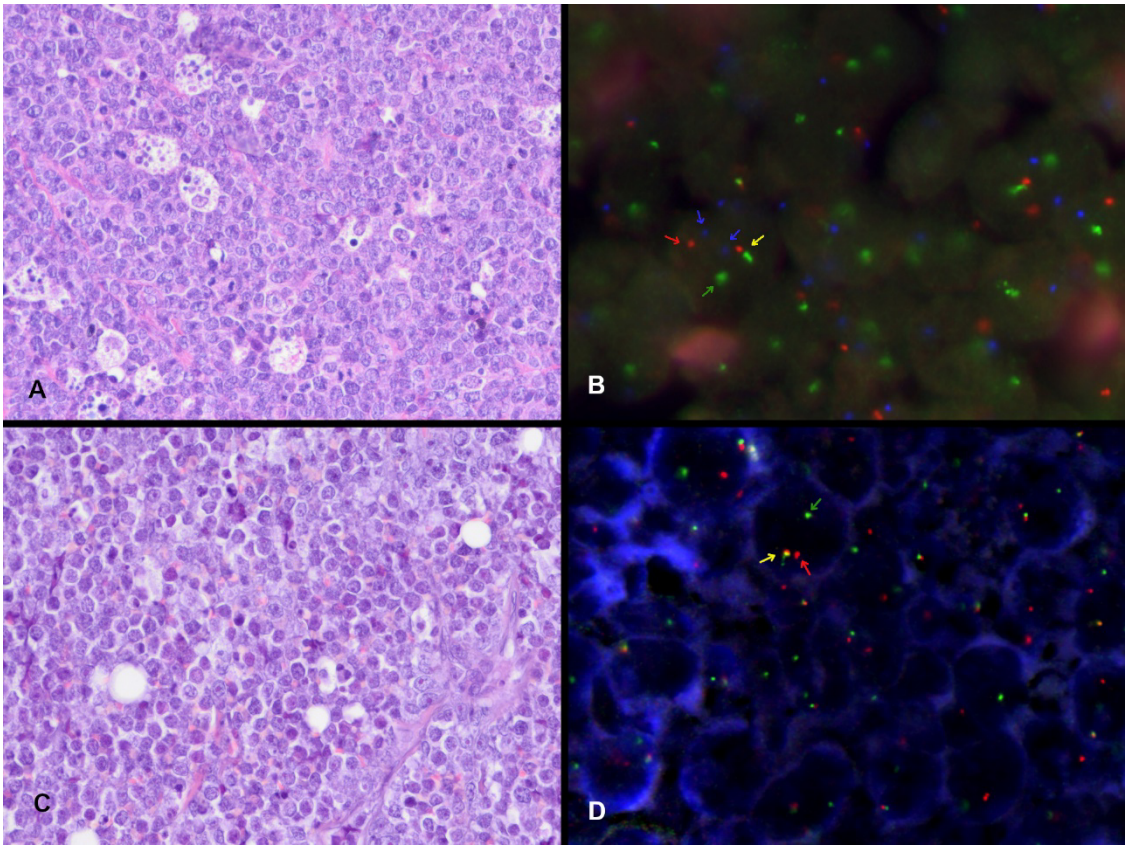

**Supplemental Figure 2. Histopathological features of case p38. (A)** H&E staining (original magnification 40x), showing DLBCL morphology. **(B)** CD20 staining (original magnification 10x). **(C)** CD10 expression (original magnification 20x). **(D)** EBV *in situ* hybridization showing positivity in virtually all tumor cells (original magnification 20x). **(E)** Negative LMP1 immunostaining (original magnification 20x). **(F)** Negative EBNA2 immunostaining (original magnification 20x); **(G)** KI-67 immunostaining (original magnification 20x). **(H)** FISH with *MYC* break-apart probe, showing split signals demonstrating the rearrangement (original magnification 100x). **(I)** FISH with IGH::*MYC* dual color dual fusion probe, showing fusion signals demonstrating the t(8;14) rearrangement (original magnification 100x).

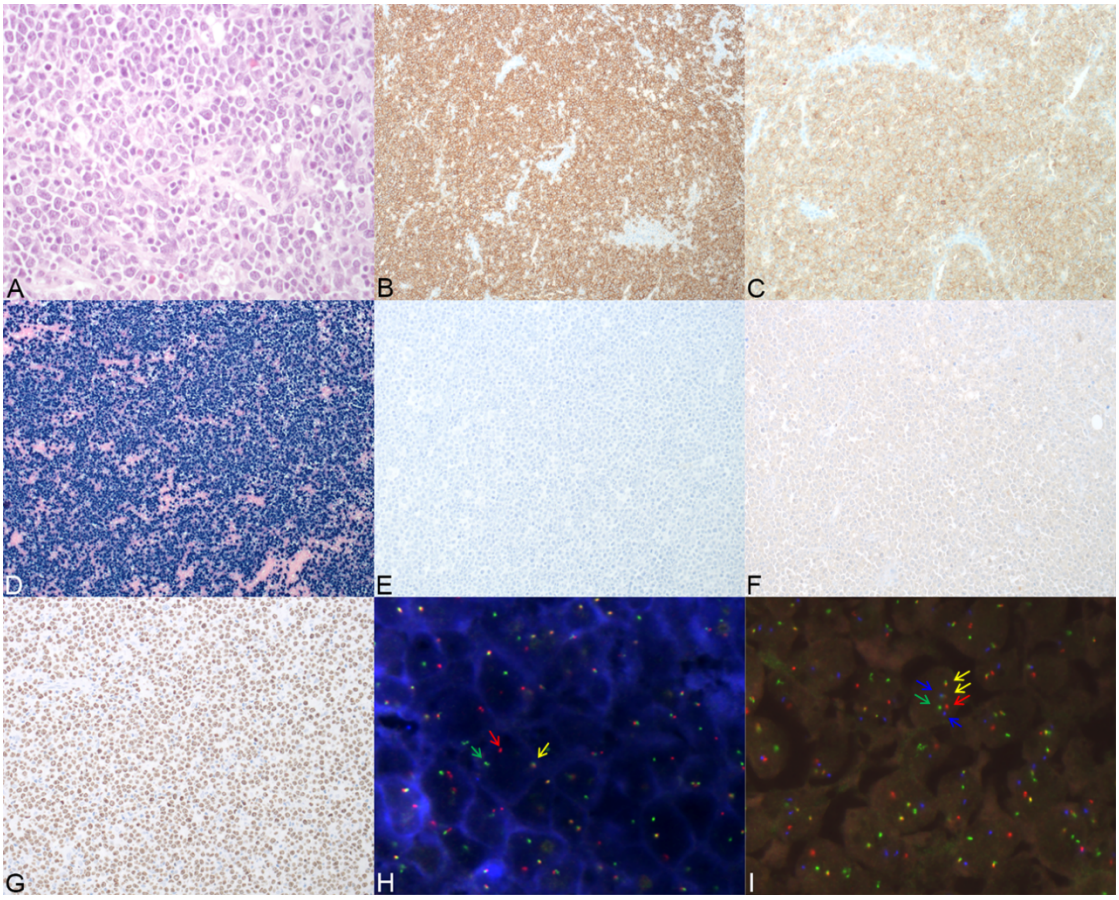

**Supplemental Figure 3**. **Results from FISH analysis performed on 31 post-SOT mPTLD** to investigate the status of *MYC*, *PAX5*, *IRF4*, *IGH*, *BCL2* and *BCL6* loci as well as 11q region. # Marks case p27, with IGH-FR3 was polyclonal, but no further analyses of IGH-FR1 and IGH-FR2 could be performed due to DNA quality.

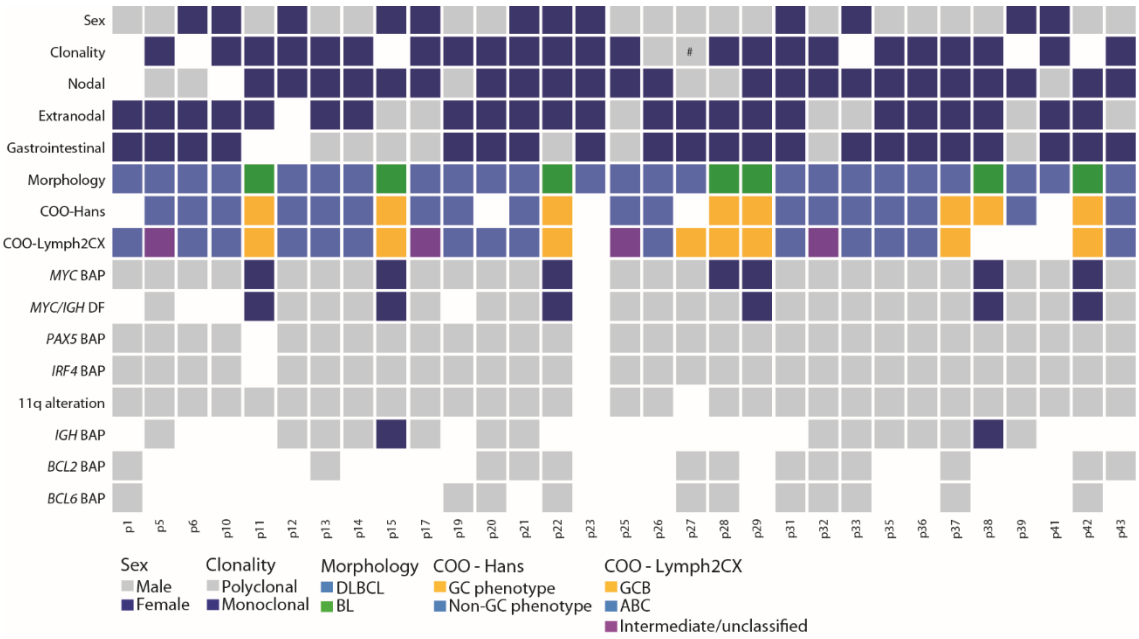

**Supplemental Figure 4. (A) Comparison of mutational profile** between pediatric PTLD-BL and previously published BL series, stratified according to EBV status.[16–18] To perform statistical analysis using comparable data, only exonic *MYC* mutations in PTLD-BL were considered. **(B) Genetic landscape of seven PTLD-BL** representing mutations and CNA frequently associated to previously defined genetic subgroups.[19]

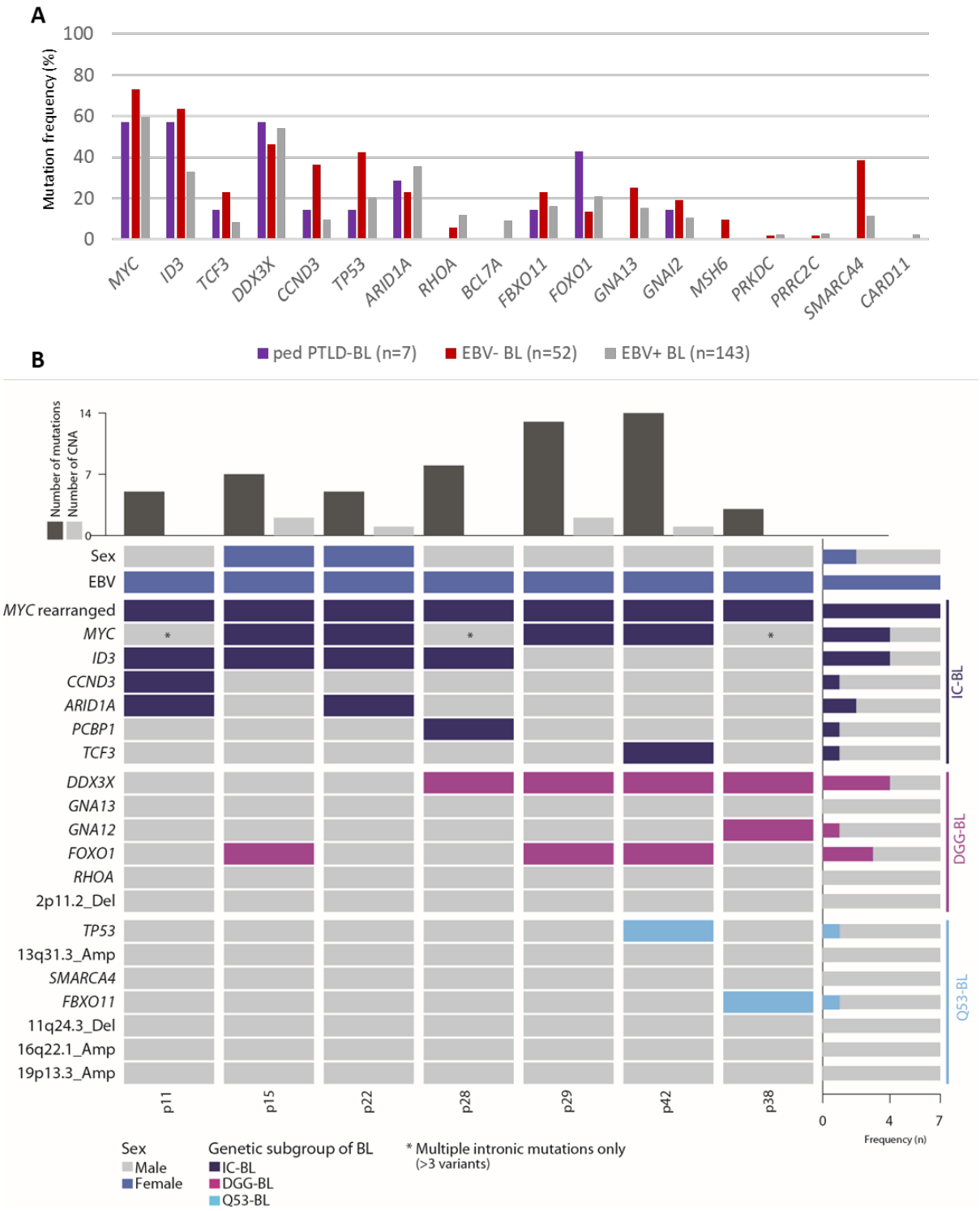

**Supplemental Figure 5**. **Pathway enrichment analysis** on PTLD-DLBCL and comparison with pediatric IMC-DLBCL.[13] The horizontal axis represents frequency of pathway alteration (%) and each pathway is represented in the vertical axis. Asterisks mark significant differences between the two groups, according to Fisher's exact test P < 0.1.

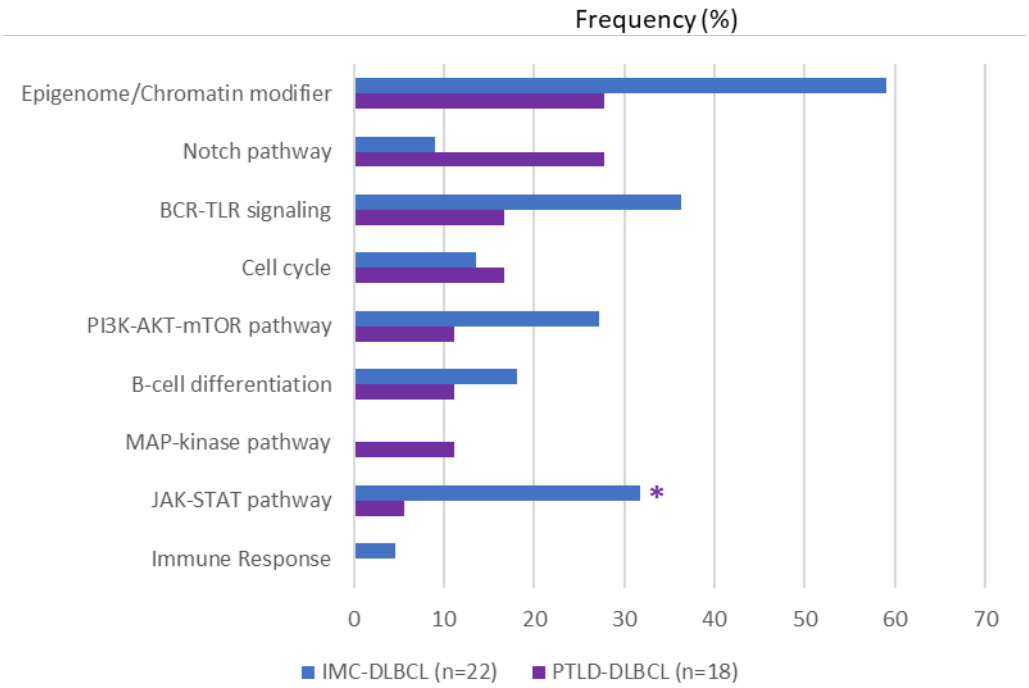

**Supplemental Figure 6. Disease-free survival (DFS) probability of post-SOT mPTLD stratified according to EBV latency pattern and replication information.**

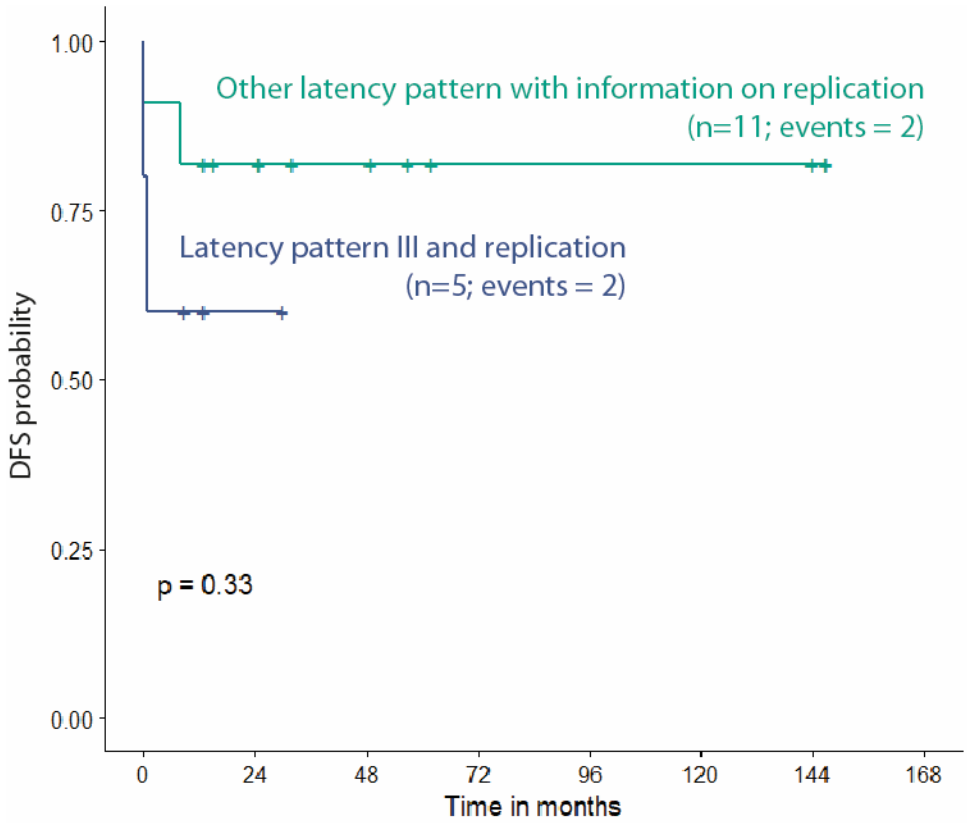

## References


1. Murata T, Sugimoto A, Inagaki T, et al. Molecular Basis of Epstein-Barr Virus Latency Establishment and Lytic Reactivation. *Viruses*. 2021;13(12):2344.

2. Wright GW, Huang DW, Phelan JD, et al. A Probabilistic Classification Tool for Genetic Subtypes of Diffuse Large B Cell Lymphoma with Therapeutic Implications. *Cancer Cell*. 2020;37(4):551-568.e14.

3. Li H, Durbin R. Fast and accurate short read alignment with Burrows-Wheeler transform. *Bioinformatics*. 2009;25(14):1754–1760.

4. McKenna A, Hanna M, Banks E, et al. The genome analysis toolkit: A MapReduce framework for analyzing next-generation DNA sequencing data. *Genome Res.* 2010;20(9):1297–1303.

5. Wang K, Li M, Hakonarson H. ANNOVAR: Functional annotation of genetic variants from high-throughput sequencing data. *Nucleic Acids Res.* 2010;38(16):e164–e164.

6. Karube K, Enjuanes A, Dlouhy I, et al. Integrating genomic alterations in diffuse large B-cell lymphoma identifies new relevant pathways and potential therapeutic targets. *Leukemia*. 2018;32(3):675–684.

7. Reva B, Antipin Y, Sander C. Predicting the functional impact of protein mutations: Application to cancer genomics. *Nucleic Acids Res.* 2011;39(17):e118.

8. Kumar P, Henikoff S, Ng PC. Predicting the effects of coding non-synonymous variants on protein function using the SIFT algorithm. *Nat. Protoc.* 2009;4(7):1073–1082.

9. Adzhubei IA, Schmidt S, Peshkin L, et al. A method and server for predicting damaging missense mutations. *Nat. Methods*. 2010;7(4):248–249.

10. Kircher M, Witten DM, Jain P, et al. A general framework for estimating the relative pathogenicity of human genetic variants. *Nat. Genet.* 2014;46(3):310–315.

11. Carter H, Chen S, Isik L, et al. Cancer-Specific High-Throughput Annotation of Somatic Mutations: Computational Prediction of Driver Missense Mutations. *Cancer Res*. 2009;69(16):6660–6667.

12. Scholtysik R, Kreuz M, Klapper W, et al. Detection of genomic aberrations in molecularly defined burkitt's lymphoma by array-based, high resolution, single nucleotide polymorphism analysis. *Haematologica*. 2010;95(12):2047–2055.

13. Ramis-Zaldivar JE, Gonzalez-Farré B, Balagué O, et al. Distinct molecular profile of IRF4-rearranged large B-cell lymphoma. *Blood*. 2020;135(4):274–286.

14. Rinaldi A, Capello D, Scandurra M, et al. Single nucleotide polymorphism-arrays provide new insights in the pathogenesis of post-transplant diffuse large B-cell lymphoma. *Br. J. Haematol.* 2010;149(4):569–577.

15. Finalet Ferreiro J, Morscio J, Dierickx D, et al. EBV-Positive and EBV-Negative Posttransplant Diffuse Large B Cell Lymphomas Have Distinct Genomic and Transcriptomic Features. *Am. J. Transplant.* 2016;16(2):414–425.

16. Abate F, Raffaella Ambrosio M, Mundo L, et al. Distinct Viral and Mutational Spectrum of Endemic Burkitt Lymphoma. *PLOS Pathog.* 2015;11(10):e1005158.

17. Kaymaz Y, Oduor CI, Yu H, et al. Comprehensive Transcriptome and Mutational Profiling of Endemic Burkitt Lymphoma Reveals EBV Type-Specific Differences. *Mol. cancer Res.* 2017;15(5):563–576.

18. Grande BM, Gerhard DS, Jiang A, et al. Genome-wide discovery of somatic coding and noncoding mutations in pediatric endemic and sporadic Burkitt lymphoma. *Blood*. 2019;133(12):1313–1324.

19. Thomas N, Dreval K, Gerhard DS, et al. Genetic Subgroups Inform on Pathobiology in Adult and Pediatric Burkitt Lymphoma. *Blood*. 2023;141(8):904–916.

20. Hans CP, Weisenburger DD, Greiner TC, et al. Confirmation of the molecular classification of diffuse large B-cell lymphoma by immunohistochemistry using a tissue microarray. *Neoplasia*. 2004;103(2):275–282.

21. Johnson NA, Slack GW, Savage KJ, et al. Concurrent expression of MYC and BCL2 in diffuse large B-cell lymphoma treated with rituximab plus cyclophosphamide, doxorubicin, vincristine, and prednisone. *J. Clin. Oncol.* 2012;30(28):3452–3459.

22. Ramburan A, Kriel R, Govender D. Plasmablastic lymphomas show restricted EBV latency profile and MYC gene aberrations. *Leuk. Lymphoma*. 2021;63(2):370–376.

23. Menter T, Juskevicius D, Alikian M, et al. Mutational landscape of B-cell post-transplant lymphoproliferative disorders. *Br. J. Haematol.* 2017;178(1):48–56.

24. Butzmann A, Sridhar K, Jangam D, et al. Mutations in JAK/STAT and NOTCH1 Genes Are Enriched in Post-Transplant Lymphoproliferative Disorders. *Front. Oncol.* 2022;11:790481.

**Supplemental Table 1.** Clinical features of 31 pediatric post-SOT mPTLD detailed per case

| Case | Age at DX (years), gender | Morphological diagnosis | Allograft | TX-PTLD (months) | EBV in blood | LDH high | Extranodal | BM/CNS | Stage* | RIS | Rituximab | Chemotherapy |
|---|---|---|---|---|---|---|---|---|---|---|---|---|
| p1 | 2, M | PTLD-DLBCL | Kidney | 10 | Pos | Yes | Yes | NA | NA | NA | NA | NA |
| p5 | 2, M | PTLD-DLBCL | Liver | 6 | Pos | NA | Yes | No | III | Yes | Yes | No |
| p6 | 2, F | PTLD-DLBCL | Liver | 8 | Pos | No | Yes | No | III | Yes | Yes | No |
| p10 | 5, F | PTLD-DLBCL | Kidney | 18 | Pos | yes | Yes | No | III | NA | Yes | No |
| p11 | 16, M | PTLD-BL | Heart | 88 | Pos | Yes | Yes | Both | IV | Yes | Yes | SOC-BNHL[1] |
| p12 | 9, F | PTLD-DLBCL | Liver | 73 | Neg | NA | NA | NA | NA | NA | NA | NA |
| p13 | 4, M | PTLD-DLBCL | Heart | 5 | Pos | No | Yes | No | III | Yes | Yes | SOC-BNHL[1] |
| p14 | 3, M | PTLD-DLBCL | Intestine | 2 | Pos | No | Yes | NA | NA | Yes | Yes | No |
| p15 | 15, F | PTLD-BL | Liver | 170 | Neg | No | No | No | I | Yes | Yes | SOC-BNHL[2] |
| p17 | 12, F | PTLD-DLBCL | Kidney | 7 | Pos | Yes | No | No | III | Yes | Yes | No |
| p19 | 4, F | PTLD-DLBCL | Liver | 16 | Pos | No | Yes | No | II | Yes | Yes | LDCT |
| p20 | 4, M | PTLD-DLBCL | Kidney | 10 | Pos | No | Yes | No | III | Yes | Yes | LDCT |
| p21 | 6, F | PTLD-DLBCL | Liver | 10 | Pos | NA | Yes | NA | NA | Yes | No | No |
| p22 | 6, F | PTLD-BL | Liver | 35 | Pos | No | Yes | BM | IV | Yes | Yes | SOC-BNHL[1] |
| p23 | 14, F | PTLD-DLBCL | Lung | 8 | Pos | Yes | Yes | NA | NA | Yes | Yes | LDCT |
| p25 | 17, M | PTLD-DLBCL | Kidney | 6 | Pos | No | No | No | III | Yes | Yes | No |
| p26 | 3, M | PTLD-DLBCL | Kidney | 9 | Pos | Yes | Yes | No | III | No | Yes | No |
| p27 | 12, M | PTLD-DLBCL | Heart | 141 | Neg | No | Yes | No | II | Yes | No | SOC-BNHL[1] |
| p28 | 14, M | PTLD-BL | Heart | 73 | Pos | No | Yes | No | III | Yes | No | SOC-BNHL[2] |
| p29 | 13, M | PTLD-BL | Heart | 88 | Pos | Yes | Yes | BM | IV | Yes | No | SOC-BNHL[2] |
| p31 | 9, F | PTLD-DLBCL | Heart | 16 | Pos | No | Yes | No | III | Yes | No | SOC-BNHL[1] |
| p32 | 4, M | PTLD-DLBCL | Kidney | 6 | Pos | No | No | No | I | Yes | No | No |
| p33 | 6, F | PTLD-DLBCL | Intestine | 2 | NA | NA | Yes | No | II | Yes | Yes | SOC-BNHL |
| p35 | 14, M | PTLD-DLBCL | Kidney | 54 | Neg | No | Yes | No | III | Yes | No | SOC-BNHL[4] |
| p36 | 7, M | PTLD-DLBCL | Heart | 90 | NA | NA | Yes | No | III | NA | NA | NA |
| p37 | 13, M | PTLD-DLBCL | Liver and kidney | 53 | NA | No | Yes | No | III | Yes | Yes | SOC-BNHL[1] |
| p38 | 5, M | PTLD-BL | Liver | 32 | NA | NA | Yes | No | III | Yes | No | SOC-BNHL[5] |
| p39 | 17, F | PTLD-DLBCL | Heart | 4 | Pos | No | No | BM | IV | Yes | Yes | SOC-BNHL[1] |
| p41 | 8, F | PTLD-DLBCL | Liver | 14 | Pos | No | Yes | No | III | Yes | Yes | LDCT |
| p42 | 13, M | PTLD-BL | Kidney | 35 | Pos | Yes | Yes | BM | IV | Yes | Yes | SOC-BNHL[1] |
| p43 | 12, M | PTLD-DLBCL | Kidney | 8 | Pos | No | No | No | III | Yes | Yes | LDCT |

M, male; F, female; DX, diagnosis; PTLD, post-transplant lymphoproliferative disorder; TX-PTLD, months from transplant to PTLD; EBV, Epstein-Barr Virus; Pos, positive; Neg, negative; LDH, lactate dehydrogenase; BM, bone marrow immunosuppression; LDCT, low dose chemotherapy; SOC-BNHL, standard of care for mature B-cell non-Hodgkin lymphomas; CR, complete remission; PD, progressive disease; F-PTLD: fulminant PTLD; NA: not assessable. The LDH the reference laboratory of each hospital.

*Stage was established according Murphy or International pediatric NHL staging system (IPNHLSS)

†Patient p7 received COP followed by dexamethasone and bortezomib administration; Patient p24 received COP and GEM/STEROID/CYS/ICE
SOC-BNHL: 1, Inter-B-NHL-2010; 2, Inter-B-NHL 2004; 3, SIOP-98; 4, SIOP-94
Cellular therapy: a, specific T cells against EBV; b, memory T cells

| Antiviral | Other treatment strategy | Outcome, Follow-up (months) | Cause of death |
|---|---|---|---|
| NA | NA | PD, 0 | F-PTLD |
| Pharmacologic therapy | Surgery | CR, 169 | |
| Pharmacologic therapy | | CR, 101 | |
| No | | CR, 30 | |
| Pharmacologic therapy | | CR, 25 | |
| NA | NA | PD, 8 | PD |
| Pharmacologic therapy | | CR, 1 | Toxicity |
| Pharmacologic therapy | | CR, 13 | Transplant related |
| No | | CR, 49 | |
| No | | CR, 13 | |
| Pharmacologic therapy | | CR, 147 | |
| No | | CR, 13 | |
| Pharmacologic therapy | | CR, 15 | |
| Pharmacologic therapy | Surgery | CR, 62 | |
| Pharmacologic therapy | | PD, 0 | F-PTLD |
| Pharmacologic therapy | | CR, 32 | |
| Pharmacologic therapy | | CR, 33 | |
| No | | CR, 37 | |
| No | | CR, 144 | |
| No | Surgery | CR, 128 | |
| No | Surgery | CR, 17 | |
| No | Surgery | CR, 4 | |
| Pharmacologic therapy | Surgery | CR, 86 | |
| Pharmacologic therapy | | CR, 136 | |
| NA | | PD, 0 | F-PTLD |
| No | | CR, 88 | |
| Pharmacologic therapy | Surgery | CR, 271 | |
| Pharmacologic therapy | Surgery | CR, 51 | Other |
| No | | CR, 8 | |
| No | | CR, 57 | |
| No | | CR, 6 | |

r; CNS, central nervous system; RIS, reduction of
H high levels were defined as above twice the normal value of

**Supplemental Table 2.** Details of all antibodies used for immunohistochemical characterization, including source and conditions of use.

| Antibody | Clone | Source | Antigen retrieval/visualization | Dilution |
|---|---|---|---|---|
| **CD20** | L26 | DAKO, (Copenhagen, Denmark) | EDTA 1 mM pH 9/ ENVISION FLEX (DAKO) | RTU |
| **CD79a** | JCB 117 | DAKO | EDTA 1 mM pH 9/ ENVISION FLEX (DAKO) | RTU |
| **PAX-5** | SP34 | Roche | CC1 solution / ultraView Universal DAB Detection Kit. Automated immunostainer (Benchmark XT; Ventana) | RTU |
| **CD3** | Polyclonal | DAKO | EDTA 1 mM pH 9/ ENVISION FLEX (DAKO) | RTU |
| **CD5** | 4C7 | DAKO | EDTA 1 mM pH 9/ ENVISION FLEX (DAKO) | RTU |
| **CD10** | 56C6 | DAKO | EDTA 1 mM pH 9/ ENVISION FLEX (DAKO) | RTU |
| **BCL6** | PG-B6p | DAKO | EDTA 1 mM pH 9/ ENVISION FLEX (DAKO) | RTU |
| **BCL2** | 124 | DAKO | EDTA 1 mM pH 9/ ENVISION FLEX (DAKO) | RTU |
| **Ki67** | Mib-1 | DAKO | Citrate 10 mM pH 6/ ENVISION FLEX (DAKO | RTU |
| **MUM1** | MRQ-43 | Ventana, Roche (Oro Walley, AR, USA) | CC1 solution / ultraView Universal DAB Detection Kit. Automated immunostainer (Benchmark XT; Ventana) | RTU |
| **MYC** | Y69 | Ventana, Roche | CC1 solution / ultraView Universal DAB Detection Kit. Automated immunostainer (Benchmark XT; Ventana) | RTU |
| **CD21** | EP3093 | Ventana, Roche | CC1 solution / ultraView Universal DAB Detection Kit. Automated immunostainer (Benchmark XT; Ventana) | RTU |
| **EBNA-2** | PE2 | Abcam | CC1 solution / ultraView Universal DAB Detection Kit. Automated immunostainer (Benchmark XT; Ventana) | 0.09375 |
| **LMP-1** | CS1-4 | Roche | CC1 solution / ultraView Universal DAB Detection Kit. Automated immunostainer (Benchmark XT; Ventana) | RTU |
| **ZEBRA** | | Argene | CC1 solution / ultraView Universal DAB Detection Kit. Automated immunostainer (Benchmark XT; Ventana) | 1:100 |

RTU, ready to use.

According to previous reports, MYC, BCL2,[21] BCL6 and MUM1[22] were considered positive when ≥40%, ≥50%, ≥30% or ≥30% of the cells were positive, respectively. Staining for EBNA-2 or LMP-1 were assessed as positive when any neoplastic cell showed nuclear or cytoplasmic/membranous positivity, respectively.[22]

**Supplemental Table 3.** One-hundred sixty-seven genes included in the SureSelectXT custom panel used for the NGS analysis of pediatric post-SOT mPTLD cases and pathway in which they are involved.

| Gene | Transcript | Position (GRCh37/hg19) | Exons | Pathway |
|---|---|---|---|---|
| *ABCA7* | NM_019112.3 | chr19:1041361-1065424 | All CDS E2-47 | |
| *ACTB* | NM_001101.3 | chr7:5567379-5569288 | All CDS E2-6 | |
| *APC* | NM_000038.5 | chr5:112090588-112179823 | All CDS E2-16 | |
| *ARID1A* | NM_006015.4 | chr1:27022895-27107247 | All CDS E1-20 | Epigenome/Chromatin modifier |
| *ATM* | NM_000051.3 | chr11:108098352-108236235 | All CDS E2-63 | |
| *B2M* | NM_004048.2 | chr15:45003745--45008540 | All CDS E1-3 | Immune Response |
| *BCL10* | NM_003921.4 | chr1:85733310-85742035 | All CDS E1-3 | BCR-TLR signaling pathway |
| *BCL2* | NM_000633.2 | chr18:60795858-60985899 | All CDS E1-2 | |
| *BCL6* | NM_001706.4 | chr3:187440245-187451481 | All CDS E3-10 | B-cell differentiation |
| *BCL7A* | NM_020993.4 | chr12:122459997-122497069 | All CDS E1-6 | |
| *BLM* | NM_000057.2 | chr15:91290623-91358509 | All CDS E2-22 | |
| *BRAF* | NM_004333.4 | chr7:140453075-140481493 | E11-15 | MAP-kinase pathway |
| *BRCA2* | NM_000059.3 | chr13:32890598-32972907 | All CDS E2-27 | |
| *BTG1* | NM_001731.2 | chr12:92537856-92539311 | All CDS E1-2 | |
| *BTG2* | NM_006763.2 | chr1:203274735-203276566 | All CDS E1-2 | |
| *BTK* | NM_000061.2 | chrX:100604873-100630272 | All CDS E2-19 | BCR-TLR signaling pathway |
| *CARD11* | NM_032415.4 | chr7:2946272-2998140 | All CDS E2-25 | BCR-TLR signaling pathway |
| *CCND1* | NM_053056 | chr11:69456082-69466050 | All CDS E1-5 | Cell cycle |
| *CCND3* | NM_001760.3 | chr6:41903678-41909387 | All CDS E1-5 | Cell cycle |
| *CD58* | NM_001779.2 | chr1:117057435-117113594 | All CDS E1-6 | Immune Response |
| *CD70* | NM_001252.3 | chr19:6586031-6591013 | All CDS E1-3 | |
| *CD79A* | NM_001783.3 | chr19:42381375-42385047 | All CDS E1-5 | BCR-TLR signaling pathway |
| *CD79B* | NM_001039933.2 | chr17:62006585-62009621 | All CDS E1-6 | BCR-TLR signaling pathway |
| *CIITA* | NM_000246.3 | chr16:10971188-11017160 | All CDS E1-19 | Immune Response |
| *CREBBP* | NM_004380.2 | chr16:3777719-3929917 | All CDS E1-31 | Epigenome/Chromatin modifier |
| *DDX3X* | NM_001356.3 | chrX:41193506-41206972 | All CDS E1-17 | |
| *DIS3* | NM_014953.3 | chr13:73333933-73355970 | All CDS E1-21 | |
| *EGR1* | NM_001964.2 | chr5:137801451-137803770 | All CDS E1-2 | |
| *EP300* | NM_001429.3 | chr22:41489009-41574960 | All CDS E1-31 | Epigenome/Chromatin modifier |
| *ETS1* | NM_001143820.1 | chr11:128332256-128443025 | All CDS E2-10 | MAP-kinase pathway |

| | | | | |
|---|---|---|---|---|
| *ETV6* | NM_001987.4 | chr12:11803062-12043980 | All CDS E1-8 | |
| *EZH2* | NM_004456.4 | chr7:148504738-148508812 | E16-20 | Epigenome/Chromatin modifier |
| *FAM46C* | NM_017709.3 | chr1:118165491-118166666 | All CDS E2 | |
| *FBXW7* | NM_033632.3 | chr4:153244033-153332955 | All CDS E2-12 | Notch pathway |
| *FOXO1* | NM_002015.3 | chr13:41133660-41240349 | All CDS E1-2 | |
| *GNA13* | NM_006572.4 | chr17:63010375-63052711 | All CDS E1-4 | PI3K-AKT-mTOR pathway |
| *HDAC7* | NM_015401.3 | chr12:48177624-48213568 | All CDS E1-26 | |
| *HIST1H1D* | NM_005320.2 | chr6:26234496-26235161 | All CDS E1 | Epigenome/Chromatin modifier |
| *HIST1H1E* | NM_005321.2 | chr6:26156619-26157278 | All CDS E1 | Epigenome/Chromatin modifier |
| *HIST1H2BC* | NM_003526.2 | chr6:26123752-26124132 | All CDS E1 | Epigenome/Chromatin modifier |
| *HIST1H3B* | NM_003537.3 | chr6:26031878-26032288 | All CDS E1 | Epigenome/Chromatin modifier |
| *ID3* | NM_002167.4 | chr1:23885451-23885917 | All CDS E1-2 | PI3K-AKT-mTOR pathway |
| *IRF4* | NM_002460.3 | chr6:393153-407598 | All CDS E2-9 | B-cell differentiation |
| *IRF8* | NM_002163.2 | chr16:85936622-85954888 | All CDS E2-9 | B-cell differentiation |
| *KLHL6* | NM_130446.2 | chr3:183209715-183273441 | All CDS E1-7 | |
| *KMT2D* | NM_003482.3 | chr12:49415563-49449107 | All CDS E1-54 | Epigenome/Chromatin modifier |
| *KMT2C* | NM_170606 | chr7:151833918-152132871 | All CDS E1-59 | Epigenome/Chromatin modifier |
| *KRAS* | NM_033360.2 | chr12:25368375-25398318 | All CDS E2-5 | MAP-kinase pathway |
| *MAP2K1* | NM_002755.3 | chr15:66679686-66782953 | All CDS E1-11 | MAP-kinase pathway |
| *MAPK1* | NM_002745.4 | chr22:22123493-22221730 | All CDS E1-8 | MAP-kinase pathway |
| *MEF2B* | NM_001145785.1 | chr19:19256606-19261544 | All CDS E2-9 | Epigenome/Chromatin modifier |
| *MYC* | NM_002467.4 | chr8:128748840-128753674 | All CDS E1-3 + intron1 | Cell cycle |
| *MYD88* | NM_002468.4 | chr3:38180153-38182777 | All CDS E1-5 | BCR-TLR signaling pathway |
| *MYOM2* | NM_003970.2 | chr8:1998881-2092905 | All CDS E2-37 | |
| *NFKB1* | NM_003998.3 | chr4:103446676-103537751 | All CDS E2-24 | BCR-TLR signaling pathway |
| *NFKBIE* | NM_004556.2 | chr6:44226956-44233500 | All CDS E1-6 | BCR-TLR signaling pathway |
| *NOTCH1* | NM_017617.3 | chr9:139390023-139399556 | E26-27, 34 + 3'UTR | Notch pathway |
| *NOTCH2* | NM_024408.3 | chr1:120457929-120459317 | E34 | Notch pathway |
| *NRAS* | NM_002524.4 | chr1:115251156-115258781 | All CDS E2-5 | MAP-kinase pathway |
| *PCBP1* | NM_006196 | chr2:70314876-70315946 | All CDS E1 | |
| *PDGFRA* | NM_006206.4 | chr4:55124936-55161439 | All CDS E2-23 | |
| *PIK3CD* | NM_005026.3 | chr1:9770513-9787104 | All CDS E3-24 | PI3K-AKT-mTOR pathway |
| *PIK3R1* | NM_181523.2 | chr5:67522504-67593429 | All CDS E2-16 | PI3K-AKT-mTOR pathway |

| | | | | |
|---|---|---|---|---|
| *PIM1* | NM_001243186.1 | chr6:37138079-37141867 | All CDS E1-6 | |
| *POU2F2* | NM_001207025.2 | chr19:42595704-42636563 | All CDS E1-14 | |
| *PRDM1* | NM_001198.3 | chr6:106534429-106555361 | All CDS E1-7 | B-cell differentiation |
| *PRKCB* | NM_002738.6 | chr16:23847497-24226137 | All CDS E1-17 | BCR-TLR signaling pathway |
| *PRKDC* | NM_006904.6 | chr8:48686734-48872686 | All CDS E1-87 | |
| *PTPN1* | NM_002827 | chr20:49127065-49199252 | Al CDS E1-10 | |
| *RB1* | NM_000321 | chr13:48878049-49054207 | All CDS E1-27 | Cell cycle |
| *RELN* | NM_005045.3 | chr7:103113259-103629803 | All CDS E1-65 | |
| *SEMA5A* | NM_003966.2 | chr5:9043008-9380058 | All CDS E3-23 | |
| *SETD2* | NM_014159.6 | chr3:47058583-47205414 | All CDS E1-21 | |
| *SGK1* | NM_001143676.1 | chr6:134491406-134638598 | All CDS E1-14 | Notch pathway |
| *SMARCA4* | NM_001128844.1 | chr19:11132400-11144541 | E20-28 | |
| *SOCS1* | NM_003745.1 | chr16:11348699-11349335 | All CDS E2 | JAK-STAT pathway |
| *SP140* | NM_007237 | chr2:231090560-231177399 | All CDS E1-27 | |
| *SPTBN5* | NM_016642.2 | chr15:42140813-42185695 | All CDS E2-68 | |
| *STAT3* | NM_139276.2 | chr17:40467763-40500534 | All CDS E2-24 | JAK-STAT pathway |
| *STAT6* | NM_001178078.1 | chr12:57490355-57502061 | All CDS E2-22 | JAK-STAT pathway |
| *TAF1* | NM_004606.3 | chrX:70586165-70683896 | All CDS E1-38 | Epigenome/Chromatin modifier |
| *TBL1XR1* | NM_024665.4 | chr3:176743285-176782765 | All CDS E3-16 | |
| *TCF3* | NM_003200.3 | chr19:1611706-1650247 | All CDS E2-19 | PI3K-AKT-mTOR pathway |
| *TET2* | NM_001127208.2 | chr4:106155099-106197676 | All CDS E3-11 | Epigenome/Chromatin modifier |
| *TMEM30A* | NM_018247.3 | chr6:75965818-75994354 | All CDS E1-7 | |
| *TNFAIP3* | NM_006290.3 | chr6:138192365-138202456 | All CDS E2-9 | |
| *TNFRSF14* | NM_003820.2 | chr1:2488104-2494712 | All CDS E1-8 | |
| *TNFSF9* | NM_003811.3 | chr19:6531048-6535077 | All CDS E1-3 | |
| *TNIP1* | NM_001252390.1 | chr5:150410274-150444656 | All CDS E2-18 | |
| *TP53* | NM_000546.5 | chr17:7572927-7579912 | All CDS E2-11 | Cell cycle |
| *TRAF3* | NM_003300.3 | chr14:103336539-103372121 | All CDS E2-11 | |
| *UNC5D* | NM_080872.2 | chr8:35093303-35648081 | All CDS E1-17 | |
| *WHSC1* | NM_001042424.2 | chr4:1902382-1980636 | All CDS E2-22 | |
| *XBP1* | NM_005080 | chr22:29191534-29196512 | All CDS E1-5 | |
| *NFKBIA* | NM_020529.2 | chr14:35871219-35873850 | All CDS E1-6 | BCR-TLR signaling pathway |
| *TRAF2* | NM_021138.4 | chr9:139793193-139820353 | All CDS E2-11 | |

| | | | | |
|---|---|---|---|---|
| *NFKBIZ* | NM_031419.4 | chr3:101568473-101578400 | All CDS E1-12 | BCR-TLR signaling pathway |
| *ACTG1* | NM_001614 | chr17:79477716-79479380 | All CDS E2-6 | |
| *ALDH18A1* | NM_002860 | chr10:97366519-97413134 | All CDS E2-18 | |
| *ARID5B* | NM_032199 | chr10:63661469-39911653 | All CDS E1-10 | |
| *BCL11A* | NM_022893 | chr2:60687539-60780405 | All CDS E1-4 | |
| *BCL2L1* | NM_138578 | chr20:30253752-30310021 | All CDS E2-3 | |
| *BCOR* | NM_001123385 | chrX:39911362-39937182 | All CDS E2-15 | |
| *C10orf12* | NM_015652 | chr10:98741148-98744891 | All CDS E1 | |
| *CD83* | NM_004233 | chr6:14118043-14135467 | All CDS E1-5 | |
| *CDKN2A* | NM_000077 | chr9:21968228-21974826 | All CDS E1-3 | Cell cycle |
| *CHST2* | NM_004267 | chr3:142839659-142841251 | All CDS E2 | |
| *CLTC* | NM_004859 | chr17:57697493-57771213 | All CDS E1-32 | |
| *DAZAP1* | NM_170711 | chr19:1407773-1433826 | All CDS E1-12 | |
| *DOCK8* | NM_001190458 | chr9:286509-464219 | All CDS E2-46 | |
| *DTX1* | NM_004416 | chr12:113495998-113534744 | All CDS E1-9 | Notch pathway |
| *DUSP2* | NM_004418 | chr2:96809562-96811093 | All CDS E1-4 | |
| *EBF1* | NM_024007 | chr5:158126119-158526486 | All CDS E1-16 | |
| *EDRF1* | NM_001202438 | chr10:127408377-127452041 | All CDS E1-25 | |
| *EIF4A2* | NM_001967 | chr3:186501400-186507058 | All CDS E1-11 | |
| *EPB41* | NM_203343 | chr1:29313950-29442309 | All CDS E2-16 | |
| *FAS* | NM_000043 | chr10:90750634-90774207 | All CDS E1-9 | |
| *FBXO11* | NM_001190274 | chr2:48035257-48132859 | All CDS E1-23 | |
| *FOXC1* | NM_001453 | chr6:1610681-1612342 | All CDS E1 | |
| *GNAI2* | NM_002070 | chr3:50273768-50295122 | All CDS E1-8 | |
| *GRHPR* | NM_012203 | chr9:37422748-37436779 | All CDS E1-9 | |
| *HIST1H2BK* | NM_080593 | chr6:27114197-27114577 | All CDS E1 | |
| *HLA-A* | NM_002116 | chr6:29910331-29913232 | All CDS E1-8 | |
| *HLA-B* | NM_005514 | chr6:31322260-31324935 | All CDS E1-7 | |
| *HLA-C* | NM_002117 | chr6:31236946-31239848 | All CDS E1-8 | |
| *HLA-DMB* | NM_002118 | chr6:32902748-32908584 | All CDS E1-6 | |
| *IKBKB* | NM_001556 | chr8:42129619-42188497 | All CDS E2-22 | |
| *IL10RA* | NM_001558 | chr11:117857183-117870356 | All CDS E1-7 | |
| *IL16* | NM_172217 | chr15:81517741-81601139 | All CDS E2-19 | |

| | | | | |
|---|---|---|---|---|
| *IRF2BP2* | NM_182972 | chr1:234742883-234745240 | All CDS E1-2 | |
| *ITPKB* | NM_002221 | chr1:226822372-226925159 | All CDS E1-8 | |
| *JUNB* | NM_002229 | chr19:12902586-12903629 | All CDS E1 | |
| *KLF2* | NM_016270 | chr19:16435735-16437842 | All CDS E1-3 | |
| *KLHL14* | NM_020805 | chr18:30254620-30350554 | All CDS E2-9 | |
| *KLHL21* | NM_014851 | chr1:6653425-6662877 | All CDS E1-4 | |
| *KLHL42* | NM_020782 | chr12:27933264-27951099 | All CDS E1-3 | |
| *MED16* | NM_005481 | chr19:868100-891131 | All CDS E2-16 | |
| *MPEG1* | NM_001039396 | chr11:58978188-58980338 | All CDS E1 | |
| *NOL9* | NM_024654 | chr1:6585914-6614562 | All CDS E1-12 | |
| *OSBPL10* | NM_017784 | chr3:31703564-32022671 | All CDS E1-12 | |
| *PABPC1* | NM_002568 | chr8:101716525-101733811 | All CDS E1-14 | |
| *PIM2* | NM_006875 | chrX:48771408-48776111 | All CDS E1-6 | |
| *PPP1R9B* | NM_032595 | chr17:48212696-48227874 | All CDS E1-12 | |
| *PRRC2C* | NM_015172 | chr1:171481228-171560986 | All CDS E2-34 | |
| *RAC2* | NM_002872 | chr22:37622711-37640188 | All CDS E1-6 | |
| *RFTN1* | NM_015150 | chr3:16358335-16535376 | All CDS E2-10 | |
| *S1PR2* | NM_004230 | chr19:10334520-10335581 | All CDS E2 | |
| *SEC24C* | NM_004922 | chr10:75506591-75530853 | All CDS E3-24 | |
| *SETD1B* | NM_015048 | chr12:122242644-122268145 | All CDS E1-17 | |
| *SLC1A5* | NM_005628 | chr19:47278767-47291222 | All CDS E1-8 | |
| *SPEN* | NM_015001 | chr1:16174563-16265922 | All CDS E1-15 | Notch pathway |
| *TAP1* | NM_000593 | chr6:32813356-32821593 | All CDS E1-11 | |
| *TNRC18* | NM_001080495 | chr7:5347737-5460877 | All CDS E2-30 | |
| *TOX* | NM_014729 | chr8:59720306-60031546 | All CDS E1-9 | |
| *TP53BP1* | NM_001141979 | chr15:43699581-43785241 | All CDS E1-28 | |
| *TP63* | NM_003722 | chr3:189349305-189612291 | All CDS E13-14 | |
| *TP73* | NM_005427 | chr1:3598930-3649643 | All CDS E2-14 | |
| *TRIP12* | NM_001284214 | chr2:230632270-230725247 | All CDS E2-42 | |
| *TRRAP* | NM_001244580 | chr7:98478774-98609978 | All CDS E2-72 | |
| *UBE2A* | NM_003336 | chrX:118708675-118717218 | All CDS E1-6 | |
| *VMP1* | NM_030938 | chr17:57808808-57917272 | All CDS E2-12 | |
| *WDR24* | NM_032259 | chr16:734734-739640 | All CDS E1-9 | |

| | | | | |
|---|---|---|---|---|
| *WEE1* | NM_003390 | chr11:9595481-9610149 | All CDS E1-11 | |
| *ZC3H12D* | NM_207360 | chr6:149771819-149795679 | All CDS E2-6 | |
| *ZFP36L1* | NM_004926 | chr14:69256250-69259655 | All CDS E1-2 | |
| *ZNF516* | NM_014643 | chr18:74074453-74155010 | All CDS E3-8 | |
| *RHOA* | NM_014643 | chr3:49397642-49413024 | All CDS E2-5 | |

BCR-TLR: B-cell receptor/Toll-like receptor; CDS: coding DNA sequence

**Supplemental Table 4.** Morphologic features, COO, EBV and clonality status of 31 pediatric post-SOT mPTLD detailed per case.

| Series | Morphology | Biopsy site | Immunophenotype | | | | | | | Clonality | COO[&] | EBER | LMP-1 | EBNA-2 | Zebra-EBV | Latency pattern |
|---|---|---|---|---|---|---|---|---|---|---|---|---|---|---|---|---|
| | | | CD20 | CD79 | BCL2 | BCL6 | CD10 | MUM1 | PAX5 | | | | | | | |
| **p1** | DLBCL | Intestine | + | + | + | | - | + | | | ABC | + | + | + | + | Type III with replication |
| **p5** | DLBCL* | Small bowel | + | | + | - | - | + | | Monoclonal | Non-GC /Unc | | + | | | |
| **p6** | DLBCL | Stomach | + | | + | - | - | + | | | Non-GC /ABC | + | + | - | | Type IIa |
| **p10** | DLBCL* | Intestine | + | | + | - | - | + | + | Monoclonal | Non-GC/ ABC | + | + | + | + | Type III with replication |
| **p11** | BL | Inguinal LN | + | | - | + | + | - | | Monoclonal | GCB | + | - | - | - | Type I |
| **p12** | DLBCL | LN | + | + | - | + focal | - | + | + | Monoclonal | Non-GC /ABC | + | + | - | - | Type IIa |
| **p13** | DLBCL | Cervical LN | + | + | + | - | - | + | + | Monoclonal | Non-GC /ABC | + | + | + | + | Type III with replication |
| **p14** | DLBCL | LN | + | + | - | + | - | + | + | Monoclonal | Non-GC /ABC | + | + | + | + | Type III with replication |
| **p15** | BL | LN | + | + | - | + | + | - | + | | GCB | + | - | - | - | Type I |
| **p17** | DLBCL | LN | + | | + focal | - | - | + | + | Monoclonal | Non-GC /Unc | + | | | | |
| **p19** | DLBCL | Intestine | + | + | + | - | - | + | | Monoclonal | Non-GC /ABC | + | - | - | - | Type I |
| **p20** | DLBCL | Intestinal LN | + | + | + | - | | + | + | Monoclonal | ABC | + | + | + | - | Type III |
| **p21** | DLBCL | Mesenteric LN | + | + | + | + | - | + | + | Monoclonal | Non-GC /ABC | + | + | - | + | Type II with replication |
| **p22** | BL | Tonsil | | + | - | + focal | + | | + | Monoclonal | GCB | + | - | - | - | Type I |
| **p23** | DLBCL | Intestine | + | | | + focal | - | | | Monoclonal | | + | - | - | - | Type I |
| **p25** | DLBCL | LN | - | + focal | + | + focal | - | + focal | + focal | Monoclonal | Non-GC /Unc | + | + | - | - | Type IIa |
| **p26** | DLBCL | Mesenteric LN | + | + | + | + | - | + | + | Polyclonal | Non-GC /ABC | + | + | + | | Type III |
| **p27** | DLBCL | Intestine | + | + | - | + | NA | - | + | Polyclonal# | GCB | - | - | | | |
| **p28** | BL | Intestine | + | + | - | + | + | + | + | Monoclonal | GCB | + | - | - | - | Type I |
| **p29** | BL | Intestine | + | + | - | + | - | - | NA | Monoclonal | GCB | + | | | | |

| | | | | | | | | | | | | | | | | |
|---|---|---|---|---|---|---|---|---|---|---|---|---|---|---|---|---|
| **p31** | DLBCL | Intestine | + | + | + | - | - | + | + | Monoclonal | Non-GC /ABC | + | | + | | Type IIb-III† |
| **p32** | DLBCL | Axilar LN | + | | + | - | - | + | | Monoclonal | Non-GC /Unc | + | + | + | + | Type III with replication |
| **p33** | DLBCL* | Mesenteric LN | - | + | | - | - | + | | | Non-GC/ABC | + | + | + | | Type III |
| **p35** | DLBCL | Cervical LN | + focal | + | | - | - | + | | Monoclonal | Non-GC/ABC | + | + focal | - | | Type IIa |
| **p36** | DLBCL* | LN | + focal | + | | - | - | + | - | Monoclonal | Non-GC /ABC | + | + focal | - | | Type IIa |
| **p37** | DLBCL | Scalp | + | | | + | + | - | | Monoclonal | GCB | - | - | - | | |
| **p38** | BL | Intestine | + | | | + | + | - | | Monoclonal | GCB | + | - | - | | Type I |
| **p39** | DLBCL | Tonsil | + | + | | - | - | + | | | Non-GC | + | + | + | | Type III |
| **p41** | DLBCL* | Abdominal mass | - | + | | | | + | - | Monoclonal | | + | + | + | | Type III |
| **p42** | BL | Abdominal mass and intestine | + | + | - | + | + | + focal | + | | GCB | + | - | - | - | Type I |
| **p43** | DLBCL | Abdominal adenopathy | | | | | | | | Monoclonal | Non-GC /ABC | + | + | + | | Type III |

NA: not assessable

* cases with plasmacytic differentiation

† In the absence of LMP1 assessability, two cases with latency pattern IIb-III are included in latency pattern III group

[#] IGH clonality analysis was not complete

[&] Cell of origin determination according to Hans and/or NanoString analyses. GCB results derive from either one or both algorithms. Unc: Unclassified.

**Supplemental Table 5.** Copy number (CN) alterations and CN neutral loss of heterozygosity (CNN-LOH) detected in 23 pediatric post-SOT mPTLD.

| Case | Group | Chromosome Region (GRCh37/hg19) | Event | Length | Cytoband |
|---|---|---|---|---|---|
| **p10** | PTLD-DLBCL | No CNA | | | |
| **p11** | PTLD-BL | chr6:0-44,239,109 | CNN-LOH | 44239110 | p25.3 - p21.1 |
| **p12** | PTLD-DLBCL | chr7:92,977,364-105,256,711 | CNN-LOH | 12279348 | q21.3 - q22.3 |
| **p12** | PTLD-DLBCL | chr19:0-6,735,114 | CNN-LOH | 6735115 | p13.3 |
| **p13** | PTLD-DLBCL | No CNA | | | |
| **p14** | PTLD-DLBCL | chr1:14,244,382-23,427,526 | CNN-LOH | 9183145 | p36.21 - p36.12 |
| **p14** | PTLD-DLBCL | chr2:32,437,183-50,937,966 | CNN-LOH | 18500784 | p22.3 - p16.3 |
| **p14** | PTLD-DLBCL | chr3:59,350,609-64,821,813 | CNN-LOH | 5471205 | p14.2 - p14.1 |
| **p14** | PTLD-DLBCL | chr5:97,552,139-102,911,071 | CNN-LOH | 5358933 | q15 - q21.2 |
| **p14** | PTLD-DLBCL | chr8:139,752,488-146,364,022 | CNN-LOH | 6611535 | q24.23 - q24.3 |
| **p14** | PTLD-DLBCL | chr9:16,354,115-33,476,795 | CNN-LOH | 17122681 | p22.3 - p13.3 |
| **p14** | PTLD-DLBCL | chr11:123,273,988-128,279,122 | CNN-LOH | 5005135 | q24.1 - q24.3 |
| **p14** | PTLD-DLBCL | chr13:33,960,165-41,140,013 | CNN-LOH | 7179849 | q13.1 - q14.11 |
| **p14** | PTLD-DLBCL | chr17:7,241,535-12,838,706 | CNN-LOH | 5597172 | p13.1 - p12 |
| **p15** | PTLD-BL | chr11:12,030,761-13,113,696 | CN Loss | 1082936 | p15.3 - p15.2 |
| **p15** | PTLD-BL | chr11:45,916,091-51,575,951 | CNN-LOH | 5659861 | p11.2 - p11.12 |
| **p15** | PTLD-BL | chrX:0-155,270,560 | CN Loss | 155270561 | p22.33 - q28 |
| **p19** | PTLD-DLBCL | chr3:0-91,000,000 | CN Gain | 91000001 | p26.3 - q11.1 |
| **p19** | PTLD-DLBCL | chr8:0-7,004,147 | CN Gain | 7004148 | p23.3 - p23.1 |
| **p19** | PTLD-DLBCL | chr9:70,984,372-141,213,431 | CN Gain | 70229060 | q21.11 - q34.3 |
| **p19** | PTLD-DLBCL | chr20:29,519,156-63,025,520 | CN Loss | 33506365 | q11.21 - q13.33 |
| **p19** | PTLD-DLBCL | chr21:14,344,537-48,129,895 | CN Gain | 33785359 | q11.2 - q22.3 |
| **p20** | PTLD-DLBCL | chr9:204,738-141,054,761 | CN Gain | 140850024 | p24.3 - q34.3 |
| **p20** | PTLD-DLBCL | chr12:112,915,434-117,209,665 | CN Loss | 4294232 | q24.13 - q24.22 |
| **p21** | PTLD-DLBCL | chr3:187,566,343-189,106,752 | CN Loss | 1540410 | q27.3 - q28 |
| **p22** | PTLD-BL | chr11:45,916,586-51,575,951 | CNN-LOH | 5659366 | p11.2 - p11.12 |
| **p22** | PTLD-BL | chr20:14,819,848-14,972,461 | CN Loss | 152614 | p12.1 |
| **p25** | PTLD-DLBCL | chr8:110,835,796-116,086,438 | CNN-LOH | 5250643 | q23.2 - q23.3 |
| **p26** | PTLD-DLBCL | chr1:30,307,979-48,275,263 | CNN-LOH | 17967285 | p35.2 - p33 |
| **p26** | PTLD-DLBCL | chr2:21,494-10,020,168 | CNN-LOH | 9998675 | p25.3 - p25.1 |

| | | | | | |
|---|---|---|---|---|---|
| **p26** | PTLD-DLBCL | chr2:147,262,273-173,642,237 | CNN-LOH | 26379965 | q22.3 - q31.1 |
| **p26** | PTLD-DLBCL | chr3:63,411-10,239,161 | CNN-LOH | 10175751 | p26.3 - p25.3 |
| **p26** | PTLD-DLBCL | chr3:47,120,640-52,638,564 | CNN-LOH | 5517925 | p21.31 - p21.1 |
| **p26** | PTLD-DLBCL | chr3:130,227,840-142,566,337 | CNN-LOH | 12338498 | q22.1 - q23 |
| **p26** | PTLD-DLBCL | chr4:105,732,804-114,022,691 | CNN-LOH | 8289888 | q24 - q25 |
| **p26** | PTLD-DLBCL | chr4:163,501,404-173,005,461 | CNN-LOH | 9504058 | q32.2 - q34.1 |
| **p26** | PTLD-DLBCL | chr4:184,294,510-190,915,650 | CNN-LOH | 6621141 | q35.1 - q35.2 |
| **p26** | PTLD-DLBCL | chr5:106,804,363-142,535,605 | CNN-LOH | 35731243 | q21.3 - q31.3 |
| **p26** | PTLD-DLBCL | chr6:142,331,397-155,742,113 | CNN-LOH | 13410717 | q24.1 - q25.3 |
| **p26** | PTLD-DLBCL | chr7:68,913,353-125,848,263 | CNN-LOH | 56934911 | q11.22 - q31.33 |
| **p26** | PTLD-DLBCL | chr9:204,738-7,370,794 | CNN-LOH | 7166057 | p24.3 - p24.1 |
| **p26** | PTLD-DLBCL | chr9:9,859,772-14,903,800 | CNN-LOH | 5044029 | p23 - p22.3 |
| **p26** | PTLD-DLBCL | chr15:38,731,045-45,598,335 | CNN-LOH | 6867291 | q14 - q21.1 |
| **p26** | PTLD-DLBCL | chr17:6,645,258-12,289,647 | CNN-LOH | 5644390 | p13.1 - p12 |
| **p26** | PTLD-DLBCL | chr17:55,932,988-62,982,717 | CNN-LOH | 7049730 | q22 - q24.1 |
| **p28** | PTLD-BL | No CNA | | | |
| **p29** | PTLD-BL | chr2:100,603,279-243,052,331 | CNN-LOH | 142449053 | q11.2 - q37.3 |
| **p29** | PTLD-BL | chr11:46,541,220-51,575,951 | CNN-LOH | 5034732 | p11.2 - p11.12 |
| **p29** | PTLD-BL | chr18:1-78,077,248 | CN Gain | 78077248 | p11.32 - q23 |
| **p29** | PTLD-BL | chrY:2,660,163-28,799,935 | Homozygous Copy Loss | 26139773 | p11.31 - q11.23 |
| **p31** | PTLD-DLBCL | chr3:1-198,022,430 | CN Gain | 198022430 | p26.3 - q29 |
| **p31** | PTLD-DLBCL | chr17:38,023,745-38,504,415 | CN Loss | 480671 | q12 - q21.2 |
| **p31** | PTLD-DLBCL | chrX:76,819,736-90,582,240 | CN Gain | 13762505 | q21.1 - q21.31 |
| **p32** | PTLD-DLBCL | chr16:29,710,682-35,271,725 | CNN-LOH | 5561044 | p11.2 - p11.1 |
| **p33** | PTLD-DLBCL | chr5:36,737,343-145,702,632 | CNN-LOH | 108965290 | p13.2 - q32 |
| **p33** | PTLD-DLBCL | chr15:30,591,713-55,631,810 | CNN-LOH | 25040098 | q13.2 - q21.3 |
| **p36** | PTLD-DLBCL | chr1:149,044,448-249,212,878 | CNN-LOH | 100168431 | q21.2 - q44 |
| **p36** | PTLD-DLBCL | chr4:84,099,324-88,072,085 | CN Gain | 3972762 | q21.22 - q22.1 |
| **p36** | PTLD-DLBCL | chr4:98,696,259-101,924,060 | High Copy Gain | 3227802 | q22.3 - q24 |
| **p36** | PTLD-DLBCL | chr4:101,947,930-103,635,183 | High Copy Gain | 1687254 | q24 |
| **p36** | PTLD-DLBCL | chr4:103,647,047-107,168,578 | CN Gain | 3521532 | q24 |
| **p36** | PTLD-DLBCL | chr4:107,185,824-190,915,650 | CN Loss | 83729827 | q24 - q35.2 |
| **p36** | PTLD-DLBCL | chr19:1-59,128,983 | CN Loss | 59128983 | p13.3 - q13.43 |

| | | | | | |
|---|---|---|---|---|---|
| **p36** | PTLD-DLBCL | chr20:1-63,025,520 | CN Gain | 63025520 | p13 - q13.33 |
| **p37** | PTLD-DLBCL | chr2:60,868,614-61,178,711 | High Copy Gain | 310098 | p16.1 |
| **p37** | PTLD-DLBCL | chr2:61,179,160-63,133,418 | CN Gain | 1954259 | p16.1 - p15 |
| **p37** | PTLD-DLBCL | chr10:43,581,501-57,966,196 | CN Gain | 14384696 | q11.21 - q21.1 |
| **p37** | PTLD-DLBCL | chr18:25,473,942-60,614,806 | CN Gain | 35140865 | q12.1 - q21.33 |
| **p37** | PTLD-DLBCL | chr18:60,616,440-70,727,724 | CN Gain | 10111285 | q21.33 - q22.3 |
| **p38** | PTLD-BL | No CNA | | | |
| **p39** | PTLD-DLBCL | No CNA | | | |
| **p42** | PTLD-BL | chr8:172,417-25,544,268 | CN Loss | 25371852 | p23.3 - p21.2 |
| **p43** | PTLD-DLBCL | chr1:144,009,053-167,484,888 | CNN-LOH | 23475836 | q21.1 - q24.2 |
| **p43** | PTLD-DLBCL | chr3:1-198,022,430 | CN Gain | 198022430 | p26.3 - q29 |
| **p43** | PTLD-DLBCL | chr5:1-180,915,260 | CN Gain | 180915260 | p15.33 - q35.3 |
| **p43** | PTLD-DLBCL | chr7:81,796,619-95,692,964 | CNN-LOH | 13896346 | q21.11 - q21.3 |
| **p43** | PTLD-DLBCL | chr9:1-141,213,431 | CN Gain | 141213431 | p24.3 - q34.3 |
| **p43** | PTLD-DLBCL | chr10:70,413,477-77,689,439 | CNN-LOH | 7275963 | q21.3 - q22.2 |
| **p43** | PTLD-DLBCL | chr12:1-133,851,895 | CN Gain | 133851895 | p13.33 - q24.33 |
| **p43** | PTLD-DLBCL | chr16:19,104,616-25,077,977 | CNN-LOH | 5973362 | p12.3 - p12.1 |
| **p43** | PTLD-DLBCL | chr17:20,124,289-20,517,074 | CN Loss | 392786 | p11.2 |
| **p43** | PTLD-DLBCL | chr17:20,517,075-21,911,243 | CN Gain | 1394169 | p11.2 |
| **p43** | PTLD-DLBCL | chr18:3,444,836-8,910,868 | CNN-LOH | 5466033 | p11.31 - p11.22 |
| **p43** | PTLD-DLBCL | chr20:34,101,821-40,679,500 | CNN-LOH | 6577680 | q11.22 - q12 |

**Supplemental Table 6.** List of somatic mutations identified in the analysis of 25 pediatric post-SOT mPTLD including prediction of amino acid chan prediction.[6]

| Case | Group | Chr | Start | End | Ref | Alt | Func.refGene | Gene | Transcript |
|---|---|---|---|---|---|---|---|---|---|
| p10 | PTLD-DLBCL | chr1 | 171486769 | 171486769 | C | T | exonic | *PRRC2C* | NM_015172 |
| p10 | PTLD-DLBCL | chr8 | 2071443 | 2071443 | C | T | exonic | *MYOM2* | NM_003970 |
| p10 | PTLD-DLBCL | chr8 | 128750345 | 128750345 | C | T | intronic-MYC | *MYC* | |
| p10 | PTLD-DLBCL | chr19 | 42383204 | 42383204 | C | T | exonic | *CD79A* | NM_001783 |
| p11 | PTLD-BL | chr1 | 23885829 | 23885829 | T | - | exonic | *ID3* | NM_002167 |
| p11 | PTLD-BL | chr1 | 27100176 | 27100176 | C | A | exonic | *ARID1A* | NM_006015 |
| p11 | PTLD-BL | chr6 | 41903688 | 41903688 | A | G | exonic | *CCND3* | NM_001136125 |
| p11 | PTLD-BL | chr8 | 101733638 | 101733638 | G | C | exonic | *PABPC1* | NM_002568 |
| p11 | PTLD-BL | chr8 | 128748998 | 128748998 | A | C | intronic-MYC | *MYC* | |
| p11 | PTLD-BL | chr8 | 128749066 | 128749066 | - | AGAGGAGAAG GT | intronic-MYC | *MYC* | |
| p11 | PTLD-BL | chr8 | 128749078 | 128749078 | C | T | intronic-MYC | *MYC* | |
| p11 | PTLD-BL | chr8 | 128749671 | 128749671 | A | G | intronic-MYC | *MYC* | |
| p11 | PTLD-BL | chr8 | 128749924 | 128749924 | G | C | intronic-MYC | *MYC* | |
| p11 | PTLD-BL | chr11 | 117869503 | 117869503 | C | T | exonic | *IL10RA* | NM_001558 |
| p11 | PTLD-BL | chr14 | 103342855 | 103342855 | C | T | exonic | *TRAF3* | NM_001199427 |
| p11 | PTLD-BL | chr15 | 42145506 | 42145506 | G | A | exonic | *SPTBN5* | NM_016642 |
| p11 | PTLD-BL | chrX | 41205627 | 41205627 | C | G | exonic | *DDX3X* | NM_001193417 |
| p12 | PTLD-DLBCL | chr1 | 2492096 | 2492096 | - | C | exonic | *TNFRSF14* | NM_001297605 |
| p12 | PTLD-DLBCL | chr1 | 115256530 | 115256530 | G | T | exonic | *NRAS* | NM_002524 |
| p12 | PTLD-DLBCL | chr3 | 101578250 | 101578250 | C | T | UTR3-NFKBIZ | *NFKBIZ* | c.*35C>T;NM_031419 |
| p12 | PTLD-DLBCL | chr3 | 101578251 | 101578251 | T | G | UTR3-NFKBIZ | *NFKBIZ* | c.*36T>G;NM_031419 |
| p12 | PTLD-DLBCL | chr3 | 101578368 | 101578372 | AAAAG | - | UTR3-NFKBIZ | *NFKBIZ* | c.*153_*157delAAAAG;NI |
| p12 | PTLD-DLBCL | chr6 | 41903682 | 41903682 | A | T | exonic | *CCND3* | NM_001136125 |
| p12 | PTLD-DLBCL | chr7 | 5428547 | 5428547 | C | G | exonic | *TNRC18* | NM_001080495 |
| p12 | PTLD-DLBCL | chr9 | 139390656 | 139390656 | G | A | exonic | *NOTCH1* | NM_017617 |
| p12 | PTLD-DLBCL | chr9 | 139390861 | 139390861 | G | A | exonic | *NOTCH1* | NM_017617 |
| p12 | PTLD-DLBCL | chr12 | 12037499 | 12037499 | C | T | exonic | *ETV6* | NM_001987 |
| p12 | PTLD-DLBCL | chr13 | 32906766 | 32906766 | C | T | exonic | *BRCA2* | NM_000059 |

| | | | | | | | | | |
|---|---|---|---|---|---|---|---|---|---|
| p12 | PTLD-DLBCL | chr15 | 42154384 | 42154384 | C | T | exonic | *SPTBN5* | NM_016642 |
| p12 | PTLD-DLBCL | chr19 | 6586078 | 6586078 | G | A | exonic | *CD70* | NM_001252 |
| p13 | PTLD-DLBCL | chr11 | 117869676 | 117869676 | C | T | exonic | *IL10RA* | NM_001558 |
| p14 | PTLD-DLBCL | chr6 | 31323175 | 31323175 | C | T | exonic | *HLA-B* | NM_005514 |
| p14 | PTLD-DLBCL | chr9 | 139814840 | 139814840 | A | C | exonic | *TRAF2* | NM_021138 |
| p14 | PTLD-DLBCL | chr12 | 48190875 | 48190875 | G | A | exonic | *HDAC7* | NM_001308090 |
| p14 | PTLD-DLBCL | chr12 | 113532642 | 113532642 | G | A | exonic | *DTX1* | NM_004416 |
| p14 | PTLD-DLBCL | chrX | 39932564 | 39932564 | C | T | exonic | *BCOR* | NM_001123383 |
| p15 | PTLD-BL | chr1 | 23885664 | 23885666 | GCC | - | exonic | *ID3* | NM_002167 |
| p15 | PTLD-BL | chr1 | 23885671 | 23885675 | CTACC | - | exonic | *ID3* | NM_002167 |
| p15 | PTLD-BL | chr8 | 128748866 | 128748866 | C | G | exonic | *MYC* | NM_002467 |
| p15 | PTLD-BL | chr8 | 128748893 | 128748893 | T | G | intronic-MYC | *MYC* | |
| p15 | PTLD-BL | chr8 | 128748919 | 128748919 | A | G | intronic-MYC | *MYC* | |
| p15 | PTLD-BL | chr8 | 128748927 | 128748927 | A | G | intronic-MYC | *MYC* | |
| p15 | PTLD-BL | chr8 | 128748949 | 128748949 | G | A | intronic-MYC | *MYC* | |
| p15 | PTLD-BL | chr8 | 128748964 | 128748964 | T | A | intronic-MYC | *MYC* | |
| p15 | PTLD-BL | chr8 | 128748982 | 128748982 | T | C | intronic-MYC | *MYC* | |
| p15 | PTLD-BL | chr8 | 128749005 | 128749005 | C | T | intronic-MYC | *MYC* | |
| p15 | PTLD-BL | chr8 | 128749047 | 128749047 | - | C | intronic-MYC | *MYC* | |
| p15 | PTLD-BL | chr8 | 128749087 | 128749087 | A | G | intronic-MYC | *MYC* | |
| p15 | PTLD-BL | chr8 | 128749186 | 128749186 | A | G | intronic-MYC | *MYC* | |
| p15 | PTLD-BL | chr8 | 128749250 | 128749250 | C | T | intronic-MYC | *MYC* | |
| p15 | PTLD-BL | chr8 | 128749252 | 128749252 | G | T | intronic-MYC | *MYC* | |
| p15 | PTLD-BL | chr8 | 128749266 | 128749266 | A | T | intronic-MYC | *MYC* | |
| p15 | PTLD-BL | chr8 | 128749289 | 128749289 | A | C | intronic-MYC | *MYC* | |
| p15 | PTLD-BL | chr8 | 128749338 | 128749338 | T | C | intronic-MYC | *MYC* | |
| p15 | PTLD-BL | chr8 | 128749356 | 128749356 | G | C | intronic-MYC | *MYC* | |
| p15 | PTLD-BL | chr8 | 128749422 | 128749422 | A | C | intronic-MYC | *MYC* | |
| p15 | PTLD-BL | chr8 | 128749436 | 128749436 | T | C | intronic-MYC | *MYC* | |
| p15 | PTLD-BL | chr8 | 128749484 | 128749484 | A | T | intronic-MYC | *MYC* | |
| p15 | PTLD-BL | chr8 | 128749514 | 128749514 | G | A | intronic-MYC | *MYC* | |
| p15 | PTLD-BL | chr8 | 128749515 | 128749515 | G | C | intronic-MYC | *MYC* | |
| p15 | PTLD-BL | chr8 | 128749564 | 128749564 | T | C | intronic-MYC | *MYC* | |
| p15 | PTLD-BL | chr8 | 128749587 | 128749587 | A | - | intronic-MYC | *MYC* | |

| | | | | | | | | | |
|---|---|---|---|---|---|---|---|---|---|
| p15 | PTLD-BL | chr8 | 128749594 | 128749594 | A | G | intronic-MYC | *MYC* | |
| p15 | PTLD-BL | chr8 | 128749661 | 128749661 | G | C | intronic-MYC | *MYC* | |
| p15 | PTLD-BL | chr8 | 128749790 | 128749790 | A | G | intronic-MYC | *MYC* | |
| p15 | PTLD-BL | chr8 | 128750135 | 128750135 | T | C | intronic-MYC | *MYC* | |
| p15 | PTLD-BL | chr8 | 128750140 | 128750140 | T | A | intronic-MYC | *MYC* | |
| p15 | PTLD-BL | chr8 | 128750609 | 128750609 | A | G | exonic | *MYC* | NM_002467 |
| p15 | PTLD-BL | chr8 | 128750680 | 128750680 | A | G | exonic | *MYC* | NM_002467 |
| p15 | PTLD-BL | chr8 | 128750698 | 128750698 | A | G | exonic | *MYC* | NM_002467 |
| p15 | PTLD-BL | chr13 | 41240349 | 41240349 | T | C | exonic | *FOXO1* | NM_002015 |
| p15 | PTLD-BL | chr22 | 41525969 | 41525969 | T | C | exonic | *EP300* | NM_001429 |
| p17 | PTLD-DLBCL | chr1 | 6659354 | 6659354 | G | A | exonic | *KLHL21* | NM_001324309 |
| p17 | PTLD-DLBCL | chr3 | 50273842 | 50273842 | G | C | exonic | *GNAI2* | NM_002070 |
| p17 | PTLD-DLBCL | chr10 | 63852709 | 63852709 | T | C | exonic | *ARID5B* | NM_001244638 |
| p20 | PTLD-DLBCL | chr1 | 27106228 | 27106228 | C | T | exonic | *ARID1A* | NM_006015 |
| p20 | PTLD-DLBCL | chr3 | 16419320 | 16419320 | C | A | exonic | *RFTN1* | NM_015150 |
| p20 | PTLD-DLBCL | chr3 | 47165327 | 47165327 | C | T | exonic | *SETD2* | NM_001349370 |
| p20 | PTLD-DLBCL | chr5 | 112175528 | 112175528 | A | G | exonic | *APC* | NM_001127511 |
| p20 | PTLD-DLBCL | chr6 | 27114468 | 27114468 | C | G | exonic | *HIST1H2BK* | NM_001312653 |
| p20 | PTLD-DLBCL | chr16 | 85953739 | 85953739 | A | G | exonic | *IRF8* | NM_002163 |
| p20 | PTLD-DLBCL | chrX | 39922007 | 39922007 | C | T | exonic | *BCOR* | NM_001123384 |
| p21 | PTLD-DLBCL | chr7 | 98609012 | 98609012 | G | A | exonic | *TRRAP* | NM_003496 |
| p21 | PTLD-DLBCL | chr7 | 151878913 | 151878913 | G | A | exonic | *KMT2C* | NM_170606 |
| p22 | PTLD-BL | chr1 | 23885727 | 23885727 | A | C | exonic | *ID3* | NM_002167 |
| p22 | PTLD-BL | chr1 | 23885752 | 23885752 | G | A | exonic | *ID3* | NM_002167 |
| p22 | PTLD-BL | chr1 | 27106133 | 27106133 | T | A | exonic | *ARID1A* | NM_006015 |
| p22 | PTLD-BL | chr3 | 142840130 | 142840130 | G | A | exonic | *CHST2* | NM_004267 |
| p22 | PTLD-BL | chr8 | 128749703 | 128749703 | G | A | intronic-MYC | *MYC* | |
| p22 | PTLD-BL | chr8 | 128750381 | 128750381 | C | G | intronic-MYC | *MYC* | |
| p22 | PTLD-BL | chr8 | 128750677 | 128750677 | C | T | exonic | *MYC* | NM_002467 |
| p22 | PTLD-BL | chr11 | 128359281 | 128359281 | C | T | exonic | *ETS1* | NM_001330451 |
| p22 | PTLD-BL | chr12 | 57499332 | 57499332 | G | A | exonic | *STAT6* | NM_001178081 |
| p26 | PTLD-DLBCL | chr3 | 142839722 | 142839722 | C | T | exonic | *CHST2* | NM_004267 |
| p26 | PTLD-DLBCL | chr19 | 1650232 | 1650232 | T | C | exonic | *TCF3* | NM_001136139 |
| p27 | PTLD-DLBCL | chr1 | 203274876 | 203274876 | G | A | exonic | *BTG2* | NM_006763 |

| | | | | | | | | | |
|---|---|---|---|---|---|---|---|---|---|
| p27 | PTLD-DLBCL | chr1 | 203274877 | 203274877 | G | A | splicing | *BTG2* | exon1 |
| p27 | PTLD-DLBCL | chr2 | 96810513 | 96810513 | G | A | exonic | *DUSP2* | NM_004418 |
| p27 | PTLD-DLBCL | chr2 | 230650559 | 230650559 | G | - | exonic | *TRIP12* | NM_001284216 |
| p27 | PTLD-DLBCL | chr5 | 137801629 | 137801629 | G | A | exonic | *EGR1* | NM_001964 |
| p27 | PTLD-DLBCL | chr5 | 137801737 | 137801737 | C | T | exonic | *EGR1* | NM_001964 |
| p27 | PTLD-DLBCL | chr6 | 26157154 | 26157154 | C | T | exonic | *HIST1H1E* | NM_005321 |
| p27 | PTLD-DLBCL | chr6 | 134494418 | 134494418 | C | G | exonic | *SGK1* | NM_001143677 |
| p27 | PTLD-DLBCL | chr6 | 134494482 | 134494482 | C | T | exonic | *SGK1* | NM_001143677 |
| p27 | PTLD-DLBCL | chr6 | 134494647 | 134494647 | A | C | exonic | *SGK1* | NM_001143677 |
| p27 | PTLD-DLBCL | chr6 | 134494697 | 134494697 | G | C | exonic | *SGK1* | NM_001143677 |
| p27 | PTLD-DLBCL | chr6 | 134495155 | 134495155 | G | C | exonic | *SGK1* | NM_001143677 |
| p27 | PTLD-DLBCL | chr6 | 134495196 | 134495196 | T | G | exonic | *SGK1* | NM_001143677 |
| p27 | PTLD-DLBCL | chr6 | 134495217 | 134495217 | G | C | exonic | *SGK1* | NM_001143677 |
| p27 | PTLD-DLBCL | chr6 | 134495658 | 134495658 | G | A | exonic | *SGK1* | NM_001143677 |
| p27 | PTLD-DLBCL | chr7 | 2983994 | 2983994 | C | T | exonic | *CARD11* | NM_032415 |
| p27 | PTLD-DLBCL | chr7 | 5353327 | 5353327 | C | T | exonic | *TNRC18* | NM_001080495 |
| p27 | PTLD-DLBCL | chr10 | 90750636 | 90750636 | G | A | exonic | *FAS* | NM_000043 |
| p27 | PTLD-DLBCL | chr12 | 113496233 | 113496233 | T | A | exonic | *DTX1* | NM_004416 |
| p27 | PTLD-DLBCL | chr12 | 113496242 | 113496242 | T | G | exonic | *DTX1* | NM_004416 |
| p27 | PTLD-DLBCL | chr12 | 122460005 | 122460005 | G | C | exonic | *BCL7A* | NM_001024808 |
| p27 | PTLD-DLBCL | chr13 | 32911295 | 32911295 | G | A | exonic | *BRCA2* | NM_000059 |
| p27 | PTLD-DLBCL | chr15 | 66727441 | 66727441 | T | C | exonic | *MAP2K1* | NM_002755 |
| p27 | PTLD-DLBCL | chr15 | 81517990 | 81517990 | G | T | exonic | *IL16* | NM_172217 |
| p27 | PTLD-DLBCL | chr16 | 10996027 | 10996027 | C | A | exonic | *CIITA* | NM_000246 |
| p27 | PTLD-DLBCL | chr17 | 63014369 | 63014369 | A | T | splicing | *GNA13* | exon3 |
| p27 | PTLD-DLBCL | chr18 | 74154731 | 74154731 | C | T | exonic | *ZNF516* | NM_014643 |
| p27 | PTLD-DLBCL | chr19 | 12902770 | 12902770 | G | A | exonic | *JUNB* | NM_002229 |
| p27 | PTLD-DLBCL | chr19 | 19256795 | 19256795 | G | A | exonic | *MEF2B* | NM_005919 |
| p28 | PTLD-BL | chr1 | 23885618 | 23885618 | C | G | exonic | *ID3* | NM_002167 |

| | | | | | | | | | |
|---|---|---|---|---|---|---|---|---|---|
| p28 | PTLD-BL | chr1 | 23885710 | 23885710 | G | C | exonic | *ID3* | NM_002167 |
| p28 | PTLD-BL | chr1 | 23885755 | 23885755 | - | CA | exonic | *ID3* | NM_002167 |
| p28 | PTLD-BL | chr2 | 70315818 | 70315818 | A | C | exonic | *PCBP1* | NM_006196 |
| p28 | PTLD-BL | chr2 | 70315897 | 70315897 | A | C | exonic | *PCBP1* | NM_006196 |
| p28 | PTLD-BL | chr3 | 38180208 | 38180208 | C | T | exonic | *MYD88* | NM_001172566 |
| p28 | PTLD-BL | chr4 | 103514671 | 103514671 | G | A | exonic | *NFKB1* | NM_001165412 |
| p28 | PTLD-BL | chr5 | 112176402 | 112176402 | A | G | exonic | *APC* | NM_001127511 |
| p28 | PTLD-BL | chr5 | 112177130 | 112177130 | A | G | exonic | *APC* | NM_001127511 |
| p28 | PTLD-BL | chr6 | 26031949 | 26031949 | G | A | exonic | *HIST1H3B* | NM_003537 |
| p28 | PTLD-BL | chr6 | 149795667 | 149795667 | T | G | exonic | *ZC3H12D* | NM_207360 |
| p28 | PTLD-BL | chr7 | 5352564 | 5352564 | G | A | exonic | *TNRC18* | NM_001080495 |
| p28 | PTLD-BL | chr7 | 98507794 | 98507794 | C | G | exonic | *TRRAP* | NM_001244580 |
| p28 | PTLD-BL | chr8 | 2007287 | 2007287 | A | G | exonic | *MYOM2* | NM_003970 |
| p28 | PTLD-BL | chr8 | 128748873 | 128748873 | A | G | intronic-MYC | *MYC* | |
| p28 | PTLD-BL | chr8 | 128748874 | 128748874 | G | A | intronic-MYC | *MYC* | |
| p28 | PTLD-BL | chr8 | 128748895 | 128748895 | T | G | intronic-MYC | *MYC* | |
| p28 | PTLD-BL | chr8 | 128748973 | 128748973 | T | G | intronic-MYC | *MYC* | |
| p28 | PTLD-BL | chr8 | 128748975 | 128748975 | T | C | intronic-MYC | *MYC* | |
| p28 | PTLD-BL | chr8 | 128748995 | 128748995 | G | C | intronic-MYC | *MYC* | |
| p28 | PTLD-BL | chr8 | 128749013 | 128749013 | G | T | intronic-MYC | *MYC* | |
| p28 | PTLD-BL | chr8 | 128749035 | 128749035 | T | C | intronic-MYC | *MYC* | |
| p28 | PTLD-BL | chr8 | 128749036 | 128749036 | G | A | intronic-MYC | *MYC* | |
| p28 | PTLD-BL | chr8 | 128749037 | 128749037 | G | C | intronic-MYC | *MYC* | |
| p28 | PTLD-BL | chr8 | 128749124 | 128749124 | C | T | intronic-MYC | *MYC* | |
| p28 | PTLD-BL | chr8 | 128749135 | 128749135 | A | G | intronic-MYC | *MYC* | |
| p28 | PTLD-BL | chr8 | 128749174 | 128749174 | C | G | intronic-MYC | *MYC* | |
| p28 | PTLD-BL | chr8 | 128749212 | 128749212 | G | - | intronic-MYC | *MYC* | |
| p28 | PTLD-BL | chr8 | 128749267 | 128749267 | - | GGACCGCATATCGCCTGT | intronic-MYC | *MYC* | |
| p28 | PTLD-BL | chr8 | 128749338 | 128749338 | T | C | intronic-MYC | *MYC* | |

| | | | | | | | | | |
|---|---|---|---|---|---|---|---|---|---|
| p28 | PTLD-BL | chr8 | 128749488 | 128749488 | C | T | intronic-MYC | *MYC* | |
| p28 | PTLD-BL | chr8 | 128749504 | 128749504 | G | A | intronic-MYC | *MYC* | |
| p28 | PTLD-BL | chrX | 41204672 | 41204672 | - | TTTTTTCTTTCAGATGCTGGCTCGTGATC | exonic | *DDX3X* | NM_001193417 |
| p29 | PTLD-BL | chr1 | 118166170 | 118166170 | A | G | exonic | *FAM46C* | NM_017709 |
| p29 | PTLD-BL | chr6 | 26031910 | 26031910 | G | A | exonic | *HIST1H3B* | NM_003537 |
| p29 | PTLD-BL | chr6 | 26234965 | 26234965 | G | A | exonic | *HIST1H1D* | NM_005320 |
| p29 | PTLD-BL | chr8 | 128749108 | 128749108 | T | C | intronic-MYC | *MYC* | |
| p29 | PTLD-BL | chr8 | 128749144 | 128749144 | C | A | intronic-MYC | *MYC* | |
| p29 | PTLD-BL | chr8 | 128749431 | 128749431 | G | C | intronic-MYC | *MYC* | |
| p29 | PTLD-BL | chr8 | 128749444 | 128749444 | A | C | intronic-MYC | *MYC* | |
| p29 | PTLD-BL | chr8 | 128749478 | 128749478 | A | T | intronic-MYC | *MYC* | |
| p29 | PTLD-BL | chr8 | 128749763 | 128749763 | G | A | intronic-MYC | *MYC* | |
| p29 | PTLD-BL | chr8 | 128749810 | 128749810 | A | T | intronic-MYC | *MYC* | |
| p29 | PTLD-BL | chr8 | 128750169 | 128750169 | A | T | intronic-MYC | *MYC* | |
| p29 | PTLD-BL | chr8 | 128750284 | 128750284 | A | T | intronic-MYC | *MYC* | |
| p29 | PTLD-BL | chr8 | 128750292 | 128750292 | C | G | intronic-MYC | *MYC* | |
| p29 | PTLD-BL | chr8 | 128750512 | 128750512 | C | G | exonic | *MYC* | NM_002467 |
| p29 | PTLD-BL | chr8 | 128750522 | 128750522 | T | C | exonic | *MYC* | NM_002467 |
| p29 | PTLD-BL | chr8 | 128750632 | 128750632 | C | G | exonic | *MYC* | NM_002467 |
| p29 | PTLD-BL | chr8 | 128750663 | 128750663 | A | C | exonic | *MYC* | NM_002467 |
| p29 | PTLD-BL | chr8 | 128750671 | 128750671 | C | G | exonic | *MYC* | NM_002467 |
| p29 | PTLD-BL | chr8 | 128750743 | 128750743 | C | G | exonic | *MYC* | NM_002467 |
| p29 | PTLD-BL | chr8 | 128750771 | 128750771 | G | A | exonic | *MYC* | NM_002467 |
| p29 | PTLD-BL | chr8 | 128750921 | 128750921 | T | G | exonic | *MYC* | NM_002467 |
| p29 | PTLD-BL | chr8 | 128750953 | 128750953 | C | G | exonic | *MYC* | NM_002467 |
| p29 | PTLD-BL | chr8 | 128751210 | 128751210 | C | A | exonic | *MYC* | NM_002467 |
| p29 | PTLD-BL | chr8 | 128751251 | 128751251 | C | G | exonic | *MYC* | NM_002467 |
| p29 | PTLD-BL | chr13 | 41240288 | 41240288 | C | T | exonic | *FOXO1* | NM_002015 |
| p29 | PTLD-BL | chrX | 41205590 | 41205590 | G | A | exonic | *DDX3X* | NM_001193417 |
| p32 | PTLD-DLBCL | chr1 | 3644716 | 3644716 | G | A | exonic | *TP73* | NM_001126240 |
| p32 | PTLD-DLBCL | chr4 | 55161387 | 55161387 | T | - | exonic | *PDGFRA* | NM_001347829 |

| | | | | | | | | | |
|---|---|---|---|---|---|---|---|---|---|
| p33 | PTLD-DLBCL | chr1 | 6585940 | 6585940 | G | A | exonic | *NOL9* | NM_024654 |
| p33 | PTLD-DLBCL | chr6 | 138200098 | 138200098 | G | A | exonic | *TNFAIP3* | NM_001270507 |
| p33 | PTLD-DLBCL | chr8 | 48739308 | 48739308 | G | A | exonic | *PRKDC* | |
| p33 | PTLD-DLBCL | chr8 | 128749023 | 128749023 | G | T | intronic-MYC | *MYC* | |
| p33 | PTLD-DLBCL | chr8 | 128750260 | 128750260 | C | T | intronic-MYC | *MYC* | |
| p33 | PTLD-DLBCL | chr9 | 382626 | 382626 | G | A | exonic | *DOCK8* | NM_001190458 |
| p33 | PTLD-DLBCL | chr15 | 42147805 | 42147805 | G | A | exonic | *SPTBN5* | NM_016642 |
| p33 | PTLD-DLBCL | chr16 | 736078 | 736078 | G | T | exonic | *WDR24* | NM_032259 |
| p35 | PTLD-DLBCL | chr1 | 3648092 | 3648092 | T | C | exonic | *TP73* | NM_001204191 |
| p35 | PTLD-DLBCL | chr1 | 29379717 | 29379717 | A | - | exonic | *EPB41* | NM_203343 |
| p35 | PTLD-DLBCL | chr1 | 171509892 | 171509892 | C | T | exonic | *PRRC2C* | NM_015172 |
| p35 | PTLD-DLBCL | chr1 | 171527028 | 171527028 | C | A | exonic | *PRRC2C* | NM_015172 |
| p35 | PTLD-DLBCL | chr2 | 96811047 | 96811047 | G | T | exonic | *DUSP2* | NM_004418 |
| p35 | PTLD-DLBCL | chr3 | 187442733 | 187442733 | T | C | exonic | *BCL6* | NM_001134738 |
| p35 | PTLD-DLBCL | chr4 | 153249384 | 153249384 | C | T | exonic | *FBXW7* | NM_001013415 |
| p35 | PTLD-DLBCL | chr6 | 32820185 | 32820185 | C | T | exonic | *TAP1* | NM_000593 |
| p35 | PTLD-DLBCL | chr7 | 2956965 | 2956965 | G | - | exonic | *CARD11* | NM_032415 |
| p35 | PTLD-DLBCL | chr7 | 2983905 | 2983905 | C | T | exonic | *CARD11* | NM_032415 |
| p35 | PTLD-DLBCL | chr7 | 151860427 | 151860427 | C | T | exonic | *KMT2C* | NM_170606 |
| p35 | PTLD-DLBCL | chr7 | 5567923 | 5567923 | G | A | exonic | *ACTB* | NM_001101 |
| p35 | PTLD-DLBCL | chr8 | 128748903 | 128748903 | T | - | intronic-MYC | *MYC* | |
| p35 | PTLD-DLBCL | chr10 | 90768708 | 90768708 | T | - | exonic | *FAS* | NM_000043 |
| p35 | PTLD-DLBCL | chr10 | 90773948 | 90773948 | G | A | exonic | *FAS* | NM_152871 |
| p35 | PTLD-DLBCL | chr11 | 108206646 | 108206646 | C | G | exonic | *ATM* | NM_000051 |
| p35 | PTLD-DLBCL | chr13 | 32910767 | 32910767 | C | A | exonic | *BRCA2* | NM_000059 |
| p35 | PTLD-DLBCL | chr15 | 42167199 | 42167199 | C | T | exonic | *SPTBN5* | NM_016642 |
| p35 | PTLD-DLBCL | chr15 | 81595890 | 81595890 | C | T | exonic | *IL16* | NM_004513 |
| p35 | PTLD-DLBCL | chr16 | 735089 | 735089 | G | A | exonic | *WDR24* | NM_032259 |
| p35 | PTLD-DLBCL | chr16 | 3801727 | 3801727 | G | A | exonic | *CREBBP* | NM_001079846 |
| p35 | PTLD-DLBCL | chr19 | 6586201 | 6586201 | G | A | exonic | *CD70* | NM_001252 |

| | | | | | | | | | |
|---|---|---|---|---|---|---|---|---|---|
| p35 | PTLD-DLBCL | chr19 | 6586333 | 6586333 | C | A | exonic | *CD70* | NM_001252 |
| p35 | PTLD-DLBCL | chr19 | 42596336 | 42596336 | G | - | exonic | *POU2F2* | NM_001207025 |
| p36 | PTLD-DLBCL | chr6 | 44233425 | 44233425 | A | G | exonic | *NFKBIE* | NM_004556 |
| p36 | PTLD-DLBCL | chr9 | 139390684 | 139390684 | G | A | exonic | *NOTCH1* | NM_017617 |
| p36 | PTLD-DLBCL | chr17 | 7577538 | 7577538 | C | T | exonic | *TP53* | NM_001126115 |
| p37 | PTLD-DLBCL | chr1 | 117087113 | 117087113 | T | A | exonic | *CD58* | NM_001144822 |
| p37 | PTLD-DLBCL | chr7 | 151878676 | 151878676 | G | T | exonic | *KMT2C* | NM_170606 |
| p37 | PTLD-DLBCL | chr16 | 11016049 | 11016049 | G | A | exonic | *CIITA* | NM_001286403 |
| p37 | PTLD-DLBCL | chr17 | 7577556 | 7577556 | C | A | exonic | *TP53* | NM_001126115 |
| p37 | PTLD-DLBCL | chrX | 48772479 | 48772479 | C | T | exonic | *PIM2* | NM_006875 |
| p38 | PTLD-BL | chr2 | 48050381 | 48050381 | T | C | exonic | *FBXO11* | NM_001190274 |
| p38 | PTLD-BL | chr3 | 50294456 | 50294458 | AAG | - | exonic | *GNAI2* | NM_001282618 |
| p38 | PTLD-BL | chr8 | 128748922 | 128748922 | C | G | intronic-MYC | *MYC* | |
| p38 | PTLD-BL | chr8 | 128749034 | 128749034 | C | G | intronic-MYC | *MYC* | |
| p38 | PTLD-BL | chr8 | 128749434 | 128749434 | C | G | intronic-MYC | *MYC* | |
| p38 | PTLD-BL | chr8 | 128749779 | 128749779 | A | C | intronic-MYC | *MYC* | |
| p38 | PTLD-BL | chrX | 41205620 | 41205620 | A | C | exonic | *DDX3X* | NM_001193417 |
| p38 | PTLD-BL | chrX | 41205658 | 41205658 | A | G | exonic | *DDX3X* | NM_001193417 |
| p39 | PTLD-DLBCL | chr1 | 16259009 | 16259009 | A | G | exonic | *SPEN* | NM_015001 |
| p39 | PTLD-DLBCL | chr3 | 187447651 | 187447651 | G | A | exonic | *BCL6* | NM_001134738 |
| p39 | PTLD-DLBCL | chr6 | 1611960 | 1611960 | C | A | exonic | *FOXC1* | NM_001453 |
| p39 | PTLD-DLBCL | chr7 | 103244814 | 103244814 | G | A | exonic | *RELN* | NM_005045 |
| p39 | PTLD-DLBCL | chr7 | 151945442 | 151945442 | T | C | exonic | *KMT2C* | NM_170606 |
| p39 | PTLD-DLBCL | chr8 | 2054325 | 2054325 | C | A | exonic | *MYOM2* | NM_003970 |
| p39 | PTLD-DLBCL | chr8 | 35624487 | 35624487 | G | A | exonic | *UNC5D* | NM_001322818 |
| p39 | PTLD-DLBCL | chr14 | 69257012 | 69257022 | GCGGCTGTCTC | - | exonic | *ZFP36L1* | NM_001244698 |
| p42 | PTLD-BL | chr1 | 203274864 | 203274864 | G | C | exonic | *BTG2* | NM_006763 |
| p42 | PTLD-BL | chr3 | 47163511 | 47163528 | TGATATAAATCATCAAAA | - | exonic | *SETD2* | NM_001349370 |

| | | | | | | | | | |
|---|---|---|---|---|---|---|---|---|---|
| p42 | PTLD-BL | chr3 | 187443367 | 187443367 | C | T | exonic | *BCL6* | NM_001134738 |
| p42 | PTLD-BL | chr5 | 112174464 | 112174464 | A | G | exonic | *APC* | NM_001127511 |
| p42 | PTLD-BL | chr8 | 128749034 | 128749034 | C | G | intronic-MYC | *MYC* | |
| p42 | PTLD-BL | chr8 | 128749254 | 128749254 | G | C | intronic-MYC | *MYC* | |
| p42 | PTLD-BL | chr8 | 128749993 | 128749993 | G | A | intronic-MYC | *MYC* | |
| p42 | PTLD-BL | chr8 | 128750483 | 128750483 | C | T | intronic-MYC | *MYC* | |
| p42 | PTLD-BL | chr8 | 128750530 | 128750530 | A | G | exonic | *MYC* | NM_001354870 |
| p42 | PTLD-BL | chr8 | 128750625 | 128750625 | G | C | exonic | *MYC* | NM_001354870 |
| p42 | PTLD-BL | chr8 | 128750680 | 128750680 | A | G | exonic | *MYC* | NM_001354870 |
| p42 | PTLD-BL | chr8 | 128750705 | 128750705 | G | A | exonic | *MYC* | NM_001354870 |
| p42 | PTLD-BL | chr8 | 128750802 | 128750802 | G | C | exonic | *MYC* | NM_001354870 |
| p42 | PTLD-BL | chr8 | 128751144 | 128751144 | C | G | exonic | *MYC* | NM_001354870 |
| p42 | PTLD-BL | chr8 | 128751210 | 128751210 | C | A | exonic | *MYC* | NM_001354870 |
| p42 | PTLD-BL | chr8 | 128751221 | 128751221 | T | C | exonic | *MYC* | NM_001354870 |
| p42 | PTLD-BL | chr8 | 128751239 | 128751239 | C | T | exonic | *MYC* | NM_001354870 |
| p42 | PTLD-BL | chr13 | 41240273 | 41240273 | G | C | exonic | *FOXO1* | NM_002015 |
| p42 | PTLD-BL | chr15 | 42149184 | 42149184 | C | T | exonic | *SPTBN5* | NM_016642 |
| p42 | PTLD-BL | chr17 | 7578265 | 7578265 | A | G | exonic | *TP53* | NM_001126115 |
| p42 | PTLD-BL | chr17 | 57697512 | 57697512 | T | G | exonic | *CLTC* | NM_001288653 |
| p42 | PTLD-BL | chr19 | 1615444 | 1615444 | A | C | exonic | *TCF3* | NM_001351778 |
| p42 | PTLD-BL | chrX | 41201908 | 41201908 | T | C | splicing | *DDX3X* | exon5 |
| p43 | PTLD-DLBCL | chr12 | 122460041 | 122460041 | A | C | exonic | *BCL7A* | NM_001024808 |

ges that affect the protein function (MA, SIFT, Polyphen2, CADD) and driver variants

| HGVS.c | HGVS.p | ExonicFunc.refGene | AF | COSMIC_ID | SIFT_score | SIFT_pred |
|---|---|---|---|---|---|---|
| c.C560T | p.S187L | nonsynonymous SNV | 0.462 | . | 0.009 | D |
| c.C3583T | p.H1195Y | nonsynonymous SNV | 0.495 | . | 0.049 | D |
| | | . | 0.494 | COSN25520744 | . | . |
| c.C224T | p.T75M,CD79A | nonsynonymous SNV | 0.495 | . | 0.001 | D |
| c.89delA | p.K30fs | frameshift deletion | 0.42 | . | . | . |
| c.C3972A | p.Y1324X,ARID1A | stopgain | 0.451 | COSM907720 | . | . |
| c.T653C | p.I218T,CCND3 | nonsynonymous SNV | 0.84 | COSM5948876 | 0.001 | D |
| c.C174G | p.N58K | nonsynonymous SNV | 0.402 | . | 0 | D |
| | | . | 0.383 | COSN4876650 | . | . |
| | | . | 0.476 | . | . | . |
| | | . | 0.459 | COSN25178966 | . | . |
| | | . | 0.472 | . | . | . |
| | | . | 0.521 | . | . | . |
| c.C884T | p.P295L | nonsynonymous SNV | 0.476 | . | 0.45 | T |
| c.C563T | p.A188V,TRAF3 | nonsynonymous SNV | 0.459 | COSM6032802 | 0.155 | T |
| c.C10120T | p.R3374W | nonsynonymous SNV | 0.479 | COSM5786167 | 0.115 | T |
| c.C1413G | p.F471L,DDX3X | nonsynonymous SNV | 0.821 | . | 0 | D |
| c.495dupC | p.C165fs,TNFRSF14 | frameshift insertion | 0.271 | . | . | . |
| c.C181A | p.Q61K | nonsynonymous SNV | 0.276 | COSM580 | 0.009 | D |
| | | UTR3-NFKBIZ | 0.331 | . | . | . |
| | | UTR3-NFKBIZ | 0.322 | . | . | . |
| M_031419 | | UTR3-NFKBIZ | 0.529 | . | . | . |
| c.T659A | p.L220Q,CCND3 | nonsynonymous SNV | 0.249 | . | 0.002 | D |
| c.G908C | p.G303A | nonsynonymous SNV | 0.554 | . | 0.779 | T |
| c.C7535T | p.P2512L | nonsynonymous SNV | 0.22 | COSM27928 | 0 | D |
| c.C7330T | p.Q2444X | stopgain | 0.323 | COSM27925,COSM4775092 | . | . |
| c.C1130T | p.A377V | nonsynonymous SNV | 0.285 | COSM4384671 | 0 | D |
| c.C1151T | p.S384F | nonsynonymous SNV | 0.35 | COSM5757636 | 0.012 | D |

| | | | | | | |
|---|---|---|---|---|---|---|
| c.G7492A | p.A2498T | nonsynonymous SNV | 0.424 | . | 1 | T |
| c.C535T | p.R179X | stopgain | 0.536 | . | . | . |
| c.C1057T | p.P353S | nonsynonymous SNV | 0.464 | . | 0.351 | T |
| c.G814A | p.V272M | nonsynonymous SNV | 0.068 | . | 0 | D |
| c.A833C | p.K278T | nonsynonymous SNV | 0.499 | . | 0.003 | D |
| c.C577T | p.R193W,HDAC7 | nonsynonymous SNV | 0.493 | . | 0 | D |
| c.G1276A | p.G426S | nonsynonymous SNV | 0.477 | . | 0.058 | T |
| c.G2035A | p.V679I,BCOR | nonsynonymous SNV | 0.963 | . | 0 | D |
| c.252_254del | p.84_85del | nonframeshift deletion | 0.12 | . | . | . |
| c.243_247del | p.Q81fs | frameshift deletion | 0.127 | . | . | . |
| c.C27G | p.N9K | nonsynonymous SNV | 0.451 | COSM6205982 | 0.005 | D |
| | | . | 0.464 | . | . | . |
| | | . | 0.406 | . | . | . |
| | | . | 0.394 | . | . | . |
| | | . | 0.416 | . | . | . |
| | | . | 0.411 | . | . | . |
| | | . | 0.408 | . | . | . |
| | | . | 0.394 | COSN23137013,COSN4876655 | . | . |
| | | . | 0.427 | . | . | . |
| | | . | 0.4 | . | . | . |
| | | . | 0.403 | . | . | . |
| | | . | 0.4 | COSN23365627,COSN25205836 | . | . |
| | | . | 0.398 | . | . | . |
| | | . | 0.383 | . | . | . |
| | | . | 0.387 | . | . | . |
| | | . | 0.362 | . | . | . |
| | | . | 0.373 | . | . | . |
| | | . | 0.366 | COSN23353412 | . | . |
| | | . | 0.374 | . | . | . |
| | | . | 0.374 | . | . | . |
| | | . | 0.371 | . | . | . |
| | | . | 0.37 | COSN8574900 | . | . |
| | | . | 0.384 | . | . | . |
| | | . | 0.383 | . | . | . |

| | | | | | | |
|---|---|---|---|---|---|---|
| | | . | 0.384 | . | . | . |
| | | . | 0.384 | . | . | . |
| | | . | 0.42 | . | . | . |
| | | . | 0.416 | . | . | . |
| | | . | 0.421 | . | . | . |
| c.A146G | p.Q49R | nonsynonymous SNV | 0.417 | . | 0.041 | D |
| c.A217G | p.T73A | nonsynonymous SNV | 0.395 | COSM1163490,COSM1163491 | 0.037 | D |
| c.A235G | p.S79G | nonsynonymous SNV | 0.404 | . | 0.091 | T |
| c.A1G | p.M1V | nonsynonymous SNV | 0.412 | COSM220645,COSM220646 | 0.006 | D |
| c.T1244C | p.L415P | nonsynonymous SNV | 0.381 | COSM221269 | 0.004 | D |
| c.C1180T | p.R394C,KLHL21 | nonsynonymous SNV | 0.512 | COSM4009497 | 0.065 | T |
| c.G75C | p.E25D | nonsynonymous SNV | 0.469 | . | 0.074 | T |
| c.T2758C | p.Y920H,ARID5B | nonsynonymous SNV | 0.49 | . | 0 | D |
| c.C5839T | p.Q1947X,ARID1A | stopgain | 0.273 | COSM2235552 | . | . |
| c.G731T | p.G244V | nonsynonymous SNV | 0.28 | . | 0.246 | T |
| c.G667A | p.V223I,SETD2 | nonsynonymous SNV | 0.511 | . | 1 | T |
| c.A4183G | p.M1395V,APC | nonsynonymous SNV | 0.479 | COSM4169481 | 0.01 | D |
| c.G110C | p.S37T,HIST1H2BK | nonsynonymous SNV | 0.229 | . | 0.035 | D |
| c.A1013G | p.Q338R | nonsynonymous SNV | 0.493 | . | 0.587 | T |
| c.G4009A | p.D1337N,BCOR | nonsynonymous SNV | 0.427 | COSM4434915,COSM4434916,COSM4434917 | 0.043 | D |
| c.G11062A | p.A3688T,TRRAP | nonsynonymous SNV | 0.51 | COSM6810121,COSM6810122 | 0.614 | T |
| c.C6032T | p.S2011F | nonsynonymous SNV | 0.477 | . | 0.029 | D |
| c.T191G | p.L64R | nonsynonymous SNV | 0.277 | . | 0.001 | D |
| c.C166T | p.P56S | nonsynonymous SNV | 0.285 | COSM1159770 | 0 | D |
| c.T5744A | p.L1915X,ARID1A | stopgain | 0.273 | . | . | . |
| c.G472A | p.G158R | nonsynonymous SNV | 0.504 | . | 0.486 | T |
| | | . | 0.372 | . | . | . |
| | | . | 0.385 | . | . | . |
| c.C214T | p.P72S | nonsynonymous SNV | 0.382 | COSM3316879,COSM3316880 | 0.029 | D |
| c.G307A | p.A103T,ETS1 | nonsynonymous SNV | 0.478 | . | 0.167 | T |
| c.C401T | p.A134V,STAT6 | nonsynonymous SNV | 0.498 | COSM4043769 | 0.273 | T |
| c.C64T | p.P22S | nonsynonymous SNV | 0.484 | . | 0 | D |
| c.A16G | p.R6G,TCF3 | nonsynonymous SNV | 0.462 | . | 0 | D |
| c.G142A | p.E48K | nonsynonymous SNV | 0.35 | COSM5947100 | 0.045 | D |

| | | | | | | |
|---|---|---|---|---|---|---|
| | | splicing | 0.338 | COSM4799443 | . | . |
| c.C497T | p.P166L | nonsynonymous SNV | 0.37 | COSM3799278 | 0.001 | D |
| c.3973delC | p.R1325fs,TRIP12 | frameshift deletion | 0.094 | . | . | . |
| c.G179A | p.S60N | nonsynonymous SNV | 0.241 | . | 0.161 | T |
| c.C287T | p.P96L | nonsynonymous SNV | 0.484 | . | 0.005 | D |
| c.C536T | p.A179V | nonsynonymous SNV | 0.323 | . | 0.099 | T |
| c.G495C | p.K165N,SGK1 | nonsynonymous SNV | 0.328 | COSM1487239,COSM1487240,COSM1487241,COSM1487242,COSM1487243 | 0.019 | D |
| c.G431A | p.R144K,SGK1 | nonsynonymous SNV | 0.08 | . | 0.508 | T |
| c.T370G | p.S124A,SGK1 | nonsynonymous SNV | 0.085 | . | 0.085 | T |
| c.C320G | p.P107R,SGK1 | nonsynonymous SNV | 0.304 | . | 0.043 | D |
| c.C300G | p.N100K,SGK1 | nonsynonymous SNV | 0.273 | . | 0.164 | T |
| c.A259C | p.K87Q,SGK1 | nonsynonymous SNV | 0.308 | . | 0.27 | T |
| c.C238G | p.P80A,SGK1 | nonsynonymous SNV | 0.238 | . | 0.121 | T |
| c.C227T | p.A76V,SGK1 | nonsynonymous SNV | 0.247 | . | 0.257 | T |
| c.G536A | p.R179Q,CARD11 | nonsynonymous SNV | 0.457 | COSM6620089 | 0.101 | T |
| c.G7195A | p.A2399T | nonsynonymous SNV | 0.28 | . | 0.051 | T |
| c.G3A | p.M1I,FAS | nonsynonymous SNV | 0.453 | COSM6660632 | 0 | D |
| c.T236A | p.M79K | nonsynonymous SNV | 0.247 | . | 0.018 | D |
| c.T245G | p.F82C | nonsynonymous SNV | 0.245 | . | 0.009 | D |
| c.G8C | p.G3A,BCL7A | nonsynonymous SNV | 0.238 | . | 0.035 | D |
| c.G2803A | p.D935N | nonsynonymous SNV | 0.454 | . | 0.043 | D |
| c.T157C | p.F53L | nonsynonymous SNV | 0.335 | COSM555604 | 0.013 | D |
| c.G250T | p.A84S,IL16 | nonsynonymous SNV | 0.491 | . | 0.016 | D |
| c.C614A | p.T205N,CIITA | nonsynonymous SNV | 0.457 | . | 0.023 | D |
| exon3 | c.276+2T>A | splicing | 0.291 | COSM4170815 | . | . |
| c.G280A | p.E94K | nonsynonymous SNV | 0.292 | . | 0.048 | D |
| c.G185A | p.G62D | nonsynonymous SNV | 0.098 | . | 0.647 | T |
| c.C806T | p.P269L | nonsynonymous SNV | 0.488 | . | 0 | D |
| c.G300C | p.Q100H | nonsynonymous SNV | 0.071 | . | 0.056 | T |

| | | | | | | |
|---|---|---|---|---|---|---|
| c.C208G | p.L70V | nonsynonymous SNV | 0.071 | COSM2049209 | 0 | D |
| c.162_163insTG | p.V55fs | frameshift insertion | 0.624 | . | . | . |
| c.A943C | p.I315L | nonsynonymous SNV | 0.308 | . | 0.004 | D |
| c.A1022C | p.Y341S | nonsynonymous SNV | 0.291 | . | 0 | D |
| c.C56T | p.P19L,MYD88 | nonsynonymous SNV | 0.414 | . | 0.011 | D |
| c.G1153A | p.G385R,NFKB1 | nonsynonymous SNV | 0.296 | . | 0.006 | D |
| c.A5057G | p.K1686R,APC | nonsynonymous SNV | 0.38 | . | 0.229 | T |
| c.A5785G | p.T1929A,APC | nonsynonymous SNV | 0.4 | . | 0.174 | T |
| c.C340T | p.H114Y | nonsynonymous SNV | 0.136 | . | . | . |
| c.A13C | p.S5R | nonsynonymous SNV | 0.424 | . | 0.176 | T |
| c.C7958T | p.S2653F | nonsynonymous SNV | 0.367 | . | 0 | D |
| c.C1466G | p.T489S,TRRAP | nonsynonymous SNV | 0.43 | . | 0.214 | T |
| c.A574G | p.S192G | nonsynonymous SNV | 0.449 | . | 0.054 | T |
| | | . | 0.301 | . | . | . |
| | | . | 0.297 | . | . | . |
| | | . | 0.278 | . | . | . |
| | | . | 0.265 | . | . | . |
| | | . | 0.257 | . | . | . |
| | | . | 0.278 | COSN23179746,COSN23224107,COSN23262474,COSN25184301,COSN25264478,COSN25522845,COSN4876647,COSN4876648,COSN4876649 | . | . |
| | | . | 0.274 | . | . | . |
| | | . | 0.278 | . | . | . |
| | | . | 0.294 | . | . | . |
| | | . | 0.289 | . | . | . |
| | | . | 0.326 | . | . | . |
| | | . | 0.32 | . | . | . |
| | | . | 0.324 | COSN23136724 | . | . |
| | | . | 0.102 | . | . | . |
| | | . | 0.141 | . | . | . |
| | | . | 0.342 | . | . | . |

| | | | | | | |
|---|---|---|---|---|---|---|
| | | . | 0.237 | COSN25179444,COSN25519226 | . | . |
| | | . | 0.235 | . | . | . |
| c.1138_1139insTTTTTTCTTTCAGATGCTGGCTCGTGATC | p.F380fs,DDX3X | frameshift insertion | 0.35 | . | . | . |
| c.A680G | p.Q227R | nonsynonymous SNV | 0.425 | . | 0.796 | T |
| c.C379T | p.L127F | nonsynonymous SNV | 0.34 | COSM4171535 | . | . |
| c.C197T | p.A66V | nonsynonymous SNV | 0.416 | . | 0.081 | T |
| | | . | 0.399 | . | . | . |
| | | . | 0.394 | . | . | . |
| | | . | 0.067 | . | . | . |
| | | . | 0.354 | . | . | . |
| | | . | 0.37 | . | . | . |
| | | . | 0.382 | . | . | . |
| | | . | 0.368 | . | . | . |
| | | . | 0.433 | . | . | . |
| | | . | 0.414 | . | . | . |
| | | . | 0.409 | . | . | . |
| c.C49G | p.P17A | nonsynonymous SNV | 0.42 | . | 0.002 | D |
| c.T59C | p.V20A | nonsynonymous SNV | 0.419 | COSM1159785,COSM1159786 | 0.547 | T |
| c.C169G | p.P57A | nonsynonymous SNV | 0.059 | . | 0.002 | D |
| c.A200C | p.K67T | nonsynonymous SNV | 0.408 | . | 0 | D |
| c.C208G | p.L70V | nonsynonymous SNV | 0.42 | . | 0 | D |
| c.C280G | p.P94A | nonsynonymous SNV | 0.433 | . | 0.18 | T |
| c.G308A | p.G103D | nonsynonymous SNV | 0.427 | COSM1454788,COSM1454789 | 0.138 | T |
| c.T458G | p.F153C | nonsynonymous SNV | 0.448 | COSM1161732,COSM1161733 | 0.008 | D |
| c.C490G | p.L164V | nonsynonymous SNV | 0.442 | COSM3316931,COSM3316932 | 0.056 | T |
| c.C747A | p.S249R | nonsynonymous SNV | 0.407 | . | 0.011 | D |
| c.C788G | p.T263S | nonsynonymous SNV | 0.398 | . | 0 | D |
| c.G62A | p.R21H | nonsynonymous SNV | 0.386 | COSM5948479,COSM5948480 | 0 | D |
| c.G1376A | p.R459H,DDX3X | nonsynonymous SNV | 0.746 | COSM1161825 | 0.001 | D |
| c.G862A | p.V288I,TP73 | nonsynonymous SNV | 0.486 | COSM3934695,COSM908805 | 1 | T |
| c.3218delT | p.M1073fs,PDGFRA | frameshift deletion | 0.47 | . | . | . |

| | | | | | | |
|---|---|---|---|---|---|---|
| c.C2083T | p.P695S | nonsynonymous SNV | 0.34 | . | 0.255 | T |
| c.G1516A | p.A506T,TNFAIP3 | nonsynonymous SNV | 0.343 | . | 0.272 | T |
| | | unknown | 0.354 | . | . | . |
| | | . | 0.409 | COSN17149849,COSN17151752 | . | . |
| | | . | 0.372 | . | . | . |
| c.G2515A | p.D839N,DOCK8 | nonsynonymous SNV | 0.098 | COSM3657440,COSM3657441 | 0.102 | T |
| c.C9160T | p.R3054C | nonsynonymous SNV | 0.126 | COSM2186557 | 0.003 | D |
| c.C1441A | p.L481I | nonsynonymous SNV | 0.36 | . | 0.553 | T |
| c.T1115C | p.I372T,TP73 | nonsynonymous SNV | 0.179 | . | 0.002 | D |
| c.1633delA | p.K545fs,EPB41 | frameshift deletion | 0.18 | COSM1341625,COSM1341626,COSM6654552 | . | . |
| c.C3281T | p.T1094I | nonsynonymous SNV | 0.136 | . | 0.004 | D |
| c.C5771A | p.P1924H | nonsynonymous SNV | 0.141 | . | 0.002 | D |
| c.C47A | p.T16K | nonsynonymous SNV | 0.418 | . | 1 | T |
| c.A1805G | p.Y602C,BCL6 | nonsynonymous SNV | 0.169 | . | 0 | D |
| c.G1040A | p.R347H,FBXW7 | nonsynonymous SNV | 0.123 | COSM1149856,COSM117308,COSM117309,COSM117310,COSM22965 | 0.001 | D |
| c.G873A | p.M291I,TAP1 | nonsynonymous SNV | 0.153 | . | 0.002 | D |
| c.2662delC | p.R888fs,CARD11 | frameshift deletion | 0.131 | . | . | . |
| c.G625A | p.A209T,CARD11 | nonsynonymous SNV | 0.113 | COSM5138977 | 0.071 | T |
| c.G10235A | p.R3412Q | nonsynonymous SNV | 0.137 | . | 0 | D |
| c.C791T | p.P264L | nonsynonymous SNV | 0.142 | . | . | . |
| | | . | 0.2 | . | . | . |
| c.397delT | p.F133fs,FAS | frameshift deletion | 0.17 | COSM1349688 | . | . |
| c.G686A | p.R229Q,FAS | nonsynonymous SNV | 0.144 | COSM5703782 | 0 | D |
| c.C8226G | p.N2742K | nonsynonymous SNV | 0.113 | . | 0.011 | D |
| c.C2275A | p.L759I | nonsynonymous SNV | 0.108 | COSM946771,COSM946772 | 0.444 | T |
| c.G4343A | p.G1448E | nonsynonymous SNV | 0.439 | . | 0.008 | D |
| c.C1216T | p.Q406X,IL16 | stopgain | 0.138 | . | . | . |
| c.C2107T | p.R703C | nonsynonymous SNV | 0.092 | . | 0.021 | D |
| c.C3665T | p.T1222M,CREBBP | nonsynonymous SNV | 0.133 | . | 0.009 | D |
| c.C412T | p.R138C,CD70 | nonsynonymous SNV | 0.141 | COSM1200315 | 0.011 | D |

| | | | | | | |
|---|---|---|---|---|---|---|
| c.G280T | p.G94W,CD70 | nonsynonymous SNV | 0.117 | . | 0 | D |
| c.1285delC | p.L429fs,POU2F2 | frameshift deletion | 0.214 | COSM4611039,COSM4611040 | . | . |
| c.T76C | p.S26P | nonsynonymous SNV | 0.364 | . | 0 | D |
| c.C7507T | p.Q2503X | stopgain | 0.15 | COSM28669,COSM4775114 | . | . |
| c.G347A | p.R116Q,TP53 | nonsynonymous SNV | 0.181 | COSM10662,COSM1640830,COSM3356964,COSM99020,COSM99021,COSM99602 | 0.005 | D |
| c.A184T | p.K62X,CD58 | stopgain | 0.153 | . | . | . |
| c.C6269A | p.S2090X | stopgain | 0.066 | . | . | . |
| c.G1423A | p.V475M,CIITA | nonsynonymous SNV | 0.425 | COSM966958 | 0.164 | T |
| c.G329T | p.C110F,TP53 | nonsynonymous SNV | 0.136 | COSM10810,COSM129834,COSM129835,COSM129836,COSM1646852,COSM3378347 | 0 | D |
| c.G413A | p.G138D | nonsynonymous SNV | 0.901 | . | 0.466 | T |
| c.A1517G | p.Y506C,FBXO11 | nonsynonymous SNV | 0.498 | . | 0.078 | T |
| c.568_570del | p.190_190del,GNAI2 | nonframeshift deletion | 0.203 | . | . | . |
| | | . | 0.214 | COSN25450465 | . | . |
| | | . | 0.144 | . | . | . |
| | | . | 0.229 | . | . | . |
| | | . | 0.223 | . | . | . |
| c.A1406C | p.H469P,DDX3X | nonsynonymous SNV | 0.163 | . | 0.109 | T |
| c.A1444G | p.T482A,DDX3X | nonsynonymous SNV | 0.114 | COSM1203253 | 0 | D |
| c.A6274G | p.S2092G | nonsynonymous SNV | 0.422 | . | 0.346 | T |
| c.C542T | p.A181V,BCL6 | nonsynonymous SNV | 0.385 | . | 0.19 | T |
| c.C1280A | p.P427H | nonsynonymous SNV | 0.4 | . | 0.354 | T |
| c.C3125T | p.S1042L,RELN | nonsynonymous SNV | 0.482 | . | 0.651 | T |
| c.A2077G | p.T693A | nonsynonymous SNV | 0.472 | . | 0.159 | T |
| c.C2936A | p.T979N | nonsynonymous SNV | 0.415 | . | 0.015 | D |
| c.G2366A | p.R789H,UNC5D | nonsynonymous SNV | 0.183 | COSM1231806 | 0.001 | D |
| c.245_255del | p.R82fs,ZFP36L1 | frameshift deletion | 0.142 | . | . | . |
| c.G130C | p.E44Q | nonsynonymous SNV | 0.439 | . | 0.128 | T |
| c.2466_2483del | p.822_828del,SETD2 | nonframeshift deletion | 0.456 | . | . | . |

| | | | | | | |
|---|---|---|---|---|---|---|
| c.G1591A | p.A531T,BCL6 | nonsynonymous SNV | 0.363 | COSM220321 | 0.013 | D |
| c.A3119G | p.D1040G,APC | nonsynonymous SNV | 0.495 | COSM6503097 | 0.005 | D |
| | | . | 0.485 | . | . | . |
| | | . | 0.521 | . | . | . |
| | | . | 0.592 | COSN23136164 | . | . |
| | | . | 0.496 | . | . | . |
| c.A64G | p.T22A,MYC | nonsynonymous SNV | 0.48 | . | 1 | T |
| c.G159C | p.E53D,MYC | nonsynonymous SNV | 0.537 | COSM1159795,COSM1159796 | 0.152 | T |
| c.A214G | p.T72A,MYC | nonsynonymous SNV | 0.56 | COSM1163490,COSM1163491 | 0.037 | D |
| c.G239A | p.R80H,MYC | nonsynonymous SNV | 0.114 | . | 0 | D |
| c.G336C | p.Q112H,MYC | nonsynonymous SNV | 0.511 | COSM1159799,COSM1159800 | 0.004 | D |
| c.C678G | p.D226E,MYC | nonsynonymous SNV | 0.51 | . | 0.115 | T |
| c.C744A | p.S248R,MYC | nonsynonymous SNV | 0.457 | . | 0.011 | D |
| c.T755C | p.L252P,MYC | nonsynonymous SNV | 0.468 | . | 0.001 | D |
| c.C773T | p.T258I,MYC | nonsynonymous SNV | 0.163 | . | 0.012 | D |
| c.C77G | p.P26R | nonsynonymous SNV | 0.376 | . | 0 | D |
| c.G8675A | p.R2892Q | nonsynonymous SNV | 0.446 | . | 0.523 | T |
| c.T188C | p.I63T,TP53 | nonsynonymous SNV | 0.092 | COSM11089,COSM116921,COSM116922,COSM116923,COSM116924,COSM1645297,COSM3421936 | 0 | D |
| c.T20G | p.I7S,CLTC | nonsynonymous SNV | 0.093 | . | 0 | D |
| c.T1659G | p.N553K,TCF3 | nonsynonymous SNV | 0.416 | . | 0.001 | D |
| exon4 | c.395+2T>C;NM_001193416 | splicing | 0.675 | . | . | . |
| c.A44C | p.K15T,BCL7A | nonsynonymous SNV | 0.238 | . | 0.001 | D |

| Polyphen2_score | Polyphen2_pred | MutationAssessor_score | MutationAssessor_pred | CADD_phred | Driver Prediction |
|---|---|---|---|---|---|
| 0.013 | B | 0.955 | L | 19.41 | Passenger |
| 0.413 | B | 0.345 | N | 18.6 | Passenger |
| . | . | . | . | . | Intronic |
| 1 | D | 2.545 | M | 23.8 | Driver |
| . | . | . | . | . | Driver |
| . | . | . | . | 38 | Driver |
| 0.361 | B | 2.265 | M | 23.5 | Driver |
| 1 | D | 0.45 | N | 27 | Passenger |
| . | . | . | . | . | Intronic |
| . | . | . | . | . | Intronic |
| . | . | . | . | . | Intronic |
| . | . | . | . | . | Intronic |
| . | . | . | . | . | Intronic |
| 0.054 | B | 0.945 | L | 4.476 | Passenger |
| 0.01 | B | 0.625 | N | 19.46 | Driver |
| 0.004 | B | 0.255 | N | 13.72 | Driver |
| 1 | D | 1.62 | L | 32 | Passenger |
| . | . | . | . | . | Driver |
| 0.948 | P | 3.42 | M | 24.1 | Driver |
| . | . | . | . | . | Driver |
| . | . | . | . | . | Driver |
| . | . | . | . | . | Driver |
| 0.998 | D | 2.435 | M | 26.7 | Driver |
| 0 | B | 0.345 | N | 0.004 | Passenger |
| 1 | D | 2.88 | M | 31 | Driver |
| . | . | . | . | 40 | Driver |
| 1 | D | 3.475 | M | 34 | Driver |
| 0.994 | D | 1.87 | L | 23.4 | Benign variant (ClinVar ID 41541) |

| | | | | | |
|---|---|---|---|---|---|
| 0 | B | -0.59 | N | 0.003 | Passenger |
| . | . | . | . | 26.4 | Driver |
| 0.047 | B | 1.245 | L | 0.229 | Passenger |
| 0.938 | P | 2.225 | M | 25.7 | Driver |
| 0.999 | D | 3.02 | M | 25.2 | Driver |
| 1 | D | 3.11 | M | 32 | Driver |
| 0.05 | B | 1.53 | L | 24.6 | Passenger |
| 0.999 | D | 2.095 | M | 23.9 | Driver |
| . | . | . | . | . | Driver |
| . | . | . | . | . | Driver |
| . | . | . | . | 21.5 | Driver |
| . | . | . | . | . | Intronic |
| . | . | . | . | . | Intronic |
| . | . | . | . | . | Intronic |
| . | . | . | . | . | Intronic |
| . | . | . | . | . | Intronic |
| . | . | . | . | . | Intronic |
| . | . | . | . | . | Intronic |
| . | . | . | . | . | Intronic |
| . | . | . | . | . | Intronic |
| . | . | . | . | . | Intronic |
| . | . | . | . | . | Intronic |
| . | . | . | . | . | Intronic |
| . | . | . | . | . | Intronic |
| . | . | . | . | . | Intronic |
| . | . | . | . | . | Intronic |
| . | . | . | . | . | Intronic |
| . | . | . | . | . | Intronic |
| . | . | . | . | . | Intronic |
| . | . | . | . | . | Intronic |
| . | . | . | . | . | Intronic |
| . | . | . | . | . | Intronic |
| . | . | . | . | . | Intronic |
| . | . | . | . | . | Intronic |

| | | | | | |
|---|---|---|---|---|---|
| . | . | . | . | . | Intronic |
| . | . | . | . | . | Intronic |
| . | . | . | . | . | Intronic |
| . | . | . | . | . | Intronic |
| . | . | . | . | . | Intronic |
| 0.145 | B | 1.59 | L | 12.37 | Passenger |
| 0.994 | D | 3.195 | M | 25.7 | Driver |
| 0.961 | D | 2.385 | M | 23 | Driver |
| 0 | B | . | . | 12.55 | Driver |
| 1 | D | 2.665 | M | 24.1 | Driver |
| 0.138 | B | 0.765 | N | 24.5 | Driver |
| 0 | B | 1.68 | L | 15.52 | Passenger |
| 0.999 | D | 1.845 | L | 25.8 | Passenger |
| . | . | . | . | 42 | Driver |
| 0.977 | D | 2.08 | M | 21.7 | Driver |
| 0.001 | B | -0.255 | N | 0.001 | Passenger |
| 0.03 | B | 0.975 | L | 19.87 | Driver |
| 0.131 | B | 0.125 | N | 23.8 | Passenger |
| 0 | B | 2.03 | M | 7.112 | Driver |
| 0.839 | P | 1.355 | L | 25.2 | Driver |
| 0.493 | P | -0.28 | N | 21.2 | Driver |
| 0.976 | D | 2.48 | M | 24.7 | Driver |
| 0.998 | D | 2.445 | M | 26.7 | Driver |
| 1 | D | 3.57 | H | 28.1 | Driver |
| . | . | . | . | 37 | Driver |
| 0 | B | 0 | N | 18.37 | Passenger |
| . | . | . | . | . | Intronic |
| . | . | . | . | . | Intronic |
| 0.999 | D | 2.975 | M | 27.1 | Driver |
| 0.987 | D | 1.59 | L | 26.1 | Passenger |
| 0.252 | B | 1.87 | L | 22.1 | Driver |
| 0.98 | D | 0 | N | 15.19 | Passenger |
| 1 | D | 2.695 | M | 22.3 | Driver |
| 0.02 | B | 2.005 | M | 22.7 | Driver |

| | | | | | |
|---|---|---|---|---|---|
| . | . | . | . | 25.1 | Driver |
| 0.804 | P | 3.06 | M | 24.8 | Driver |
| . | . | . | . | . | Driver |
| 0.003 | B | -0.69 | N | 11.84 | Passenger |
| 0.022 | B | 1.445 | L | 14.72 | Passenger |
| 0.056 | B | 1.095 | L | 23.3 | Passenger |
| 0.203 | B | -0.035 | N | 22.8 | Driver |
| 0 | B | 0.835 | L | 21.3 | Passenger |
| 0 | B | 1.87 | L | 17.98 | Passenger |
| 0.265 | B | 1.955 | M | 23.5 | Driver |
| 0.004 | B | 1.67 | L | 22.7 | Passenger |
| 0.004 | B | 1.39 | L | 21.3 | Passenger |
| 0.009 | B | 0.83 | L | 22.6 | Passenger |
| 0.001 | B | 2.08 | M | 23.6 | Driver |
| 0.898 | P | 2.085 | M | 28.7 | Driver |
| 0.002 | B | 2.125 | M | 14.68 | Driver |
| 0.225 | B | . | . | 23.4 | Driver |
| 0.968 | D | 2.465 | M | 23.9 | Driver |
| 0.992 | D | 2.4 | M | 23.7 | Driver |
| 0.714 | P | 1.79 | L | 24.5 | Passenger |
| 0.055 | B | 2.67 | M | 8.869 | Benign variant detected in germline (ClinVar ID 51349) |
| 0.989 | D | 2.7 | M | 28 | Driver |
| 0.267 | B | 2.25 | M | 2.046 | Driver |
| 0.95 | P | 0 | N | 9.318 | Passenger |
| . | . | . | . | 25.2 | Driver |
| 0.976 | D | . | . | 23.9 | Driver |
| 0.005 | B | 0.345 | N | 10.29 | Passenger |
| 0 | B | 0 | N | 21 | Passenger |
| 0.115 | B | 0.805 | L | 12.86 | Passenger |

| | | | | | |
|---|---|---|---|---|---|
| 1 | D | 3.515 | H | 25 | Driver |
| . | . | . | . | . | Driver |
| 0.948 | P | 2.465 | M | 24.1 | Driver |
| 0.949 | P | 2.08 | M | 24.7 | Driver |
| 0 | B | 2.2 | M | 23.3 | Driver |
| 0.997 | D | 2.005 | M | 25.4 | Driver |
| 0 | B | 1.65 | L | 8.353 | Passenger |
| 0 | B | 1.845 | L | 8.716 | Passenger |
| . | . | . | . | 24.6 | Driver |
| 0.031 | B | 1.845 | L | 1.131 | Passenger |
| 0.985 | D | 0 | N | 6.005 | Passenger |
| 0.006 | B | 0.09 | N | 10.26 | Passenger |
| 0.109 | B | 0.84 | L | 9.801 | Passenger |
| . | . | . | . | . | Intronic |
| . | . | . | . | . | Intronic |
| . | . | . | . | . | Intronic |
| . | . | . | . | . | Intronic |
| . | . | . | . | . | Intronic |
| . | . | . | . | . | Intronic |
| . | . | . | . | . | Intronic |
| . | . | . | . | . | Intronic |
| . | . | . | . | . | Intronic |
| . | . | . | . | . | Intronic |
| . | . | . | . | . | Intronic |
| . | . | . | . | . | Intronic |
| . | . | . | . | . | Intronic |
| . | . | . | . | . | Intronic |
| . | . | . | . | . | Intronic |

| | | | | | |
|---|---|---|---|---|---|
| . | . | . | . | . | Intronic |
| . | . | . | . | . | Intronic |
| . | . | . | . | . | Driver |
| 0 | B | -1.2 | N | 1.232 | Passenger |
| . | . | . | . | 24.6 | Driver |
| 0.954 | P | 2.685 | M | 27.3 | Driver |
| . | . | . | . | . | Intronic |
| . | . | . | . | . | Intronic |
| . | . | . | . | . | Intronic |
| . | . | . | . | . | Intronic |
| . | . | . | . | . | Intronic |
| . | . | . | . | . | Intronic |
| . | . | . | . | . | Intronic |
| . | . | . | . | . | Intronic |
| . | . | . | . | . | Intronic |
| . | . | . | . | . | Intronic |
| 1 | D | 2.9 | M | 25.7 | Driver |
| 0 | B | -0.41 | N | 4.024 | Driver |
| 0.999 | D | 2.395 | M | 24.7 | Driver |
| 0.997 | D | 3.3 | M | 25.9 | Driver |
| 0.994 | D | 3.305 | M | 26 | Driver |
| 0.015 | B | 0.49 | N | 0.005 | Passenger |
| 0.807 | P | 0.69 | N | 17.6 | Driver |
| 1 | D | 3.21 | M | 27.2 | Driver |
| 0.509 | P | 2.31 | M | 23.5 | Driver |
| 0.582 | P | 2.25 | M | 23.6 | Driver |
| 0.979 | D | 0.35 | N | 21.3 | Passenger |
| 1 | D | 2.89 | M | 31 | Driver |
| 1 | D | 1.93 | L | 34 | Driver |
| 0.001 | B | -0.9 | N | 0.002 | Driver |
| . | . | . | . | . | Driver |

| | | | | | |
|---|---|---|---|---|---|
| 0.002 | B | 0.55 | N | 0.434 | Passenger |
| 0.002 | B | 0 | N | 10.33 | Passenger |
| 0.956 | P | 2.84 | M | 26.2 | Driver |
| . | . | . | . | . | Intronic |
| . | . | . | . | . | Intronic |
| 0.661 | P | 2.215 | M | 24.4 | Driver |
| 0.998 | D | 2.565 | M | 26.1 | Driver |
| 0.982 | D | 2.08 | M | 18.23 | Driver |
| 0.911 | P | . | . | 22.8 | Driver |
| . | . | . | . | . | Driver |
| 0.078 | B | 1.245 | L | 5.347 | Passenger |
| 0.688 | P | 1.15 | L | 0.984 | Passenger |
| 0 | B | 0 | N | 8.384 | Passenger |
| 1 | D | 2.39 | M | 27.1 | Driver |
| 1 | D | 1.255 | L | 35 | Driver |
| 0.998 | D | 2.705 | M | 32 | Driver |
| . | . | . | . | . | Driver |
| 0.89 | P | 1.52 | L | 28.6 | Driver |
| 1 | D | 2.395 | M | 27.6 | Driver |
| 1 | D | 4.805 | H | 24.2 | Driver |
| . | . | . | . | . | Intronic |
| . | . | . | . | . | Driver |
| 1 | D | 3.005 | M | 33 | Driver |
| 0.933 | P | 1.93 | L | 24.1 | Passenger |
| 0 | B | 0.225 | N | 0.001 | Benign variant (ClinVar ID 51264) |
| 0.983 | D | 2.135 | M | 24.1 | Driver |
| . | . | . | . | 41 | Driver |
| 0.69 | P | 1.65 | L | 21.5 | Passenger |
| 1 | D | 2.3 | M | 24.3 | Driver |
| 0.672 | P | 1.24 | L | 24.5 | Driver |

| | | | | | |
|---|---|---|---|---|---|
| 1 | D | 1.7 | L | 27.8 | Passenger |
| . | . | . | . | . | Driver |
| 0.994 | D | 0 | N | 11.98 | Passenger |
| . | . | . | . | 47 | Driver |
| 1 | D | 2.935 | M | 34 | Driver |
| . | . | . | . | 35 | Driver |
| . | . | | . | 37 | Driver |
| 0.631 | P | 1.18 | L | 0.045 | Driver |
| 1 | D | 3.325 | M | 33 | Driver |
| 0 | B | -0.75 | N | 0.483 | Passenger |
| 0.991 | D | 1.945 | M | 24.3 | Driver |
| . | . | . | . | . | Driver |
| . | . | . | . | . | Intronic |
| . | . | . | . | . | Intronic |
| . | . | . | . | . | Intronic |
| . | . | . | . | . | Intronic |
| 0.002 | B | 1.61 | L | 15.94 | Passenger |
| 1 | D | 4.01 | H | 27.2 | Driver |
| 0 | B | 0.805 | L | 8.424 | Passenger |
| 0.267 | B | 1.265 | L | 16.5 | Passenger |
| 0.214 | B | 1.04 | L | 17.67 | Passenger |
| 0 | B | 0.45 | N | 6.076 | Passenger |
| 0.022 | B | 1.245 | L | 0.001 | Passenger |
| 0.995 | D | 3.015 | M | 23.7 | Driver |
| 1 | D | 2.81 | M | 34 | Driver |
| . | . | . | . | . | Driver |
| 0.012 | B | 1.065 | L | 22.4 | Passenger |
| . | . | . | . | . | Driver |

| | | | | | |
|---|---|---|---|---|---|
| 1 | D | 0.775 | N | 26.4 | Driver |
| 0.376 | B | 0.895 | L | 22.1 | Driver |
| . | . | . | . | . | Intronic |
| . | . | . | . | . | Intronic |
| . | . | . | . | . | Intronic |
| . | . | . | . | . | Intronic |
| 0 | B | -1.125 | N | 0.002 | Passenger |
| 0.219 | B | 1.065 | L | 14.18 | Driver |
| 0.994 | D | 3.195 | M | 25.7 | Driver |
| 1 | D | 2.74 | M | 32 | Driver |
| 0.545 | P | 2.21 | M | 23.4 | Driver |
| 0.224 | B | -0.06 | N | 3.49 | Passenger |
| 0.582 | P | 2.25 | M | 23.6 | Driver |
| 0.739 | P | 0.925 | L | 12.24 | Passenger |
| 0.827 | P | 2.05 | M | 23.5 | Driver |
| 0.123 | B | 2.9 | M | 23.8 | Driver |
| 0.018 | B | 0.805 | L | 9.692 | Passenger |
| 1 | D | 3.12 | M | 23.9 | Driver |
| 0.007 | B | 3.41 | M | 24.1 | Driver |
| 0.999 | D | 3.2 | M | 27.2 | Driver |
| . | . | . | . | 24.7 | Driver |
| 0.643 | P | 2.075 | M | 13.11 | Driver |

**Supplemental Table 7.** Frequency of driver mutations in pediatric PTLD-DLBCL. IC-DLBCL[13] and in adult EBV-positive and negative PTLD-DLBCL.[23,24] Frequencies marked in bold represent statistically significant differences with pediatric PTLD-DLBCL, according to Fisher's exact test * *P* <0.1..

| Gene | Frequency of driver mutations(%) | | | | |
|---|---|---|---|---|---|
| | **Ped IC-DLBCL (n=22)** | **Ped PTLD-DLBCL (n=18)** | **Ped EBV+ PTLD-DLBCL (n=16)** | **Adult EBV+ PTLD-DLBCL (n=16)** | **Adult EVB- PTLD-DLBCL (n=28)** |
| *SOCS1* | **27.3** | 0 | 0 | 6.25 | 3.57 |
| *KMT2D* | **22.7** | 0 | 0 | **18.75** | **35.71** |
| *KMT2C* | 9.1 | 16.7 | 12.5 | 6.25 | 7.14 |
| *CARD11* | 0 | 11.1 | 6.2 | 0 | 7.14 |
| *CD70* | 4.5 | 11.1 | 12.5 | | |
| *NOTCH1* | 0 | 11.1 | 12.5 | 6.25 | 14.29 |
| *TP53* | 9.1 | 11.1 | 6.2 | 12.5 | **42.86** |
| *MYD88* | 13.6 | 0 | 0 | 6.25 | 10.71 |
| *GNA13* | 13.6 | 5.6 | 0 | 0 | 7.14 |
| *PIM1* | 13.6 | 0 | 0 | 6.25 | 10.71 |
| *BTG1* | 13.6 | 0 | 0 | 6.25 | 10.71 |
| *EZH2* | 13.6 | 0 | 0 | 6.25 | 14.29 |
| *PRDM1* | 4.5 | 0 | 0 | 0 | 10.71 |
| *PIK3CD* | | 0 | 0 | **18.75** | 3.57 |
| *DDX3X* | 4.5 | 5.6 | 6.2 | | |
| *SGK1* | 0 | 5.6 | 0 | 0 | 7.14 |
| *SPTBN5* | 0 | 11.1 | 12.5 | | |